ORGANOMETALLIC CATION-EXCHANGED PHYLLOSILICATES

BY

SHAY FLEMING

A THESIS SUBMITTED FOR THE DEGREE OF

MASTER OF SCIENCE

AT

DUBLIN CITY UNIVERSITY

SCHOOL OF CHEMICAL SCIENCES
DUBLIN CITY UNIVERSITY
GLASNEVIN
DUBLIN 9

JUNE 1991

THIS WORK IS DEDICATED

TO

MY WIFE JO

AND

DAUGHTERS KATE AND SOPHIE

ACKNOWLEDGEMENTS

I wish to express my sincere gratitude to my Research Supervisor, Dr Christopher Breen, for his guidance and encouragement throughout this work

I should also like to acknowledge the Academic Staff, Technical Staff and Fellow Post-Graduates of the School of Chemical Sciences at Dublin City University for their invaluable assistance

In particular, I wish to thank my friend and colleague, Dr Alyn Deane, for his helpful suggestions in the preparation of this manuscript

I further wish to express my thanks to Mrs Ruth Sheridan who typed the entire manuscript

In addition, I should like to record my gratitude to the Research and Post-Graduate Students Committee for the award of a Research Studentship

Finally, I would like to thank my parents and family for their understanding and kindness throughout this work

ABSTRACT

Organotin (IV) complexes formed between 0 01 M dimethyltin dichloride solutions prepared at pH 2 6 and 4 0, and trimethyltin chloride prepared at pH 3 4, with Na^{+}-montmorillonite clay have been characterised using ^{119}Sn Mössbauer spectroscopy, X-ray diffraction, thermogravimetric analysis and water sorption isotherms Following cation exchange, Mössbauer spectroscopy identified two tin species in the dimethyltin (IV)-exchanged clay prepared at pH 2 6 A cis species was characterised by an isomer shift, δ, of 1 11 mms^{-1}, and quadrupole splitting, Δ, of 3 12 mms^{-1}, and a trans species, characterised by an isomer shift, δ of 1 27 mms^{-1}, and quadrupole splitting of 4 24 mms^{-1} In the dimethyltin (IV)-exchanged clay prepared at pH 4 0, a cis species, characterised by an isomer shift, δ of 1 12 mms^{-1}, and quadrupole splitting, Δ of 2 89 mms^{-1}, along with a trans species, characterised by an isomer shift, δ, of 1 26 mms^{-1}, and quadrupole splitting, Δ, of 3 66 mms^{-1} were also identified However, a single tin species, characterised by an isomer shift, δ, of 1 32 mms^{-1} and quadrupole splitting of 3 79 mms^{-1}, was identified in the trimethyltin (IV)-exchanged clay prepared at pH 3 4

Within the temperature range 20-450°C, the intercalated species of each of the three thermally pretreated organotin (IV)-exchanged clays were found to be unstable with respect to increasing pretreatment temperature For each of the dimethyltin (IV)-exchanged clays prepared at pH 2 6 and 4 0, the thermolysis pattern of the intercalated species, as characterised using Mössbauer spectroscopy, was quite similar, with cis and trans species being converted to Me_2SnO between 20 and 230°C At temperatures greater than 200°C, Me_2SnO and remaining trans species were converted to oxides of tin The trimethyltin (IV)-exchanged clay behaved in almost identical way, where a low isomer shift component was formed, albeit at a somewhat higher pretreatment temperature than the dimethyltin (IV)-

exchanged systems However, at temperatures greater than 200°C, any remaining methylated components were similarly converted to oxides of tin

The temperatures at which these inorganic oxides of tin appeared in the dimethyltin (IV) exchanged clays were seen to coinside with a collapse in the basal spacing from 13 8Å in the clay preapred at pH 2 6, and 15 9Å in the clay prepared at pH 4 0, to 9 6Å A similar collapse in the basal spacing from 13 8Å to 9 6Å was seen for the trimethyltin (IV)-exchanged clay

Following thermal pretreatment at 120°C, both dimethyltin (IV)-exchanged clays displayed type IV isotherms in the B E T classification for the adsorption of water However, the clay prepared at pH 4 0 had a lower sorption capacity and exhibited a less marked hysteresis which closed sooner than that of the exchanged clay prepared at pH 2 6

CONTENTS

CHAPTER 1

INTRODUCTION TO CLAY MINERALOGY

1 1 GENERAL INTRODUCTION

For many years now clays and clay minerals have been successfully prepared and produced, and have found a wide application as lubricants in the drilling of oil wells, plasticisers in cements and fillers in paper, adhesives, cosmetics and paints. It is only recently that interlayering smectites with large organometallic molecules has been successful in producing high surface area solids for use as molecular sieves and novel pillared clay catalysts However, until very recently it has not been possible to accurately determine the fundamental structure of the different clay minerals, and as such the correlation of data obtained from X-ray diffraction, atomic absorption spectrometry and infra-red spectroscopy has produced much clearer pictures of the structure and properties of these materials

In order to gain some understanding of the reactions between these minerals and their intercalants it is first necessary to describe their strucutre and classification.

1 2 THE STRUCTURE OF CLAY MINERALS

Two basic structural units are involved in the atomic lattices of most of the clay minerals. The first of these units consist of two-dimensional arrays of SiO_4 tetrahedra and the second unit is a two-dimensional array of $Mg_3(OH)_6$ or $Al_2(OH)_6$ octahedra.

In each SiO_4 tetrahedra, the central silicon atom is equidistant from four oxygen atoms, (Fig. 1.1a).

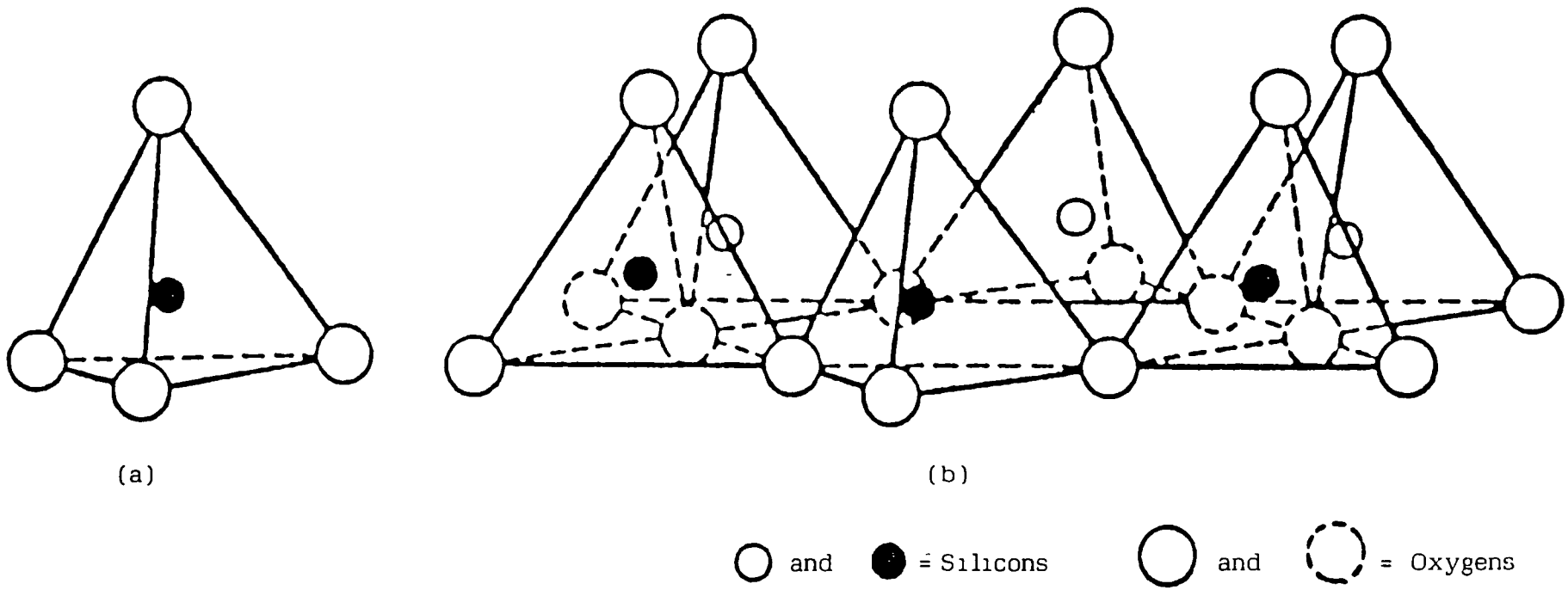

Fig. 1.1 Schematic diagram showing (a) a single silica tetrahedron and (b) the sheet structure of silica tetrahedrons arranged in a hexagonal network.

The O-O distance in each case being 2.55Å The silica tetrahedra are arranged to form a planar hexagonal network, which may be repeated indefinitely to form a sheet of composition of $Si_4O_6(OH)_4$.[9] The oxygen atoms at the base of each tetrahedron is corner shared with neighbouring tetrahedra, with the apical oxygens all pointing in the same direction, (Fig. 1.1b) In the second of these units, the aluminium or magnesium cations are directly co-ordinated to six oxygen atoms or hydroxyl groups forming an octahedron (Fig. 1 2a) The oxygen atoms and hydroxyl groups form two planes, one above and one below the cation, (Fig. 1 2b)

The analogous symmetry and almost identical dimensions in the tetrahedral and octahedral layers allow the apical oxygens of each tetrahedron to be shared by the octahedral layer. In 1·1 layer silicates such as kaolin,(Fig. 1.3), this sharing occurs between one tetrahedral and one octahedral sheet. In 2 1 layer silicates such as montmorillonite,(Fig. 1.4), the apical oxygens of two tetrahedral sheets, each directed inwards, are shared with the octahedral sheet In the layer silicates, the layers composed of an octahedral sheet and one or more tetrahedral sheets are continuous in the a and b directions and are stacked on top of one another in the c direction.

The layer silicates can be further subdivided into di-octahedral and tri-octahedral forms, depending on the valency of the central cation in the octahedral layer. In order to maintain overall electrical

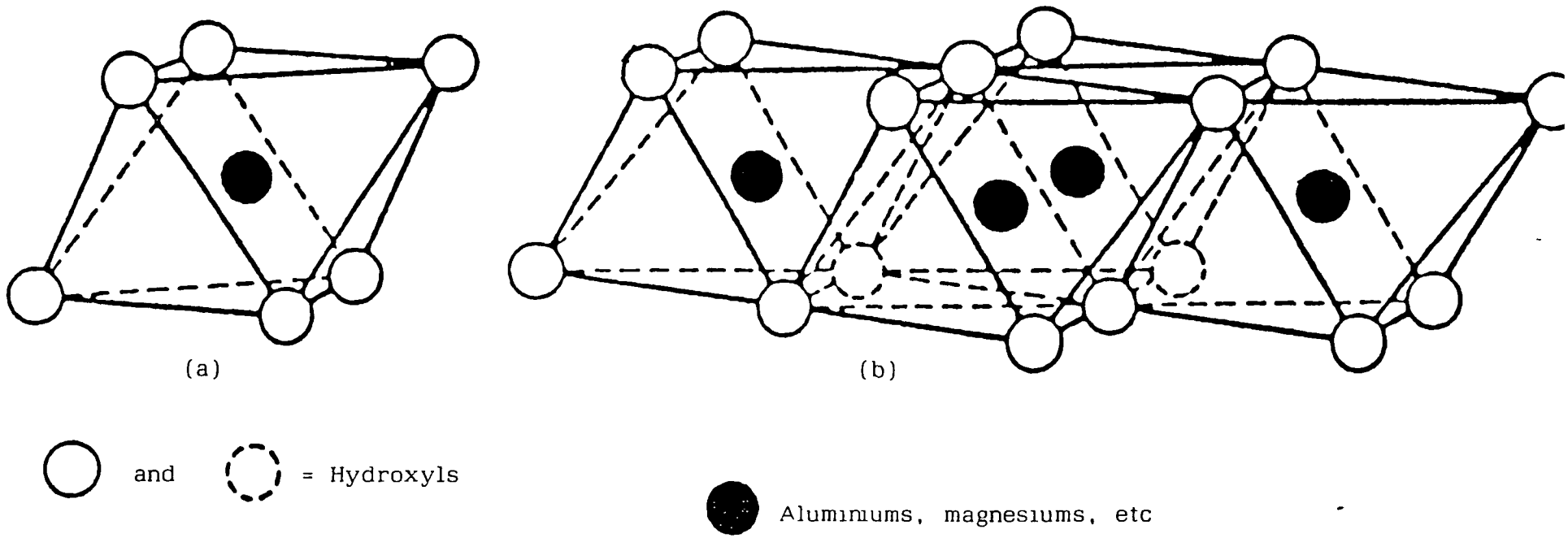

Fig. 1 2 Schematic diagram showing (a) a single octahedral unit and (b) the sheet structure of the octahedral unit

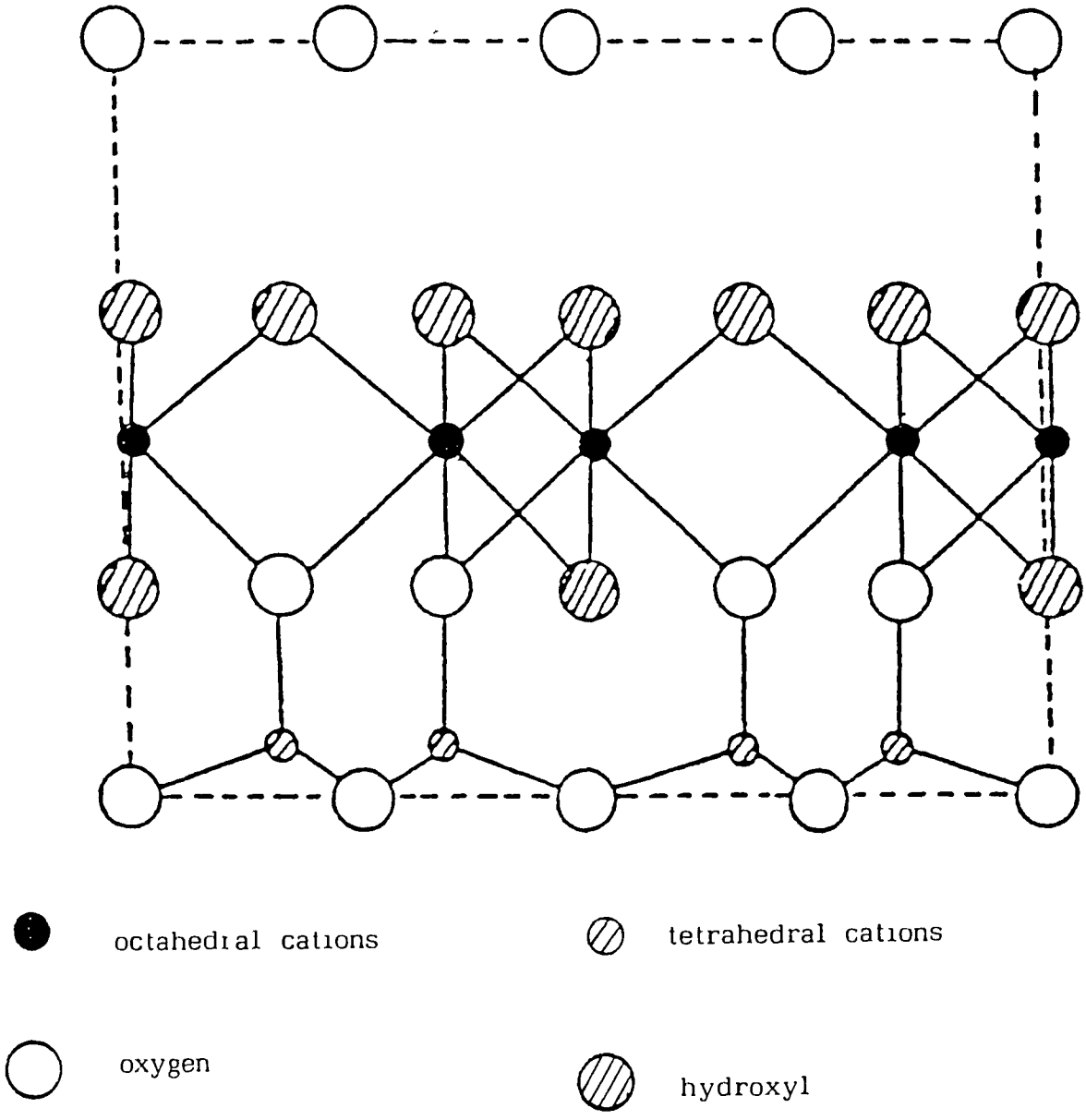

Fig 1 3 Schematic diagram showing the kaolanite structure.

neutrality, all three divalent cation sites in the octahedral sheet must be filled giving rise to a tri-octahedral mineral (e.g. $Mg_3 Si_4 O_{10} (OH)_2$) If however two of the three divalent cation sites are occupied by trivalent cations, a di-octahedral mineral (e g. $Al_2 Si_4 O_{10} (OH)_2$) is formed. This of course is an ideal situation in which all positive and negative charges are balanced generating an electrically neutral structure.

As clay minerals are formed under non-ideal conditions in nature, charge imbalance occurs. For example a trivalent cation such as aluminium being substituted for silicon in the tetrahedral layer or a divalent cation such as magnesium being substituted for aluminium in the octahedral layer. The net deficiency of positive charge is balanced by the clay layers separating and exchangable cations being sorbed into the interlayer space This phenomenon of cation exchange influences the surface properties of the layer silicates such as swelling in water.

1.3 CLASSIFICATION OF LAYER SILICATES

It was the importance of clay materials in ceramics, agriculture, geology and many other industries that led to their investigation and the elucidation of their similar and not so similar crystal structures. Although many clay minerals had been assigned names by early investigators and were classified by their chemical composition, it wasn't until the early 1920s[1,2]

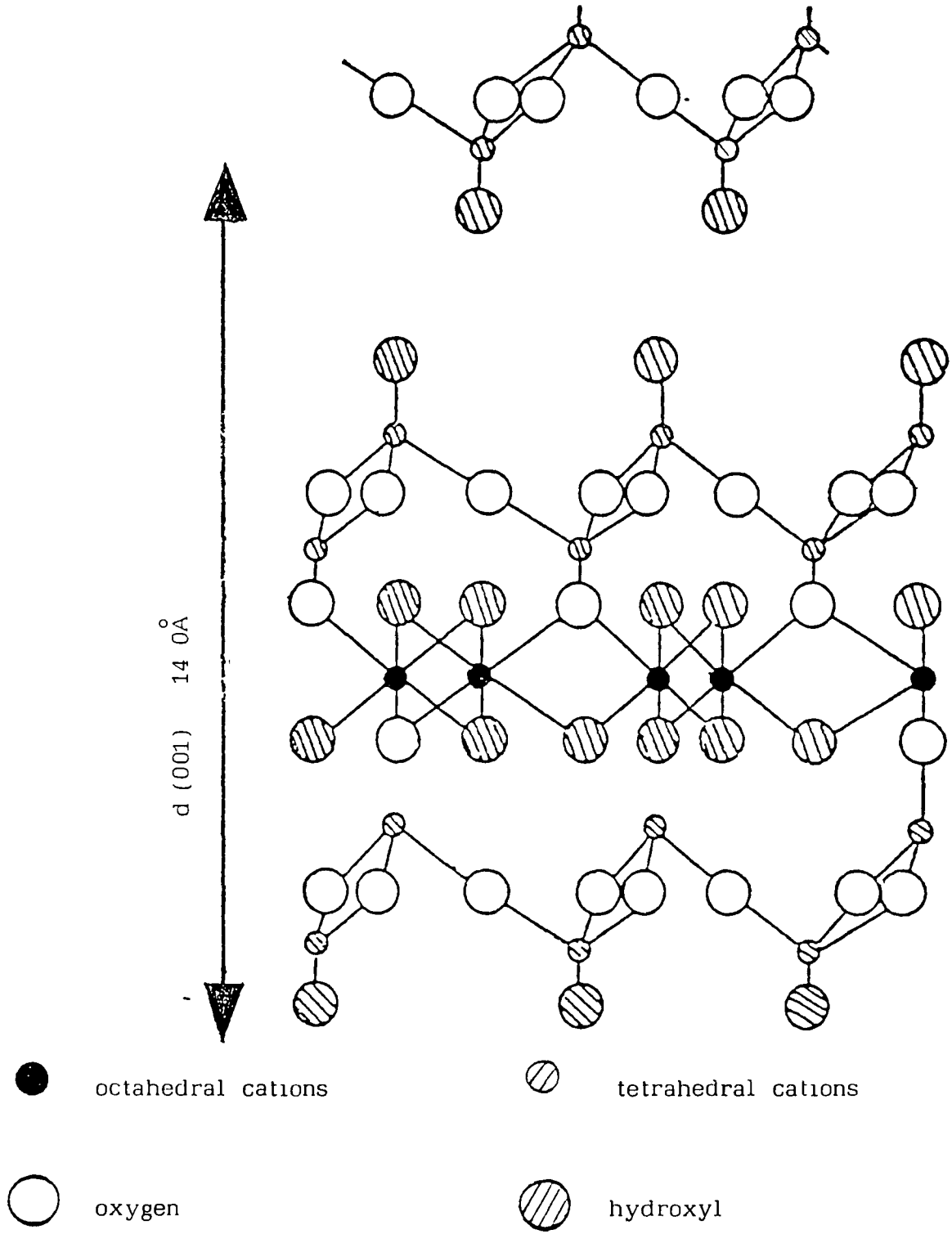

Fig 1 4 Schematic diagram showing the montmorillonite structure proposed by Edelman-Favejee

that it was shown by X-ray analysis that clay minerals were composed of crystalline material. By 1940 Linus Pauling[2] had shown that clay minerals of widely different chemical composition had very similar crystal structures, making it possible to devise the classification of these materials which is still used today.

The sheet silicates are classified by the charge on the aluminosilicate layer in order of increasing charge per formula unit. This is based on the recommendations put forward by a subcommitte of the Association International Pour L'Etude des Argiles (A I.E P.A) at the International Clay Conference in Stockholm in 1963. Table 1 1 shows a proposed classification scheme for Phyllosilicates related to clay minerals

1.3.1 1.1 Type Minerals

The charge per formula unit for this group is zero. The stacking geometry of oxygen and hydroxyl planes of successive layers in a single crystal of Kaolinite gives rise to strong Van der Waals forces and some hydrogen bonding holding the layers together The minerals in this group do not expand in water. However, absorption of organic materials is possible since some edges of Kaolinite crystals contain unsatisfied valencies occupying between 10 and 20 per cent of the total crystal area. It should be pointed out that polar molecules like dimethylsulphoxide, N-methylformamide and hydrazine can intercalate between the layers of Kaolin

TABLE 1.1 PROPOSED CLASSIFICATION SCHEME

TYPE	CHARGE PER FORMULA UNIT	GROUP	SUBGROUP
1 1	0	Kaolinite-Serpentine	Dioctahedral Trioctahedral
2:1	0	Pyrophyllite-Talc	Dioctahedral Trioctahedral
	0.25-0 6	Smectite	Dioctahedral Trioctahedral
	0.6-0.9	Vermiculite	Dioctahedral Trioctahedral
	1.5-2.0	Illite	Dioctahedral Trioctahedral
	1	Mica	Dioctahedral Trioctahedral
	2	Brittle Mica	Dioctahedral Trioctahedral
2.1:1	Variable	Chlorite	Dioctahedral Trioctahedral

FOR PHYLLOSILICATES RELATED TO CLAY MINERALS

SPECIES	FORMULA UNIT
Kaolinite	$[Al_2Si_2O_5(OH)_4]$
Chrysolite	$[Mg_3Si_2O_5(OH)_4]$
Pyrophyllite	$[Al_2Si_4O_{10}(OH)_2]$
Talc	$[Mg_3Si_4O_{10}(OH)_2]$
Montmorillonite	$[Na_{0.3}(Al_{1.7}Mg_{0.3})Si_4O_{10}(OH)_2]$
Saponite	$[Na_{0.3}Mg_3(Si_{3.8}Al_{0.3})O_{10}(OH)_2]$
Dioctahedral Vermiculite	$[Mg_{0.3}Al_2(Si_{3.4}Al_{0.6})O_{10}(OH)_2]$
Tricotahedral Vermiculite	$[Mg_{0.3}Mg_3(Si_{3.4}Al_{0.6})O_{10}(OH)_2]$
Illite	$[K_{0.8}Al_2(Si_{3.2}Al_{0.8})O_{10}(OH)_2]$
Glauconite	$[K_{0.8}Mg_3(Si_{3.2}Al_{0.8})O_{10}(OH)_2]$
Muscovite	$[K\ Al_2(Si_3Al)O_{10}(OH)_2]$
Phlogopite	$[K\ Mg_3(Si_3Al)O_{10}(OH)_2]$
Margarite	$[Ca\ Al_2(Si_2Al_2)O_{10}(OH)_2]$
Xanthophyllite	$[Ca\ Mg_3(Si_2Al_2)O_{10}(OH)_2]$
Donbassite	$[Al_4Si_{2.5}O_{11}(H_2O)3.5]$
Clinochlore	$[Mg_6Si_4O_{10}(OH)_3]$

and enter into hydrogen bonding with the layers. Of the minerals in this group Kaolinite and Halloysite are dioctahedral whereas Antigarite and Chrysolite belonging to the Serpentine sub group are trioctahedral.

1.3.2 2:1 Type Minerals

(a) Pyrophyllite-Talc Group.

This group has a tetrahedral-octahedral-tetrahedral, or 2.1 type, layer structure. In this group the isomophous substitution of Al^{3+} for Mg^{2+} or Fe^{2+} in octahedral positions, or Si^{4+} for Al^{3+} in tetrahedral positions never occurs, resulting in no interlayer adsorption of external cations In this group, Pyrophillite is dioctahedral and Talc trioctahedral.

(b) Smectite Group

The charge per formula unit for minerals in this group ranges between 0 25 and 0.6. Adsorption of external cations to balance the net negative layer charge resulting from isomorphous substitution in both the dioctahedral and trioctahedral layers takes place readily. These sorbed cations are easily exchanged in aqueous solution, the result of which is that layers may expand to a limiting d(001) spacing of 1.9nm although the Na^{+}-clay can go to infinity. Montmorillonite and Nontronite are members of the dioctahedral subgroup. Hectorite and Saponite are members of the trioctahedral subgroup.

(c) Vermiculite Group

The amount of isomorphous substitution in this group is generally greater than that occurring in the smectite group, and mainly in the tetrahedral sheet. Consequently, the charge per formula unit is also higher than the smectite group ranging from 0.6 to 0.9. This high layer charge makes interlayer expansion difficult compared to expansion of montmorillonite. However, sorption of water and organic molecules does occur. Vermiculite can occur as dioctahedral vermiculite or trioctahedral vermiculite.

(d) Illite Group.

The charge per formula unit for the Illite group ranges between 1.5 and 2 0, right between the Vermiculite and Mica groups Much greater isomorphous substitution occurs in this group than in other groups as only some of the silicon atoms in the tetrahedral sheets are replaced by aluminium. This resultant negative charge is balanced by positively charged metal ions. Illite does not appear to intercalate organic compounds and interlayer water is rarely present. Dioctahedral Illite is normally referred to as "Illite" whereas trioctahedral illite is referred to as Glauconite.

(e) Mica Group

In this group much substitution of Si^{4+} by Al^{3+} occurs in the tetrahedral sheet. Sorption of interlayer K^{+} ions balances the negative charge giving rise to strong electrostatic attraction between adjacent layers. This strong interlayer bonding makes cation exchange

difficult and intercalation seldom occurs Muscovite is a dioctahedral mica Phlogopite is a trioctahedral mica.

(f) Brittle Mica Group

In this group greater isomorphous substitution occurs in the tetrahedral sheet. The charge per formula unit is about 2, with the large sheet negative charge being balanced by Ca^{2+} rather than K^{+} as in the True Mica Group The interlayer cations are not exchangable and swelling is very rare Margarite is a dioctahedral Brittle Mica, Xanthophillite is trioctahedral

1 3 3 Modified 2 1 1 Type Minerals

The chlorite structure consists of alternate mica-like and brucite-like layers. The mica-like layers are trioctahedral and are unbalanced by the substitution of Al^{3+} for Si^{4+}. This charge deficiency is balanced by the substitution of Al^{3+} for Mg^{2+} in the brucite sheet. Hence, no net layer charge exists in this group. Cations are not exchangable and swelling is only observed when the hydrogen bonding between the silicate and brucite layers is disrupted. The charge per formula unit ranges from 0.5 to about 1.5 Donbassite is a dioctahedral chlorite mineral, Clinochlore is a trioctahedral chlorite mineral.

1 4 MONTMORILLONITE.

The name montmorillonite was first proposed in 1847 by Damour and Salvetat[3] for a mineral from Montmorillon in France Analysis of this mineral[4]

showed it to be a hydrous aluminium silicate containing small quantities of alkali and alkaline earth metals The structure of montmorillonite was first proposed by Hofmann, Endell and Wilm [5] This structure was then modified by Marshall,[6] Maegdefrau, Hofmann[7] and Hendricks,[8] (Fig. 1.5), and is now the generally accepted structure According to this structure montmorillonite is a 2 1 type clay mineral, negatively charged due to the isomorphous substitution of Mg^{2+} for Al^{3+} in the octahedral sheet and Al^{3+} for Si^{4+} in the tetrahedral sheet The net negative charge is balanced by sorption of exchangable cations between the layers Consequently, water is also readily adsorbed in the interlayer space as an integral number of complete layers of molecules, depending on the nature of the exchangable cation, causing the lattice to expand in the c direction [9] The c direction in montmorillonite can vary from 9 5Å in the totally dehydrated form to about 19 5Å depending on the type and degree of hydration of the interlayer cation, and in some cases layers can dissociate completely [10]

However, this structure as proposed by Marshall,[6] Magdefrau and Hofmann,[7] and Hendricks[8] does not adequately account for the ion exchange capacity of montmorillonite

Edelman and Favajee[11] in 1940 suggested a model in which alternative SiO_4 tetrahedra in both silica sheets are inverted This structure gives rise to the situation where not all silicon atoms are in a single

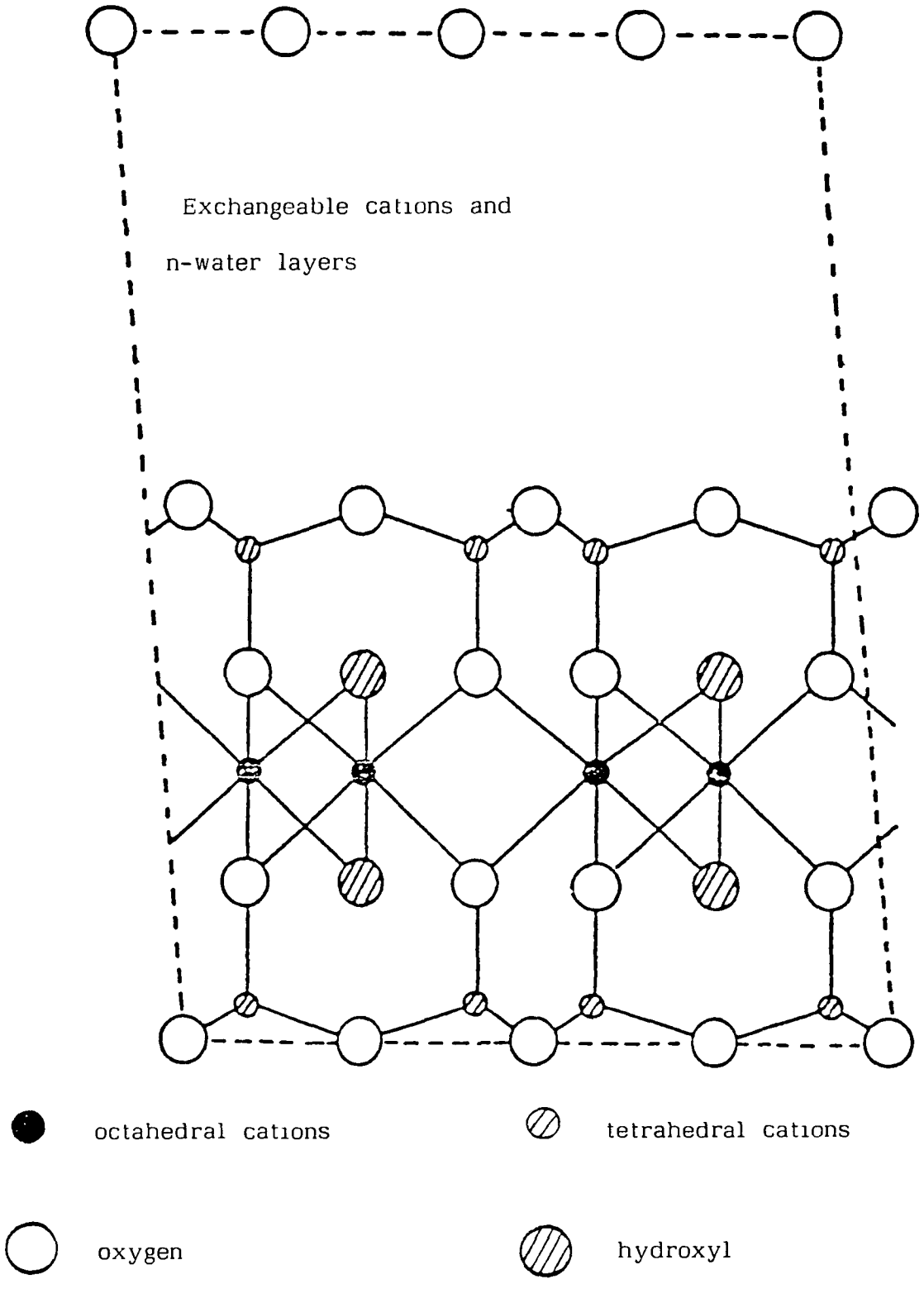

Fig 1 5 Schematic diagram showing the montmorillonite structure proposed by Hofmann-Endell-Wilm, and modified by Marshall-Maegdefrau-Hendricks

plane in the silica tetrahedral sheets resulting in some substitutions of OH for O in octahedral layers to balance the charge However, in 1950 Fourier synthesis of X-ray diffraction data[12] showed this structure as presented to be incorrect In 1950, McConnell[13] suggested a revision of the structure previously proposed by Hofmann et al [5] in 1933, whereby some of the oxygens on the base of the silica tetrahedrons are replaced by hydroxyl groups

Finally, on the basis of the structural changes taking place when montmorillonite is heated, Franzen, Muller-Hesse, and Schwiete[14] suggested in 1955 a structure in which two tetrahedral layers are bound together with an octahedral layer with water molecules lying between the octahedral layer of one package and the silica layer of the next although, no diffraction evidence for this structure was presented

For the purpose of this research the Hofmann-Endell-Wilm structure of Montmorillonite modified by Marshall, Maegdefrau and Hendricks as seen in Fig 1 5 is considered to be correct.

1.4 1 The Cation Exchange Capacity (C.E.C.) of Clay Minerals.

Clay minerals can sorb certain cations and hold them until they are exchanged stoichiometrically by another cation from aqueous solution. Although cation exchange had been observed for centuries[15] in so far as liquid manures were decolourized and deodourized by

filtering through soils it wasn't until 1850 that Forschamer[16] showed that calcium and magnesium are released from soil by leaching with sea water.

Exchangable cations are held around the outside of the silica-alumina clay mineral structural unit and do not affect the structure of the clay mineral packet.[9] The cation exchange capacity of clay minerals is measured in terms of milliequivalents per gram or more often per 100 grams of clay Table 2 shows the CEC's of Clay Minerals presented as milliequivalents per hundred grams of clay

1.4.2 The causes of Cation Exchange and Exchange Sites

Generally cation exchange is considered to arise from three types of exchange site

(i) Broken bonds around the edges of the silica-alumina units.

These broken bonds tend to occur on non-cleavage surfaces parallel to the c axis of the layer clay minerals leaving a net negative charge on the layer which is balanced by adsorbed cations. Cation exchange capacity increases as particle size and degree of crystalinity decreases. In the Kaolinite and halloysite minerals, broken bonds are probably the major cause of exchange capacity.

(ii) Isomorphous Substitution within the lattice structure.

This factor accounts for about eighty per cent of the total exchange capacity in vermiculites and montmorillonites. The substitution of Al^{3+} for Si^{4+} in

TABLE 1.2 THE CATION EXCHANGE CAPACITIES OF CLAY MINERALS
presented as millequivalents per hundred grams of clay

MINERAL	C.E.C.
Kaolinite	3-15
Halloysite.2 H_2O	5-10
Halloysite.4 H_2O	50-50
Montmorillonite	80-150
Illite	10-40
Vermiculite	100-150
Chlorite	10-40
Sepiolite-Attapulgite-Palygorskite	20-30

tetrahedral sheets and Mg^{2+} for Al^{3+} in octahedral sheets again leaves a net negative charge on the layer which requires balancing by exchangable cations To a lesser extent the layer charge may be balanced by other lattice charges in the silica-alumina unit such as replacing oxygens by hydroxyl groups or filling more than sixty six per cent of all possible octahedral positions It should be pointed out that isomorphous sites account for up to 80% of the cation exchange capacity whereas edge sites account for only 20%.

(iii) The Hydrogen of exposed Hydroxyls.

This type of cation exchange capacity is also important in kaolinite and halloysite due to the presence of the sheet of hydroxyls on one side of the basal cleavage plane However, the hydrogen of exposed hydroxyls would probably be tightly bound compared to broken bonds and may not be easily replaced.

1.4.3 The Position and Rate of Exchange of Exchangable Cations.

The position of the exchangable cations within or around a layer surface depends on the location of the negative charge, whereas the rate of cation exchange depends on the nature and concentration of the cations in solution and also on the clay mineral itself. In clay minerals in which the cation exchange results from broken bonds the adsorbed cation will be held around the edge of the clay sheet. However, in cation exchange due to isomorphous substitution, the exchanged cations are

mostly found on or between the basal plane surfaces. The rate of cation exchange due to broken bonds is almost instantaneous but penetration between the sheets of montmorillonite where isomorphous substitution is responsible for about eighty per cent of cation exchange takes a while longer In zeolites, however cation exchange takes place much more slowly.

When clays adsorb small amounts of water it is likely that the adsorbed cations at the edge sites are held very close to or at the clay mineral surface. However, Brown[12] showed that for montmorillonite under these hydration conditions the adsorbed cations between the basal plane surfaces are held midway between the clay mineral surfaces In anhydrous Na^+-montmorillonite, Pezerat and Mering[17] showed that the sodium cations occupied the hexagonal cavity in the tetrahedral layer and stayed there in the presence of one H_2O molecule When two or more H_2O molecules were adsorbed, the cation moved out of this cavity and was separated from each of the basal surfaces of the clay by a water molecule

The positions of all exchangable cations in such systems are not the same Mering and Glaeser[18] pointed out that cations compensating for lattice unbalance tend to take on a position as close to the negative charge as possible. Whereas sodium would occupy the hexagonal hole, calcium on the other hand would go into the hole nearest to one negative charge However, as soon as

water is adsorbed calcium leaves this hexagonal hole and becomes hydrated, the clay behaving as if saturated completely with sodium

Ion exchange is a diffusion controlled process where the rate of diffusion depends on ionic mobility. Walker[19] pointed out that the increase in basal spacing accompanying the cation exchange of montmorillonite was related to the rate of cation exchange, and earlier showed that as the surface charge density on the clay increased the rate of exchange decreased.[20]

1.4.4 The Replaceability of Exchangable Cations

The following are some of the factors controlling the replaceability of exchangable cations

(i) The nature of the cation

(ii) The nature of the clay mineral

(iii) The ionic concentration of the exchanging cations.

(iv) The population of exchange positions.

(v) The nature of the anion in the exchange solution.

(vi) Heating the clay

In general, all cations do not have the same replaceability or replacing power within a clay lattice.[15] A divalent cation will replace a monovalent one except hydrogen which can behave like a di- or tri-valent ion. For cations having equal valence, those which are least hydrated have the better replacing ability and are very difficult to displace once exchanged [21] Schachtschabel[22] demonstrated the

existance of a cation replaceability series for individual clay minerals

The effect of increasing the concentration of the replacing cation was shown by Gedroiz [23] The replacement of Ca^{2+} and Mg^{2+} by NH_4^+ increased as the concerntration of NH_4^+ increased. Wicklander[24] showed that the ability of a cation to be released from its position within a lattice was affected by the nature of the replacing cations and on the degree to which the replaced ion saturated the exchange sites The replaceability of Na^+ by Ca^{2+} in a Na^+-montmorillonite was shown to depend on whether $Ca(OH)_2$ or $CaSO_4$ was used,[9] and the work by Hofmann and Endell[25] showed that when Na^+-montmorillonite is moderately heated its exchange capacity is reduced before its swelling property is lost.

1.5 CLAY-WATER SYSTEMS

Under ambient conditions, water is probably the most common polar compound present in the interlayer space of montmorillonite, the clay mineral used in this study Many physical properties of clay minerals such as plasticity, bonding, compaction and suspension depend largely on the water adsorbed by clay minerals. Water adsorption in montmorillonites may be placed into two categories.

(i) The water held in pores, on the surfaces and around the edges of the particles making up the clay mineral.

(ii) The interlayer water between the aluminosilicate layers

Surface water is easily removed by drying at temperatures just above room temperature, whereas interlayer water requires much more energy for its complete removal, and once removed rehydration of the mineral is difficult if not impossible unless water associated with the interlayer cations is still present [26] Walker et al.[27] demonstrated by X-ray diffraction the existance of two types of the interlayer water in vermiculites The first being an inner hydration shell around the exchangeable cation and the second forming an outer co-ordination sphere around the cation Mooney et al [28] showed that water was readily adsorbed into the interlayer space and that the adsorption was not only related to partial pressure but also to the size, valency, and polarizing power of the exchangeable cation.

When hydrated montmorillonite is heated to high temperatures it contracts in a series of steps to a basal spacing of 9.6Å. These series of steps are thought to be related to the basal spacings of stable hydrates of the interlayer cation until eventually no interlayer water remains.[29] However, cation exchanged montmorillonites contract on heating to a minimum basal spacing depending on the size and arrangement of the exchanged cations within the interlayer

Partially dehydrated exchanged montmorillonites are easily rehydrated as explained above so long as the

dehydration temperature does not exceed 500-600°C, the dehydroxylation temperature range for montmorillonite. The dehydroxylation does not depend on the nature of the exchange cation but instead is due to the collapse of the clay structure itself resulting in the complete removal of the lattice hydroxyl groups, usually complete by 800°C.[30]

1.6 INTERCALATION OF ORGANIC SPECIES

Hofmann et al.[31] demonstrated the variation of basal spacing when montmorillonite was exposed to alcohol, acetone and ether Clay mineral/organic interaction can be of two types

(i) Organic Cation Exchange and

(ii) Intercalation of Organic Molecules.

Organic cations are adsorbed by cation exchange replacing inorganic cations in the interlamellar space, whereas polar organic molecules can be adsorbed by eliminating water from the system,[32] quite often forming complexes with multiple layers of organic species.

Hendricks[33] suggested that organic cations are held by Van der Waal's forces and large organic ions are difficult or impossible to replace with smaller ions. He also showed that the organic ions were oriented between the montmorillonite layers in such a way as to minimise expansion. Brindley and Hofmann[34] suggested that the adsorbed polar organic molecules interact with the interlayer cation, showing once again the dependence of intercalation on the polarizing power of an exchanged

cation The introduction of infra-red spectroscopy has led to major advances in the understanding and interpretations of clay/organic interactions [35]

1 7 ZEOLITES: A STRUCTURAL COMPARISON

1 7 1 Basic Zeolite Structure

Zeolites are crystalline aluminosilicates composed of primary building blocks which are either silicon or aluminium ions surrounded by four larger oxygen anions [36] These tetrahedra combine, linking silicon and aluminium ions together through silicon bridges resulting in well ordered three-dimensional frameworks. There are thirty four known natural zeolites and about one hundred and twenty structures that are entirely synthetic

Like clay minerals, zeolites having common strucutral elements can be grouped together The sodalite unit (Fig. 1 6a) is the secondary building unit made up of a cubo-octahedral arrangement of twenty four silica or alumina tetrahedra The mineral sodalite is formed by linking eight sodalite units in such a way that the two four membered rings are shared by two cubo-octahedra. (Fig 1.6b) If the sodalite units are connected by bridging oxygen atoms between the four-membered rings, Zeolite A is formed. (Fig. 1.6c) However, linking the sodalite units by oxygen bridges between the hexagonal faces gives the structure known as faujasite. (Fig. 1 6d) This is also referred to as Zeolite X or Zeolite Y, depending on the silicon-aluminium ratio

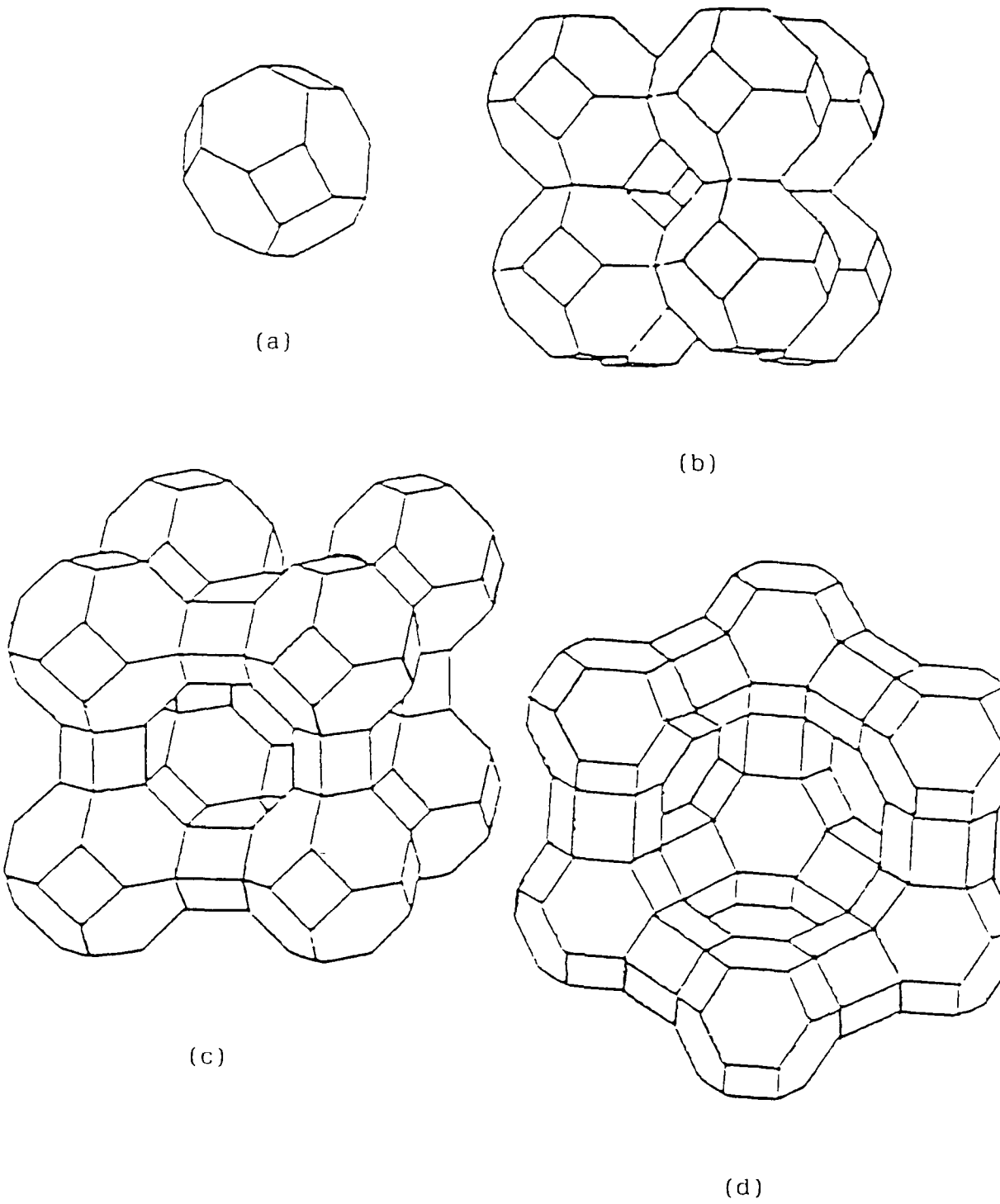

Fig 1 6 Schematic diagram depicting some common zeolite structures (a) sodalite unit, (b) sodalite, (c) zeolite A, (d) faujasite

Each of the three zeolite structures, sodalite, zeolite A and faujasite have a three-dimensional network of channels, or linked cavities These cavities can absorb molecules which are small enough and as such have access to the interal surface of the zeolite The free pore aperture of sodalite is 2.6Å, and as such can only adsorb very small molecules The pore size of zeolite A, is about 11.4Å. Faujasite has particularly large cavities, about 12Å in diameter. Entry to these cavities is by way of the twelve membered oxygen rings and as such are accessible to molecules with diameters less than 7 4Å.

Some zeolites have channel systems running in one direction only, for example mordenite or zeolite A, whereas others have two-dimensional nets of channels with dimensions different from those of the main network.

1.7.2 Cation-Exchange

As with clay minerals, zeolites have cation exchange capacities. In zeolites it is the aluminium-based tetrahedra which are negatively charged Charge imbalance is brought about by the substitution of aluminium for silicon, occuring in three dimensions in the interstices throughout the network. The overall behaviour, both physical and chemical, of zeolites is modified by the number, location and size of the intracrystalline cations which neutralize the overall negative charge on the framework. The open structures of zeolites allow ready migration of water molecules and

ZEOLITE	GROUP	IDEALIZED COMPOSITION	CATION EXCHANGE CAPACITY meq/100g
EDINGTONITE	NATROLITE	$Ba[Al_2Si_3O_{10}]\ 4H_2O$	390
LEVYNITE	CHABAZITE	$Ca[Al_2Si_4O_{12}]\ 6H_2O$	400
HARMOTOME	PHILLIPSITE	$(K_2Ba)[Al_2Si_5O_{14}]\ 5H_2O$	390
ZEOLITE X	FAUJASITE	$(CaHa_2)[Al_2Si_5O_{14}]\ 6H_2O$	390
STILBITE	HEULANDITE	$(Ha\|Ca)[Al\ Si_3O_8]\ 3H_2O$	320

TABLE 1.3 Classification and Cation Exchange Capacities of some zeolites.

cations involved in cation-exchange Since cations are exchangeable, modified sorbents can be made from a given framework topology by cation exchange

Because the negatively charged anions are rigidly held in the zeolite lattice, and the balancing cations are not, zeolites have found widespread use as cation exchange materials. Cation exchange of zeolites is used routinely in modifying the properties of zeolite products used in adsorption,[37] and catalysis, and a large body of literature on cation exchange selectivities,[38] structural characteristics, thermodynamics,[37] and ion-exchange separations[39] exists, Table 1 3.

1 7 3 Zeolite Synthesis

Synthetic zeolites are formed by crystallisation under hydrothermal conditions from solutions containing species such as sodium aluminate, sodium silicate and sodium hydroxide. The product obtained is determined by the synthesis conditions, temperature, time, pH and other variable parameters. The early era of the discovery of zeolites in the late 1940's and early 1950's led to about twenty novel synthetic zeolites [40] Barrer et al.[41,42] first reported the synthesis of zeolite N-A, a siliceous analog of zeolite A, by adding tetramethylammonium cations to sodium aluminosilicate gels, noting the effect of the alkylammonium ion on the increasing framework Si/Al composition. Techniques such as n.m.r. using ^{29}Si or ^{27}Al show promise in the elucidation of synthetic pathways.

CHAPTER 2

LITERATURE SURVEY

CHAPTER 2

2 1 INTRODUCTION

Generally speaking, a clay can be considered to be a natural, fine grained, earthy material which develops plasticity when it is mixed with a limited amount of water. Plasticity, in this sense describes the property of the moistened material to become deformed under pressure, and retaining this shape when the pressure is removed Chemical analysis of clays show them to be composed of silica, alumina, magnesia and water. Other materials including iron, alkalies, alkaline earths and organics are also frequently included in clay compositions.

Clays are composed of crystalline particles of less than 2 micrometers in size. The small particle size largely determines both the physical and chemical properties of the clay Along with their small particle size and intercalation properties, clays afford an appreciable surface area for the adsorption of organic molecules and catalysis. The catalytic role of clay minerals, specifically the smectite group, is related to the acidic nature of the interlayer and has been recognised in several "natural" processes,[1] including petroleum-forming reactions,[2,3] chemical transformations in soils,[4] and reactions related to chemical evolution.[5] In most cases, however, the clay appears to be acting purely as a solid source of protons.[6,7]

Cation exchanged montmorillonites have been

shown to be useful catalysts in the oxidation of acetaldehyde at room temperature,[8] the low temperature production of methyl-t-butyl ether (MTBE) from methanol and isobutene,[9] and the production of carbolactones from cyclo-octene-5-carboxylic acid.[9] It has also been shown that in some examples of catalysis by ion-exchanged montmorillonites there is shape selectivity,[10] similar to that exhibited in zeolites.[11] Identifying the most suitable cation exchanged clay - solvent - reaction temperature system ensures high reaction yields. Also the shape selective nature of the system reduces the number of side products formed.

The intercalation of polynuclear hydroxy metal cations and metal cluster cations in montmorillonites generates new Pillared clay materials [12] The pillaring phenomenon leads to the formation of porous networks analogous to zeolites

Within the last ten years research has been carried out to investigate the nature and structure of several intercalated inorganic species in a Wyoming montmorillonite, using numerous physico-chemical techniques such as infra-red spectroscopy, X-ray diffraction, thermogravimetric analysis and adsorption studies. From this, much information has been obtained concerning the interlamellar dynamics of these species, the identification of reaction sites, and some restrictions relating to possible catalytic reactions, including solvent effects.[13,14,15]

In this present work, the resonance absorption

technique of Mössbauer Spectroscopy is used in conjunction with X-ray diffraction, thermogravimetric analysis, and water vapour isotherm studies to characterise and investigate the stability of various organotin (IV)-exchanged montmorillonites as low temperature pillared layered clays (PILC's).

Since most of the reactions performed over montmorillonite clays utilise the acid properties of the clay itself, it is therefore prudent to include a discussion of the nature of the interlayer acidity associated with intercalated clay catalysts and zeolites. This is particularly useful as background to the thermogravimetric studies of the desorption of bases from the dimethyltin exchanged clays to be reported in Chapter 4.

2.2 CLAY ACIDITY

The acidic properties of cation exchanged montmorillonite catalysts are related to the nature, number and strength of acid sites existing throughout the solid clay matrix. The ability of an ion-exchanged montmorillonite to produce the hydrogen ions, H^+, and hydronium ions, H_3O^+ necessary for the protonation of organic molecules in the inter-layer region is one of its most important and striking features. This acidity is considered to be produced by the polarization of water in hydration shells of the interlayer cations. Mortland et al.[16] found that the interlayer water is dissociated to a greater degree than bulk water. It has also been shown that the hydrogen

ion concentration in the interlayer regions of Ca^{2+} and Mg^{2+} exchanged clays may be as high as 10 mol dm^{-3}.[17] The acid strength of hydrated cations can be described by the reaction

$$[M(H_2O)_x]^{n+} + H_2O \quad [MOH(H_2O)_{x-1}]^{(n-1)+} + H_3O^+$$

Within the clay interlayer, acidity can occur in two ways, the first being via proton transfer, denoted as Brønsted acidity, and the second via electron transfer denoted as Lewis acidity. As the water of hydration dissociates in the interlayer region of a clay it is considered that only Brønsted acidity occurs within these regions In the case of ion-exchanged montmorillonites, Lewis sites are considered to be associated with the Al^{3+} and Fe^{3+} cations exposed at the crystal edges[13] of the octahedral sheet The resultant acidity of these sites is due to the net negative charge at these sites Lewis sites are also considered to be involved in reactions where the clay is dehydrated, i e at temperatures greater than 100°C, and also when the clay is dehydrated under vacuum. This type of acidity persists even after destruction or collapse of the clay structure which may be caused by heating the solid at 900°C. The distinction between the two types of site also helps in determining reaction pathways over solid acid catalysts. The number and type of adsorption sites on a wide range of solid surfaces exhibiting catalytic properties has been studied using the technique of temperature programmed desorption

(TPD) Very recently Breen et al.[14] used the (TPD) technique to help clarify the number and type of acid sites in trivalent cation-exchanged montmorillonites which earlier had been shown to be efficient catalysts[18] for a number of novel and industrially significant reactions.[6]

The amount of acid in a solid acid catalyst can be measured by exposing the surface to a liquid and allowing equilibrium to be reached Thermogravimetric analysis (TGA) and differential thermal analysis (DTA) have been used to quantify the acid strength of solid acids.[19] These techniques involve exposing the solid sample to a base vapour followed by thermal treatment to determine both the amount of vapour adsorbed and the temperatures at which the physi- and chemisorbed species desorb.

As with ion-exchanged layered silicates, the inherent catalytic activity of zeolites is attributable to the presence of acidic sites throughout the solid matrix and may be Brønsted or Lewis in character. Lewis sites in zeolites are similar to those in the ion-exchanged layered silicates in that they are surface sites. In Zeolites, Lewis sites are generated by the replacement of Si^{4+} by Al^{3+} atoms in the alumino-silicate framework. Brønsted acidity is generated in the same way in both zeolites and cation exchanged montmorillonites, that is, by the exchange and subsequent hydrolysis of monovalent ions by polyvalent cations. Lewis sites in faujasites can also be generated by the

dehydration of Brønsted sites in the hydrogen or ammonium exchanged forms [20]

In zeolites, most acid catalysed reactions are related to Brønsted acidity The nature and quantitation of the acid sites can be determined by the infra-red spectra of pyridine, and to a lesser extent ammonia adsorbed on to the zeolite surface [21,22]

2 3 CLAY CATALYSIS

As the number and diversity of intercalated clay-catalysed reactions grows, it is apparent that there is little information readily available outlining the dynamic and steady state behaviour of these systems Adams et al [9] have derived a preliminary set of "rules" for acid catalysis by ion-exchanged montmorillonites from the reactions of alkenes, alcohols and alicyclic ethers over such catalysts The results of their studies are helpful in the design of new reactions in helping to decide whether a particular acid-catalysed reaction would succeed over a clay and also suggest procedures to optimise yields for particular reactions

The protons responsible for the acidic nature of the clay are produced by the polarization of the interlayer water. The degree of polarization produced in the interlamellar space of a cation exchanged montmorillonite is dependent on many factors,[23] including the nature, size and charge of the interlayer cation. Trivalent rather than divalent or monovalent exchanged montmorillonites would be expected to be more active in catalytic processes Adams et al [9] have confirmed

experimentally that Cr(III), Fe(III) and Al(III) are the most active interlayer cations used in catalytic processes involving alkenes, alcohols and alicyclic ethers They have also shown that temperature plays an important role in the formation of the carbocation intermediates produced in these reactions, and the necessity of ensuring solvent compatibility with the reactants used and products produced. Some of these reactions will be examined in detail in a later section.

2.3.1 Reaction Sites

When organic reactions take place over trivalent metal-exchanged montmorillonites there are two possible reaction sites involved. These are (i) within the interlayer region itself and (ii) surface sites. Remembering that the protons necessary for acid catalysis are produced in the interlayer region of the clay, as soon as they are produced they immediately set about protonating molecules present in the interlayer region

In the case of an organic molecule, the process can be described as

$$M(OH)_n^{m+} + R \rightleftharpoons [M(OH_2)_{n-1}OH]^{(m-1)} + [RH]^+$$

The probability of the forward reaction occurring depends on the interlayer concentration of organic molecules, and also on the basicity of the organic species relative to water. When more than one organic species is present the situation becomes much more complicated.

In their study of the reactions of alcohols with alkenes over an aluminium-exchanged montmorillonite, Adams et al [24] suggested that carbocations reacted with hydrocarbons in the interlayer region producing dimers. This is consistent with the view that high electric field gradients cause polarization and activation of alkene double bonds. They also suggested that carbocations can react with oxygenated (polar) species such as alcohols and water at surface sites, but not with unsaturated hydrocarbons. This showed that the active sites in the metal-exchanged montmorillonite are not confined exclusively to the interlayer region.

2 3.2 Solvent Effects

Saturated hydrocarbon solvents have been used in liquid phase cation exchanged clay reactions to avoid the possibility of co-ordination of the solvents to the interlayer cations.[25,26] It was considered that such co-ordination could result in the reduced polarization of the interlayer water and poisoning of the catalysts. However, when a cyclic-ether type solvent, in this case, 1 4-dioxan was used in the production of methyl-t-butyl ether (MTBE)[26] from methanol and isobutene over montmorillonite catalysts (Fig. 2.1), comparable yields of MTBE were produced at temperatures $\sim$ 30°C lower than when hydrocarbon solvents were used. This reduction in temperature from 90°C to 60°C had the added effect of reducing the production of unwanted dimers of isobutene. As all the reactants and products of this reaction were miscible in the solvent 1,4-dioxan, the

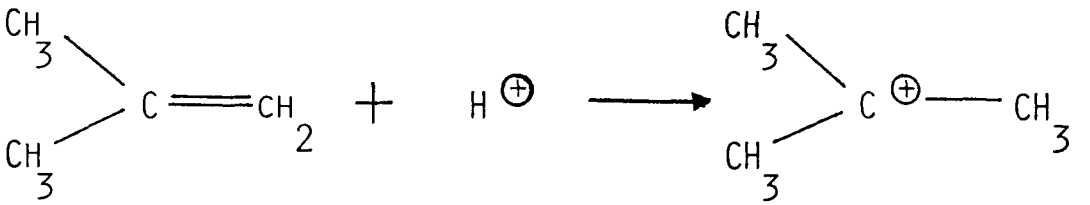

isobutene

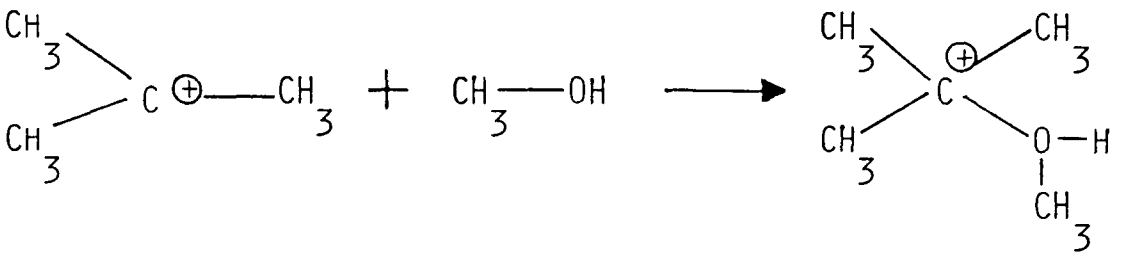

methanol

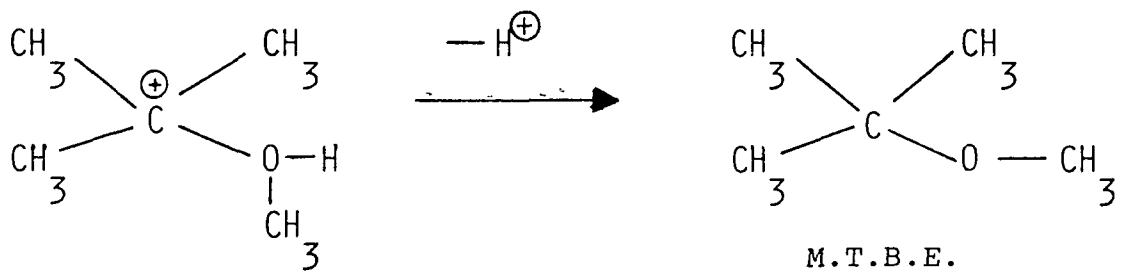

M.T.B.E.

Fig. 2.1 Schematic diagram showing the production of MTBE from isobutene and methanol over an exchanged montmorillonite catalyst.

reaction was able to proceed more rapidly with the lower temperature. The displacement of some interlayer water by the dioxan might also have increased the interlayer acidity.

When tetrahydrofuran (THF) b.p. 65°C, and tetrahydropyran (THP) b.p. 88°C, were used as solvents, over Fe(III) and Cr(III) exchanged montmorillonites, about 35% yields of MTBE were obtained at 60°C in 4 hours Reaction over an Al(III) exchanged montmorillonite produced only a 4% yield using these solvents. However, when 1,4-dioxan was used with the Al(III) catalyst a significant yield of 61% MTBE was obtained The yields from these reactions as seen in Table 2 1 demonstrate the important specific cation-solvent effects involved

Nevertheless, in simple acid-catalysed processes at temperatures below 100°C, it appears most advantageous to use a solvent which promotes miscibility even where only a weak acid is required to protonate the organic species.

CLAY	SOLVENT	% YIELD
Al(III)-mont	1,4-Dioxan	61
	THP	4
	THF	0
Cr(III)-mont	1,4-Dioxan	63
	THP	42
	THF	28
Fe(III)-mont	1,4-Dioxan	65
	THP	35
	THF	32

Experimental Conditions 1g clay, 1cm^{3}MeOH, 3cm^3 solvent, 25mmol isobutene at 60°C for 4 hours.

TABLE 2.1

Cation-Solvent pairing relationship to reaction yield.

2.3 3 Restrictions on Possible Reactions

The acid-catalysed reactions of alcohols with alkenes over ion-exchanged montmorillonites at temperatures below 100°C were studied by Adams et al.[25] Of the eight reactions studied, Table 2.2, only two proceeded to form products. They concluded that, for reaction to occur at these temperatures it was necessary that a tertiary carbocation be formed from one of the reactants directly on protonation for reaction to occur This conclusion was confirmed by a literature survey[10] of other low temperature acid-catalysed reactions over ion-exchanged montmorillonites

There was an exception though. In the formation of di-2,2'-alkyl ethers from the addition of water to alkenes over ion-exchanged montmorillonites However, it was shown that the water used in the reaction came from the clay layer itself and as such could not be replenished, therefore the reaction could not be claimed to be catalytic.[27] When these reactions are carried out at temperatures greater than 100°C primary and secondary carbocations are shown to be involved. These carbocations are believed to be derived directly from alkene protonation, or by protonation of the alcohol followed by dehydration

For reactions below 100°C, reactivity is explained by (i) a sufficiently acidic interlayer environment to protonate the tertiary but not the primary or secondary carbocations, and (ii) the greater stability of the tertiary over the primary and secondary

ALKENE	t-ethers	t-alcohols	BuOH
2-methylpent-1-ene	1.74	0 45	4.51
2-methylkept-1-ene	1.40	0 32	4.85

The following alkenes did not react·

4-methylpent-1-ene, cis 4-methylpent-2-ene, trans 4-methylpent-2-ene, 3,3-dimethyl but-1-ene, hex-1-ene, hex-2-ene

TABLE 2.2

Summary of results for the reaction of various alkenes with butan-1-ol over 0 5g Aluminium exchanged montmorillonite at 95°C Both alkene and butan-1-ol concentrations are 6 25mmol respectively.

species For reactions above 100°C a high proton concentration is derived from the polarization of water molecules co-ordinated to the exchanged cation after all non-coordinated water is lost This high proton concentration is required for processess involving primary and secondary carbocations

2.3.4 Catalysis by Zeolites

The main catalytic characteristics of acid zeolites in hydrocarbon reactions are their selectivity as molecular sieves, high acid strength, and electrolytic properties influencing reaction kinetics These characteristics are very similar to those of the ion-exchanged layered silicates Many reactions involving carbonium ions are catalysed by acidic zeolites,[28] and the reaction mechanisms are not fundamentally different from those seen in ion-exchanged layered silicates. Some of the more important properties of zeolite catalysts over ion-exchanged catalysts are

(i) A high density of catalytic sites due to their high specific surface area afforded through cage effects, and arising from the highly ionizing power of zeolites.[29]

(ii) Well defined sites of catalytic activity due to the regular crystalline structure, along with well identified locations of balancing cations.[30]

(iii) Molecular sieving properties due to the spaces within the crystallites having dimensions close to those of the reactant or product molecules.

(iv) Controllable electrostatic fields[31] brought about when multivalent cations replace monovalent ones and position themselves where each one is best able to relate to three separate AlO_4^{5-} tetrahedra

(v) Sites for occluded and grafted species being generated when small particles of metal are deposited within a zeolite and resultant material displaying the properties associated with a supported metal catalyst, but only for molecules small enough to pass through the zeolite sieve

In 1978, Coughlan et al [32] reported that cation exchanged alkyltin (IV) zeolites Y, and L, prepared from methanol were catalytically more active in the dehydration of n-pentanol than the unexchanged parent forms A similar catalytic activity for dimethyltin (IV) aqueous exchanged zeolite Y systems prepared at pH 1.8 and 3 3 was also reported, both activities being higher than the dimethyltin (IV) methanol exchanged zeolite Y system. Furthermore, they found the dibutyltin (IV) exchanged zeolite Y system to be catalytically more active than either of the dimethyltin (IV) exchanged forms even though the former system was least exchanged. In each case they related the catalytically active centres in the exchanged zeolites to the hydrolysis of the alkyltin (IV) cations[33] introduced either during exchange or subsequently within the zeolite cavities providing the greater number of

acid centres. In this study Coughlan et al. concluded that the dehydration of n-pentanol was a useful probe reaction for determining the activity of catalysts of low to medium acidity.

The future trends in materials will, no doubt, see the development of new commercial zeolites and ion-exchanged layered silicates. Due to the cost incentives of the bulk chemical and consumer markets, the chemical modification of the present ion-exchanged layered silicate and zeolite commercial products will continue for years to come.

2.4 PILLARED LAYERED CLAYS

Within the last ten years new classes of selective heterogenous catalysts have been developed through the intercalation of metal complex cations in clay materials.[34] These new structures are generated by first intercalating the clay mineral with polynuclear metallic cations and then thermally transforming the exchanged intercalated species to pillars of various metal oxides which are cross-linked to the silicate layers.[35] The resulting thermally pretreated intercalated clays are commonly referred to as "Pillared Layered Clays", abbreviated PILC's.

The concept of pillaring smectite clays was demonstrated more than thirty years ago by Barrer and McLeod[36] using tetraalkyl-ammonium ions to induce interlayer porosity in montmorillonite. However, organic pillaring agents were found to decompose below 250°C,[36] while metal chelate complexes degraded below

500°C.[37] Although the chemistry of alkylammonium clays was further developed,[38] the idea of pillaring clays to achieve porous networks was overshadowed by the rapid advances being made in the synthesis and application of synthetic zeolites. Within the same time frame, more than one hundred species of zeolites have been synthesized, though only a few have found any significant industrial application[39] as a result of the limited range of pore sizes, (2 to 8Å). There is now a renewed interest in pillared clays due to the realization that their pore sizes can be made larger than those of faujastic zeolites Moreover, by varying the size of the intercalated pillar or the spacing between pillars, or both, the pore size may be altered to suit a particular application. Furthermore, on calcination, the conversion of the intercalated hydrated cations to immobile or fixed oxide pillars leads to the generation of permanent microporosity in the interlayers. Thus, the structure of pillared layered clays, (PILC's), consists of a labyrinth of pores with sizes in the 1-10nm range having a total surface area between 200 and 500m^2/g, while a pronounced Bronsted and Lewis acidity prevails in the interlayer space.[40] Also, for each class of pillared clay, the pore size and it's distribution along with the thermal stability of the clay have been found to depend on the method of preparation.[41,42]

The potential use of pillared clays as catalysts and molecular sieves has been extensively studied. In

1980, Vaughan and Lussier[42] demonstrated that the interlayering of montmorillonite with hydroxy-aluminium oligomers generated materials which could be used in conventional petrochemical processes, such as catalytic cracking and hydrocracking. As a result of their sorptive properties their interlayered montmorillonites, (Wyoming bentonite intercalated with chlorhydrol, and calcined to 550°C), appeared to behave like two-dimensional molecular sieves, sorbing 1,3,5-trimethyl benzene having a kinetic diameter of 7.6Å but not perfluorobutylamine, 10.4Å. The catalytic properties of this PILC was investigated in 1983 by Occelli and Tindwa,[43] who showed that the aluminium chlorohydroxide exchanged bentonite retained it's high conversion ability and catalytic activity up to 540°C, comparable to that of a clay-based commercial cracking catalyst containing about 15% faujasite.

Although polynuclear hydroxy metal ions formed by hydrolysis in aqueous solution can yield pillared clays with interlayer free spacings between 5 and 20Å, the number of metals that form suitable oligomeric species is limited. Endo et al.,[44,45] produced a silicic acid-clay complex having an interlayer free spacing of $\sim$3Å and a nitrogen surface area of $\sim 200 m^2/g$ after heating to 550°C, by the hydrolysis of silicon acetylacetonate cations in the interlayer region. In 1978, Van Damme et al.,[46] reported the adsorption of mesosubstituted porphyrins and their reactivity in the interlamellar space of smectites in terms of their

ability to react with exchangeable cations, and also on the stability of Fe^{3+}, and Sn^{4+} metallo porphyrins on the clay surface. They found that upon adsorption, weak complexes of Fe(III) mesotetraphenyl porphyrin were irreversibly demetallated and protonated, whereas the strongly acid-resistant Sn(IV) species could be adsorbed with only partial demetallation in the hydrated clay. An X-ray photoelectron study of the Sn(IV) mesotetra pyridylporphyrin complex showed that this species demetallated completely when the clay was completely dehydrated and attributed this to the increased interlayer acidity on dehydration In a later study of these systems Abdo et al ,[47] demonstrated that upon demetallation, the Sn(IV) cations remain in the vicinity of the porphyrin dication and were able to re-enter the porphyrin rings as the water content of the clay increased and the interlayer H^+ concentration decreased

A study of tin exchanged smectites for utilisation as catalysts or selective sorbents can be considered in terms of both the extensive chemistry of tin and it's rationalisable organometallic chemistry. This provides a number of opportunities to tailor the molecular architecture of the type of cation which can be used to fabricate materials with high interlayer surface areas and large pore volumes similar to the layer silicates exchanged with bulky, highly charged cations as discussed above, Fig. 2.2. In one such study, Molloy et al.,[48] prepared an N-methyl-(3-triphenylstannyl) pyridium-exchanged montmorillonite

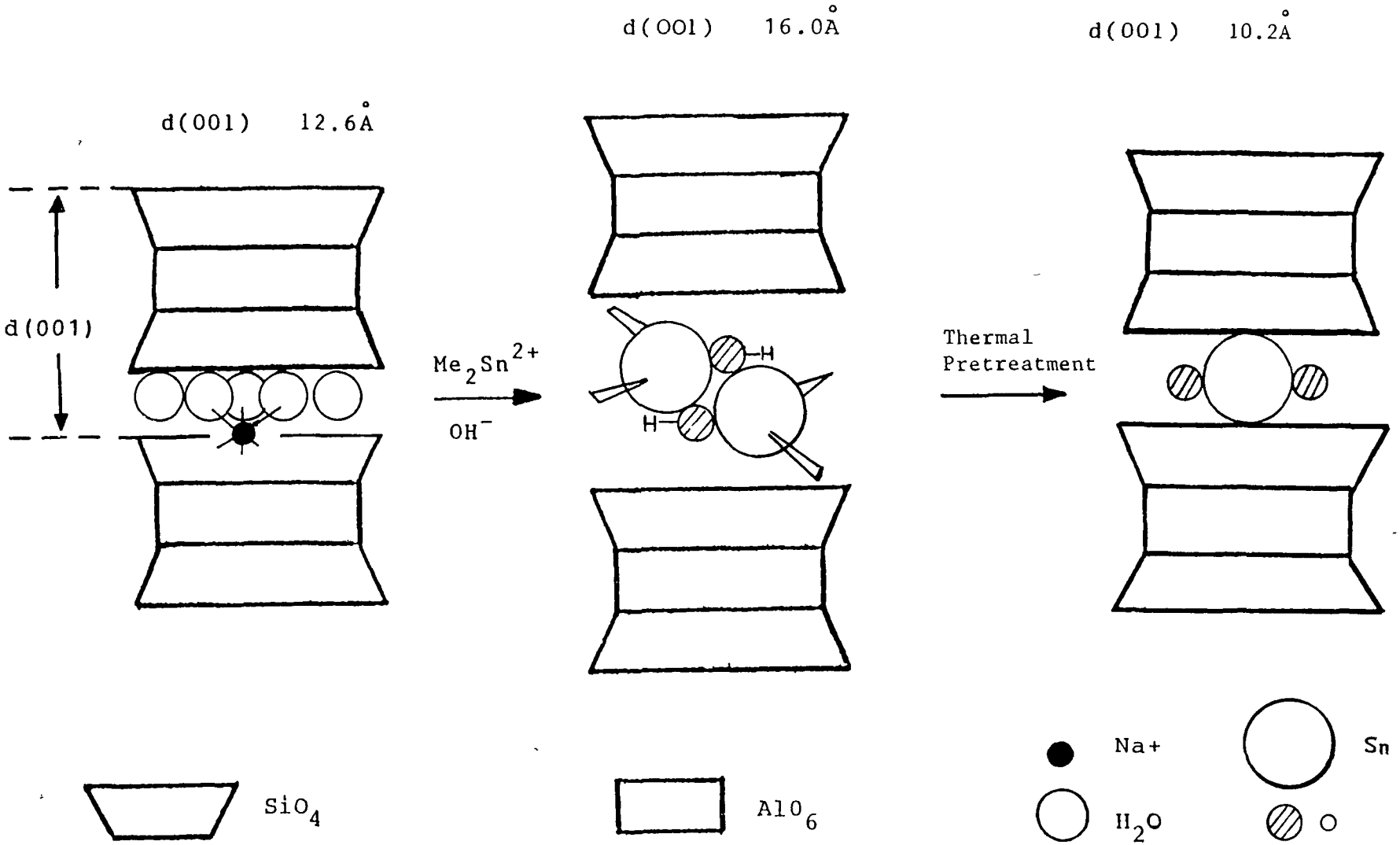

Fig. 2.2 Schematic representation of the exchange of sodium montmorillonite with the alkyltin (IV) cation prepared at pH 4.0, and the pillaring effect produced after thermal pretreatment

which demonstrated the possibility of generating high-spacing phyllosilicate materials using organo-metallic cation pillars. Intercalation of this organotin (IV) cation was confirmed using X-ray diffraction by an increase in basal spacing from 12.6Å for the monolayer hydrate of the unexchanged montmorillonite, to 19.1Å. Subsequent dehydration at room temperature under vacuum reduced the basal spacing to 17 7Å, corresponding to a gallery height of 8.1Å In the same study, Mössbauer spectroscopy was used as a post-exchange probe of the organotin (IV) environment within the interlayer, and demonstrated that the hyperfine parameters, of isomer shift and quadrupole splitting observed for the exchanged cation were very similar to those prior to intercalation This was good evidence that a unique tin environment was present in the clay, and showed that the structural integrety of the organotin (IV) cation was maintained during the exchange process. In addition, they concluded that although only ~40% of the possible exchange sites were occupied by pillar cations, further exchange with catalytically active Al^{3+}, Cr^{3+} and Fe^{3+}, cations was possible. As such, catalytically active phyllosilicate materials incorporating dissimilar catalytic agents could be produced in which additional organometallic pillars could be used to engineer the spatial accessibility of the catalyst and hence maximize its size, shape and stereochemical selectivity. Moreover, as a result of the inherent problem of the relatively small pore size of zeolite catalysts, the use

of stable, high spacing pillared clays, whose gallery height can be modified in a controlled way, is of particular importance in the preparation and utilisation of various cation-exchanged clays as acid catalysts in a range of novel and industrially significant processes

2.5 SORPTION BY CLAY MINERALS AND ZEOLITES

When a clay mineral such as montmorillonite is dispersed in aqueous solution, water molecules along with any other ionic species present can be removed from the bulk solution This phenomenon is a result of the attractive field of a solid surface on molecules or charged substances close to the solid liquid interface, and may take the form of sorption at the surface (adsorption) or occlusion by the solid, (absorption). Sorption of gases on solid surfaces is also possible. In general, two kinds of adsorption behaviour can be distinguished. Physisorption due to the operation of forces between the solid surface and the adsorbate molecules, and similar to the Van der Waals forces between molecules, is generally reversible.
For chemisorption to occur, stronger bonding forces comparable to those leading to the formation of chemical compounds are required Chemisorption is seldom reversible at low temperatures, and sometimes as in the case of adsorption of oxygen on charcoal at 150K, desorption of another species, in this case carbon monoxide occurs instead of oxygen

Differentiating between physisorption and chemisorption is often useful and necessary when

discussing the interaction of gases with metals. However, no clear difference is observed in the case of clay minerals and zeolites In this case differentiation between mobile and immobile sorption on to localized and non-localized sorption sites is much more advantageous.[15]

2.5.1 Vapour Phase Adsorption on to Ion Exchanged Montmorillonites.

The interaction of adsorbed molecules with montmorillonite clays has been studied over the years by many investigators, and special interest has been focussed on the swelling properties of the systems.

The influence of adsorbed water on acetone uptake by montmorillonite was demonstrated as early as 1943 by Glaeser [49] In this case it was found that one-layer complexes having a basal spacing of 13 2Å were found when Na^{+}- and Ca^{2+}- montmorillonites, previously dried by evacuation at 225°C, were exposed to acetone vapour. However, two-layer complexes having a basal spacing of 17.5Å were generated when the clays were exposed to saturated acetone and water vapour (50% relative humidity). Glaeser concluded that the acetone uptake was facilitated by the hydrated clay initially expanding the clay interlayers.

The interaction of organic vapours with montmorillonite containing different interlayer cations was examined by Parfitt and Mortland.[50] They concluded that adsorption of the organic species acetone and acetylacetone was facilitated by co-ordination to the

exchanged cations of low hydration energy. In addition, the formation of metal acetylacetonates is indicated for acetylacetone adsorbed by aluminium and copper montmorillonites brought about by electrovalent bonding through proton donation to the clay.

Barrer and MacLeod[36,51] followed the adsorption of polar and non-polar vapours on a sodium-exchanged montmorillonite. By comparing adsorption isotherms, they showed that non-polar vapours were physically adsorbed only on the external surfaces of the clay through weak Van der Waals forces whereas polar vapours were readily intercalated.

Sorption/desorption and surface-area data form the basis of thermodynamic investigations of the free energy for the reaction between clay minerals and water or other liquids Although many methods have been tried to determine the surface-area of clay minerals, the most trustworthy results are obtained using the method developed by Brunauer, Emmet and Teller,[36] (B.E.T.). This method is based on the adsorption of simple molecules such as nitrogen at temperatures in the neighbourhood of their boiling points.

In 1955, Dyal and Hendricks,[52] described a technique for determining both the external crystal and interlayer area of montmorillonite minerals based on the amount of ethylene glycol retained under conditions in which a monolayer of the organic molecules was presumed to be present on all planar surfaces.

In 1972, Van Assche et al.[53] used homologous

series of alcohols and amines to investigate vapour phase adsorption, in which the interlamellar swelling was followed by X-ray diffraction. Thermodynamic data including the heats of adsorption for methanol and butylamine along with the energy of interlayer expansion, and the heat of monolayer formation were derived. In 1979, Annabi-Bergaya et al ,[54,55,56] reported several studies regarding the desorption of alcohols by a series of charge deficient calcium-montmorillonites using gravimetry and X.R.D. They found that about half of the adsorbed alcohol molecules were occluded in micropores between the clay particles They also suggested that the apparent molecular packing of the alcohol in the interlamellar space is related specifically to the nature of the exchange cation In 1987, Deane,[15] calculated diffusion coefficients and activation energies for the vapour phase adsorption of alcohols and ethers onto Al^{3+}-, Fe^{3+}- and Cr^{3+}- exchanged montmorillonite. It was shown that the activation energies were dependent on the exchange cation and increased as $Fe^{3+} < Al^{3+} < Cr^{3+}$, and concluded that this sequence was caused by the displacement of some water molecules from the co-ordination shell of the cation. The derived diffusion rates for the three cyclic ethers were larger than those of the alcohols used, and also, that the 1,4-dioxan diffused at a slower rate than both THP and THF. This suggested that there was an enhanced interaction between the solvent and the exchanged cation

resulting in the clay layers being propped apart more efficiently, resulting in catalysis occuring when 1,4-dioxan was used in conjunction with these trivalent ion exchanged clays.

2.5.2 Liquid Phase Adsorption.

At room temperature and humidity, water is perhaps the most common polar compound present in the interlayer space of montmorillonite Water also plays an important part in the binding and transformation of polar organic compounds at the montmorillonite surface [57] The adsorption of species from solution not only depends on the nature of the species itself but also on the size, shape and charge of the interlayer cation, and by the presence of pre-adsorbed molecules such as water. Uncharged non-polar organic molecules, like water, are either directly co-ordinated to the cation, or indirectly linked to the cation through bridging with water molecules.[58] Polar organic compounds, on the other hand compete with water for the same ligand positions around the interlayer cation,[23] and as such the adsorption process is largely dependent on the polarizing power of the cation.

In 1971, German and Harding,[59] showed that the adsorption of alcohols on to Na^{+}- and Ca^{2+}- exchanged montmorillonites was much more favourable for the Ca^{2+}-exchanged clay and suggested that this enhanced adsorption was related to the solution energy of the calcium cation.

In the case of liquid adsorption, the type of

resulting in the clay layers being propped apart more efficiently, resulting in catalysis occuring when 1,4-dioxan was used in conjunction with these trivalent ion exchanged clays.

2.5.2 Liquid Phase Adsorption

At room temperature and humidity, water is perhaps the most common polar compound present in the interlayer space of montmorillonite Water also plays an important part in the binding and transformation of polar organic compounds at the montmorillonite surface [57] The adsorption of species from solution not only depends on the nature of the species itself but also on the size, shape and charge of the interlayer cation, and by the presence of pre-adsorbed molecules such as water. Uncharged non-polar organic molecules, like water, are either directly co-ordinated to the cation, or indirectly linked to the cation through bridging with water molecules.[58] Polar organic compounds, on the other hand compete with water for the same ligand positions around the interlayer cation,[23] and as such the adsorption process is largely dependent on the polarizing power of the cation.

In 1971, German and Harding,[59] showed that the adsorption of alcohols on to Na^{+}- and Ca^{2+}- exchanged montmorillonites was much more favourable for the Ca^{2+}-exchanged clay and suggested that this enhanced adsorption was related to the solution energy of the calcium cation.

In the case of liquid adsorption, the type of

isotherm obtained seems to be related to the solvent system used. The amount of species adsorbed along with the isotherm maximum and minimum are all influenced by the exchangeable cation and the presence of pre-adsorbed molecules.[60]

In 1987, Deane[15] reported the adsorption of methanol from the cyclic ethers 1,4-Dioxan, THP and THF onto Al^{3+}- and Cr^{3+}-exchanged montmorillonites. It was shown that the isotherm type according to the Schay-Nagy classification, is greatly affected by the binary system involved Exposing the dehydrated clay to water before exposure to the mixtures resulted in a 50% increase in the uptake of THF X-ray diffraction data reveals the exclusive presence of methanol in some interlayers, suggesting the adsorption of THF and methanol into separate layers

2.5 3 Sorption by Zeolites

Zeolites provide stable, high capacity, microporous sorbents with diverse moleculer sieving properties [61] As a direct consequence of their open, porous structures, zeolites have large internal surface areas resulting in high sorption capacities for molecules which are small enough to pass through the entrance ports. The adsorption properties of zeolites can be modified in one or more of the following ways.

(i) Changing the Si to Al ratio[62] will alter the unit cell dimensions in zeolites. For example, in the case of faujasite there is a linear dependence on the size of the cubic unit cell as

isotherm obtained seems to be related to the solvent system used The amount of species adsorbed along with the isotherm maximum and minimum are all influenced by the exchangeable cation and the presence of pre-adsorbed molecules.[60]

In 1987, Deane[15] reported the adsorption of methanol from the cyclic ethers 1,4-Dioxan, THP and THF onto Al^{3+}- and Cr^{3+}-exchanged montmorillonites It was shown that the isotherm type according to the Schay-Nagy classification, is greatly affected by the binary system involved Exposing the dehydrated clay to water before exposure to the mixtures resulted in a 50% increase in the uptake of THF. X-ray diffraction data reveals the exclusive presence of methanol in some interlayers, suggesting the adsorption of THF and methanol into separate layers

2 5 3 Sorption by Zeolites

Zeolites provide stable, high capacity, microporous sorbents with diverse moleculer sieving properties.[61] As a direct consequence of their open, porous structures, zeolites have large internal surface areas resulting in high sorption capacities for molecules which are small enough to pass through the entrance ports The adsorption properties of zeolites can be modified in one or more of the following ways·

(i) Changing the Si to Al ratio[62] will alter the unit cell dimensions in zeolites. For example, in the case of faujasite there is a linear dependence on the size of the cubic unit cell as

the Si-Al ratio changes from 3.0 to 1 18

(ii) The incorporation of appropriate cations into zeolites by ion-exchange can influence the size of the voids and hence the surface area available for adsorption

(iii) Increasing the temperature at which adsorption occurs enables larger molecules to enter cavities

Under appropriate conditions zeolites can adsorb non-polar and polar molecules Isotherms of non-polar sorbed molecules are as a rule of type I in Brunauer's classification [63]

In general, the amount of substance adsorbed by a given weight of zeolite depends only on the vapour pressure of the sorbent and the sorption temperature. However, the ease of penetration of the outgassed zeolite by guest molecules depends on

(i) The size and shape of the windows controlling entry to the channels and cavities in the zeolite.

(ii) The size and shape of the sorbed molecules.

(iii) The number, size and location of the exchangeable cations.

(iv) The presence or absence of defects such as stacking faults which may narrow the diffusion pathways at planes where such faults occur.

(v) The presence or absence of other strongly held guest molecules such as water, ammonia and salts.

The ability to modify slightly both the channel size and the nature of the exposed zeolite surfaces is of great importance when zeolites are used as catalysts

the Si-Al ratio changes from 3 0 to 1.18

(ii) The incorporation of appropriate cations into zeolites by ion-exchange can influence the size of the voids and hence the surface area available for adsorption

(iii) Increasing the temperature at which adsorption occurs enables larger molecules to enter cavities

Under appropriate conditions zeolites can adsorb non-polar and polar molecules Isotherms of non-polar sorbed molecules are as a rule of type I in Brunauer's classification [63]

In general, the amount of substance adsorbed by a given weight of zeolite depends only on the vapour pressure of the sorbent and the sorption temperature However, the ease of penetration of the outgassed zeolite by guest molecules depends on

(i) The size and shape of the windows controlling entry to the channels and cavities in the zeolite.

(ii) The size and shape of the sorbed molecules.

(iii) The number, size and location of the exchangeable cations.

(iv) The presence or absence of defects such as stacking faults which may narrow the diffusion pathways at planes where such faults occur.

(v) The presence or absence of other strongly held guest molecules such as water, ammonia and salts.

The ability to modify slightly both the channel size and the nature of the exposed zeolite surfaces is of great importance when zeolites are used as catalysts

or catalyst supports.

2 6 ANALYTICAL TECHNIQUES USED IN CLAY-MINERAL STUDIES

Over the years numerous investigators have used many techniques in characterising the physico-chemical properties of the ion-exchanged layered silicates No one technique on its own is sufficient to investigate the changes taking place in and around the interlayer. This has resulted in a combination of differing instrumental methods being used, and data from each method combined in identifying and characterising the many events taking place within the clay mineral structure

X-ray diffraction is probably the most valuable method used to study the structure of the complexes formed between expanding layered silicates and their intercalated species.[64] However, its usefulness in investigating the changes taking place in the structure of the adsorbed species is quite limited.

Thermal methods of analysis can give a considerable amount of information on the hydration state of a clay and its intercalated cations

The application of Mössbauer spectroscopy to clay minerals with sheet and chain silicate structures allows the oxidation states, site occupancy and molecular symmetry of exchanged cations in these complex materials[65] to be investigated.

Infra-red spectroscopy can be used to determine the mode of bonding in the adsorbed or intercalated organic molecules,[66] while atomic-absorption

or catalyst supports

2 6 ANALYTICAL TECHNIQUES USED IN CLAY-MINERAL STUDIES

Over the years numerous investigators have used many techniques in characterising the physico-chemical properties of the ion-exchanged layered silicates. No one technique on its own is sufficient to investigate the changes taking place in and around the interlayer This has resulted in a combination of differing instrumental methods being used, and data from each method combined in identifying and characterising the many events taking place within the clay mineral structure

X-ray diffraction is probably the most valuable method used to study the structure of the complexes formed between expanding layered silicates and their intercalated species [64] However, its usefulness in investigating the changes taking place in the structure of the adsorbed species is quite limited.

Thermal methods of analysis can give a considerable amount of information on the hydration state of a clay and its intercalated cations

The application of Mössbauer spectroscopy to clay minerals with sheet and chain silicate structures allows the oxidation states, site occupancy and molecular symmetry of exchanged cations in these complex materials[65] to be investigated.

Infra-red spectroscopy can be used to determine the mode of bonding in the adsorbed or intercalated organic molecules,[66] while atomic-absorption

spectrophotommetry can be used to accurately determine both the elemental content and the cation-exchange capacity of layered silicates

The major techniques used throughout this work were Mössbauer Spectroscopy, Thermogravimetric Analysis, X-ray diffraction, and Water Vapour Isotherms. A brief disscussion of their applications in clay mineral studies will be outlined in the following sections

2.6 1 Mössbauer Spectroscopy

The non-destructive technique of Mössbauer Spectroscopy was the major method used throughout this work, and as such a brief discussion of its application in clay mineral studies will be included at this point

The direct application of the Mössbauer effect to chemistry, of which clay mineral studies are included, is due to it's ability to detect the slight variations in nuclear energy levels brought about by interactions between the absorbing nucleus and the extra-nuclear electrons For many years these interactions were considered to be negligible.

The Mössbauer technique is only applicable to a few atoms of which Sn and Fe are the most common.

The application of the technique to silicate mineralogy has been well described by Bancroft et al.[67] They were able to correlate the influence of electronic configuration, oxidation state, and co-ordination symmetry of iron cations in silicates of known structure[67] to those in silicates of unknown and complex structures [68] In 1969, adsorption studies of Fe^{3+} on

spectrophotommetry can be used to accurately determine both the elemental content and the cation-exchange capacity of layered silicates

The major techniques used throughout this work were Mössbauer Spectroscopy, Thermogravimetric Analysis, X-ray diffraction, and Water Vapour Isotherms. A brief disscussion of their applications in clay mineral studies will be outlined in the following sections

2 6.1 Mössbauer Spectroscopy

The non-destructive technique of Mössbauer Spectroscopy was the major method used throughout this work, and as such a brief discussion of its application in clay mineral studies will be included at this point

The direct application of the Mössbauer effect to chemistry, of which clay mineral studies are included, is due to it's ability to detect the slight variations in nuclear energy levels brought about by interactions between the absorbing nucleus and the extra-nuclear electrons. For many years these interactions were considered to be negligible.

The Mössbauer technique is only applicable to a few atoms of which Sn and Fe are the most common.

The application of the technique to silicate mineralogy has been well described by Bancroft et al.[67] They were able to correlate the influence of electronic configuration, oxidation state, and co-ordination symmetry of iron cations in silicates of known structure[67] to those in silicates of unknown and complex structures [68] In 1969, adsorption studies of Fe^{3+} on

illite and montmorillonite were carried out by Malathi et al.[69]

Although the literature abounds with ^{57}Fe-clay mineral Mössbauer studies,[70] very little work has been presented for ^{119}Sn located in similar environments.

In 1983, Ruiying[71] developed a computer program for fitting ^{119}Sn - Mössbauer spectra and used his program to compute the component spectral lines in Pt-^{119}Sn/Al_2O_3 reforming catalyst

In 1987, Molloy et al ,[48] used ^{119}Sn-Mössbauer spectroscopy to characterise the structure and interlayer environment of an N-methyl-(3-triphenylstannyl) pyridinium exchanged montmorillonite, and found that the isomer shift and quadrupole splitting parameters were in close agreement with those observed for the organotin (IV) complex salt before intercalation.

Very recently Simopoulous et al.[72] used ^{119}Sn-Mössbauer Spectroscopy to investigate the structure of cationic dimethyltin (IV) complexes exchanged into a Wyoming montmorillonite, and their interactions with the clay lattice. In this study, although the Mössbauer spectra recorded at both liquid nitrogen temperature, (78K), and room temperature could be fitted to two broad doublets, revealing the presence of more than one Sn environment, a pronounced asymmetry was exhibited by the spectrum recorded at room temperature. Comparison of spectral data recorded between 80 and 300K explained this asymmetry in terms of the melting of water in the

illite and montmorillonite were carried out by Malathi et al.[69]

Although the literature abounds with ^{57}Fe-clay mineral Mössbauer studies,[70] very little work has been presented for ^{119}Sn located in similar environments

In 1983, Ruiying[71] developed a computer program for fitting ^{119}Sn - Mössbauer spectra and used his program to compute the component spectral lines in Pt-$^{119}Sn/Al_2O_3$ reforming catalyst.

In 1987, Molloy et al.,[48] used ^{119}Sn-Mössbauer spectroscopy to characterise the structure and interlayer environment of an N-methyl-(3-triphenylstannyl) pyridinium exchanged montmorillonite, and found that the isomer shift and quadrupole splitting parameters were in close agreement with those observed for the organotin (IV) complex salt before intercalation.

Very recently Simopoulous et al.[72] used ^{119}Sn-Mössbauer Spectroscopy to investigate the structure of cationic dimethyltin (IV) complexes exchanged into a Wyoming montmorillonite, and their interactions with the clay lattice. In this study, although the Mössbauer spectra recorded at both liquid nitrogen temperature, (78K), and room temperature could be fitted to two broad doublets, revealing the presence of more than one Sn environment, a pronounced asymmetry was exhibited by the spectrum recorded at room temperature. Comparison of spectral data recorded between 80 and 300K explained this asymmetry in terms of the melting of water in the

interlayer region of the clay at about 220K. This was verified in a similar set of variable temperature experiments using an exchanged clay dried at 70°C for three hours under vacuum

In 1989, Petridis et al.,[73] used ^{119}Sn-Mössbauer spectroscopy in conjunction with XRD and IR spectroscopy to study the thermal transformation of dimethyltin (IV)-intercalated montmorillonite to a pillared clay. They demonstrated that thermal pretreatment of the exchanged clay above 250°C leads to a collapsed interlayer However, thermal pretreatment after glycerol solvation of the exchanged complex at 240°C leads to a tin oxide pillared clay which is stable to about 500°C.

The three main hyperfine interactions which can be observed by Mössbauer Spectroscopy are reflected in the Mössbauer parameters known as the chemical isomer shift, the quadrupole splitting and magnetic splitting As the tin atom is diamagnetic, only chemical isomer shift and quadrupole splitting data are measured. Further deductions can be made from line-width data and the sign of the quadrupole interactions.

2 6 2 X-Ray Diffraction.

Over the years X-ray diffraction techniques have been used in many clay-mineral investigations.[64] In 1956, Greene-Kelly[74] showed, using X-ray diffraction that there were four pyridine molecules and two water molecules around the interlamellar Na^+-ions in the Na^+-montmorillonite pyridine/water clay intercalate He suggested from his measurement of a 23.3Å basal spacing

interlayer region of the clay at about 220K. This was verified in a similar set of variable temperature experiments using an exchanged clay dried at 70°C for three hours under vacuum

In 1989, Petridis et al.,[73] used ^{119}Sn-Mössbauer spectroscopy in conjunction with XRD and IR spectroscopy to study the thermal transformation of dimethyltin (IV)-intercalated montmorillonite to a pillared clay. They demonstrated that thermal pretreatment of the exchanged clay above 250°C leads to a collapsed interlayer However, thermal pretreatment after glycerol solvation of the exchanged complex at 240°C leads to a tin oxide pillared clay which is stable to about 500°C

The three main hyperfine interactions which can be observed by Mössbauer Spectroscopy are reflected in the Mössbauer parameters known as the chemical isomer shift, the quadrupole splitting and magnetic splitting. As the tin atom is diamagnetic, only chemical isomer shift and quadrupole splitting data are measured. Further deductions can be made from line-width data and the sign of the quadrupole interactions

2.6.2 X-Ray Diffraction

Over the years X-ray diffraction techniques have been used in many clay-mineral investigations.[64] In 1956, Greene-Kelly[74] showed, using X-ray diffraction that there were four pyridine molecules and two water molecules around the interlamellar Na^+-ions in the Na^+-montmorillonite: pyridine/water clay intercalate He suggested from his measurement of a 23.3Å basal spacing

that these complex interlamellar species formed pillars which held the alumino-silicate layers apart

In 1980, Endo et al.,[75] using thin, orinented film samples which were obtained by slow evaporation of aqueous suspension under ambient conditions, showed that four orders of reflection could readily be identified for a silica intercalate obtained by reaction of Na^+-hectorite with acetyl acetone [H(acac)] and $SiCl_4$. Adams and Breen[76] in 1981 used X-ray diffraction as a main tool in determining the effect of temperature, flow rate for N_2 carrier gas, and partial pressure of water on the conversion of the high spacing intercalates of Na^+-montmorillonite pyridine/water systems to the low spacing intercalates Their results showed that the conversion was greatly affected by the amount of water made available to the sample.

Deane in 1987[15] used X-ray diffraction to show that Al^{3+}- and Cr^{3+}- exchanged montmorillonites exposed to 1,4-dioxan/methanol mixtures resulted in the diffraction profile being dominated by that of the 1,4-dioxan intercalate.

2 6.3 Thermal Studies.

Thermal methods of analysis are defined as techniques which measure the change in some physical or chemical property of a material as a function of temperature, as the sample is subjected to a defined temperature programme. In thermogravimetry (TG) the weight change of a material is quantitatively measured. The resultant thermogram provides information about the

that these complex interlamellar species formed pillars which held the alumino-silicate layers apart

In 1980, Endo et al ,[75] using thin, oriented film samples which were obtained by slow evaporation of aqueous suspension under ambient conditions, showed that four orders of reflection could readily be identified for a silica intercalate obtained by reaction of Na^+-hectorite with acetyl acetone [H(acac)] and $SiCl_4$ Adams and Breen[76] in 1981 used X-ray diffraction as a main tool in determining the effect of temperature, flow rate for N_2 carrier gas, and partial pressure of water on the conversion of the high spacing intercalates of Na^+-montmorillonite pyridine/water systems to the low spacing intercalates Their results showed that the conversion was greatly affected by the amount of water made available to the sample

Deane in 1987[15] used X-ray diffraction to show that Al^{3+}- and Cr^{3+}- exchanged montmorillonites exposed to 1,4-dioxan/methanol mixtures resulted in the diffraction profile being dominated by that of the 1,4-dioxan intercalate.

2.6.3 Thermal Studies

Thermal methods of analysis are defined as techniques which measure the change in some physical or chemical property of a material as a function of temperature, as the sample is subjected to a defined temperature programme. In thermogravimetry (TG) the weight change of a material is quantitatively measured The resultant thermogram provides information about the

thermal stability and composition of the initial sample, any intermediates formed and the resulting residue.

Derivative Thermogravimetry (DTG) converts the TG signal to its first derivative form and as such is a plot of the rate of weight change as a function of temperature. Both methods can yield accurate information providing that a single stoichiometric reaction occurs in the temperature range of interest.[77] Consequently,the weight loss due to a dehydroxylation step can be used to determine the clay content. However, although DTG contains no more information than TG it is sometimes easier to interpret the derivatised thermograms.

The use of thermogravimetry and its associated techniques as tools in the identification and classification of clay minerals has been well documented.[78] As TG and DTG curves alone do not usually provide sufficient information to identify a species with certainty, quite often the observation of characteristic thermal events will identify to which group a clay mineral belongs. For example, Schultz[79] was able to distinguish from eighty samples four types of montmorillonite (Wyoming, Tatatilla, Otay and Chambers) using a combination of X-ray chemical analyses and thermogravimentric techniques. The examination of the metal-organic link involved in the co-ordination of ethylenediamine to Copper II ions in montmorillonite interlayers[80] again showed the compatibility of thermogravimetric analysis with other techniques. Mackenzie[81] showed using TG techniques that the level of

thermal stability and composition of the initial sample, any intermediates formed and the resulting residue.

Derivative Thermogravimetry (DTG) converts the TG signal to its first derivative form and as such is a plot of the rate of weight change as a function of temperature. Both methods can yield accurate information providing that a single stoichiometric reaction occurs in the temperature range of interest.[77] Consequently,the weight loss due to a dehydroxylation step can be used to determine the clay content. However, although DTG contains no more information than TG it is sometimes easier to interpret the derivatised thermograms

The use of thermogravimetry and its associated techniques as tools in the identification and classification of clay minerals has been well documented.[78] As TG and DTG curves alone do not usually provide sufficient information to identify a species with certainty, quite often the observation of characteristic thermal events will identify to which group a clay mineral belongs. For example, Schultz[79] was able to distinguish from eighty samples four types of montmorillonite (Wyoming, Tatatilla, Otay and Chambers) using a combination of X-ray chemical analyses and thermogravimentric techniques. The examination of the metal-organic link involved in the co-ordination of ethylenediamine to Copper II ions in montmorillonite interlayers[80] again showed the compatibility of thermogravimetric analysis with other techniques. Mackenzie[81] showed using TG techniques that the level of

hydration of a cation exchanged clay depends on the cation present and is also directly related to the polarising power of that cation. Deane[15] showed that the dehydroxylation of various cation exchanged montmorillonites occurred in almost the same temperature range and also that the peaks in the derivative thermograms had approximately the same shape and intensity. From this he concluded that the dehydroxylation of a clay mineral is directly related to the clay used and does not depend upon the exchangeable cation present in the interlayer. The experimental dehydroxylation region in these studies was between 550°C and 750°C as expected [6]

2.6.4 Water Vapour Isotherms

The interlayers of swelling clay minerals such as montmorillonite can be pillared by exchanging their interlayer cations for polyoxymetal species, followed by dehydration into respective oxide pillars The silicate interlayers can then be permanently propped apart forming zeolitic micropores. Although the size of the interlayer pillars can be estimated from the difference in basal spacings of the clay before and after intercalation and pillaring, water adsorption isotherms are used to characterise the internal pore structure of the interlayers. In 1959, Johansen and Dunning[82] demonstrated that montmorillonite samples adsorbed water vapour strongly and exhibited a pronounced hysteresis loop in their adsorption-desorpton isotherms. The desorption isotherm was reproducible but adsorption was

hydration of a cation exchanged clay depends on the cation present and is also directly related to the polarising power of that cation Deane[15] showed that the dehydroxylation of various cation exchanged montmorillonites occurred in almost the same temperature range and also that the peaks in the derivative thermograms had approximately the same shape and intensity. From this he concluded that the dehydroxylation of a clay mineral is directly related to the clay used and does not depend upon the exchangeable cation present in the interlayer. The experimental dehydroxylation region in these studies was between 550°C and 750°C as expected.[6]

2.6.4 Water Vapour Isotherms

The interlayers of swelling clay minerals such as montmorillonite can be pillared by exchanging their interlayer cations for polyoxymetal species, followed by dehydration into respective oxide pillars. The silicate interlayers can then be permanently propped apart forming zeolitic micropores. Although the size of the interlayer pillars can be estimated from the difference in basal spacings of the clay before and after intercalation and pillaring, water adsorption isotherms are used to characterise the internal pore structure of the interlayers. In 1959, Johansen and Dunning[82] demonstrated that montmorillonite samples adsorbed water vapour strongly and exhibited a pronounced hysteresis loop in their adsorption-desorpton isotherms. The desorption isotherm was reproducible but adsorption was

found to be sensitive to the original condition of the clay. Senich et al.,[83] in a later study reported the first-order basal spacing of a calcium-exchanged montmorillonite to vary in a continuous but non-uniform manner upon adsorption or desorption of water. The sorption isotherms were shown to be completely reversible at relative vapour pressures between zero and 0.2, with adsorption isotherms being more closely reproducible on successibe cycles than desorption isotherms. Also they reported that their experimental data fitted the B.E.T. multimolecular adsorption model more closely than the Langmuir monomolecular adsorption model.

The comparison of water adsorption-desorption isotherms for Na^{+}-, and Ca^{2+}-montmorillonites[84] demonstrated that the hysteresis behaviour for the Na^{+}-clay was much more pronounced than for the Ca^{2+}-clay, and may have been related to one or more of the following factors:- (i) capillary condensation, (ii) the change in rigidity of the water adsorption on the exchangeable ions between the clay platelets, and (iii) a variety of geometric situations in which pore filling and emptying paths were different. Analysis of these adsorption isotherms using the B.E.T. theory indicated that in the Ca^{2+}-clay the energy of interaction between the first mono-layer of water molecules adsorbed and the total active surface was greater than the energy of condensation of the subsequent layers. However, in the Na^{+}-clay the difference between these two energy terms

found to be sensitive to the original condition of the clay. Senich et al.,[83] in a later study reported the first-order basal spacing of a calcium-exchanged montmorillonite to vary in a continuous but non-uniform manner upon adsorption or desorption of water. The sorption isotherms were shown to be completely reversible at relative vapour pressures between zero and 0.2, with adsorption isotherms being more closely reproducible on successibe cycles than desorption isotherms. Also they reported that their experimental data fitted the B.E.T. multimolecular adsorption model more closely than the Langmuir monomolecular adsorption model.

The comparison of water adsorption-desorption isotherms for Na^{+}-, and Ca^{2+}-montmorillonites[84] demonstrated that the hysteresis behaviour for the Na^{+}-clay was much more pronounced than for the Ca^{2+}-clay, and may have been related to one or more of the following factors.- (i) capillary condensation, (ii) the change in rigidity of the water adsorption on the exchangeable ions between the clay platelets, and (iii) a variety of geometric situations in which pore filling and emptying paths were different. Analysis of these adsorption isotherms using the B.E.T. theory indicated that in the Ca^{2+}-clay the energy of interaction between the first mono-layer of water molecules adsorbed and the total active surface was greater than the energy of condensation of the subsequent layers. However, in the Na^{+}-clay the difference between these two energy terms

was less, indicating that the hydration forces in the Na^+-clay were less than those in the Ca^{2+}-clay.

In the case of alumina pillared clays however, water adsorption isotherms were shown to be unusual for microporous solids,[85] in that they fitted neither the B.E T. nor the Langmuir linear equations. Yamanaka et al.,[85] concluded that the shape of these isotherms could be interpreted in terms of hydrophobic properties, where the adsorption of water was suppressed until higher relative vapour pressures were introduced and adsorbate-adsorbate interactions began to play an important role. In a parallel study, Malla and Komarneni[86] demonstrated that the hydrophobicity of the aluminium oxide-exchanged montmorillonite apparently developed on thermal pretreatment, whereby protons migrated from the interlayers to the octahedral sheets where negative charge was located. However, after exposure to NH_3 vapour these protons migrated back into the interlayers, where NH_3 was subsequently converted to NH_4^+. In addition, in the further exchange of NH_4^+ for Ca^{2+}, the exchanged clay exhibited hydrophilic properties reflected both in the shape of the water isotherm (close to moderate Brunaur type I), the heat of sorption, and the total sorption capacity.

was less, indicating that the hydration forces in the Na^+-clay were less than those in the Ca^{2+}-clay.

In the case of alumina pillared clays however, water adsorption isotherms were shown to be unusual for microporous solids,[85] in that they fitted neither the B.E.T. nor the Langmuir linear equations. Yamanaka et al.,[85] concluded that the shape of these isotherms could be interpreted in terms of hydrophobic properties, where the adsorption of water was suppressed until higher relative vapour pressures were introduced and adsorbate-adsorbate interactions began to play an important role. In a parallel study, Malla and Komarneni[86] demonstrated that the hydrophobicity of the aluminium oxide-exchanged montmorillonite apparently developed on thermal pretreatment, whereby protons migrated from the interlayers to the octahedral sheets where negative charge was located. However, after exposure to NH_3 vapour these protons migrated back into the interlayers, where NH_3 was subsequently converted to NH_4^+. In addition, in the further exchange of NH_4^+ for Ca^{2+}, the exchanged clay exhibited hydrophilic properties reflected both in the shape of the water isotherm (close to moderate Brunaur type I), the heat of sorption, and the total sorption capacity.

CHAPTER 3

EXPERIMENTAL

CHAPTER 3

EXPERIMENTAL

CHAPTER 3

3 1 THE GENERAL PRETREATMENT AND PREPARATION OF THE BASIC CLAY

The parent clay used in this study was a Wyoming montmorillonite supplied by Volclay Ltd., Wallasey, Cheshire In order to remove any impurities present such as quartz and mica etc , a sedimentation technique was used The sedimentation technique is based on Stoke's Law for particles of radius, a, falling with a terminal velocity, V, through a liquid medium of viscosity, η The force on any particle, F, is given by the equation,

$$F = 6\pi a \eta V$$

At a loading of about 10g of the raw clay per litre of distilled water, the suspension was mechanically stirred until the clay was distributed evenly through the volume of water and left to stand for 24 hours, after which the top 10cm fraction was siphoned off and centrifuged to remove excess water. The siphoned suspension was replaced with water and the process repeated until the suspension became transluscent At this point the remaining suspension was disgarded as it contained mostly the impurities from the raw clay

The centrifuged clay, containing particles of approximately 2μm in diameter was then dried at 110°C for 24 hours, cooled in a desiccator and ground to a fine powder. The clay was then converted to its sodium form by mixing it in a 1 0 M sodium chloride solution overnight. It is then washed free of electrolyte,

CHAPTER 3

3 1 THE GENERAL PRETREATMENT AND PREPARATION OF THE BASIC CLAY

The parent clay used in this study was a Wyoming montmorillonite supplied by Volclay Ltd., Wallasey, Cheshire In order to remove any impurities present such as quartz and mica etc., a sedimentation technique was used The sedimentation technique is based on Stoke's Law for particles of radius, a, falling with a terminal velocity, V, through a liquid medium of viscosity, η The force on any particle, F, is given by the equation,

$$F = 6\pi a \eta V$$

At a loading of about 10g of the raw clay per litre of distilled water, the suspension was mechanically stirred until the clay was distributed evenly through the volume of water and left to stand for 24 hours, after which the top 10cm fraction was siphoned off and centrifuged to remove excess water The siphoned suspension was replaced with water and the process repeated until the suspension became transluscent At this point the remaining suspension was disgarded as it contained mostly the impurities from the raw clay.

The centrifuged clay, containing particles of approximately 2μm in diameter was then dried at 110°C for 24 hours, cooled in a desiccator and ground to a fine powder. The clay was then converted to its sodium form by mixing it in a 1.0 M sodium chloride solution overnight. It is then washed free of electrolyte,

centrifuged and dried at room temperature This sodium exchanged clay is then ground with a mortar and pestle and stored, and for the purpose of this study will be referred to as the "base" clay.

Chemical analysis of this sample by standard literature methods[1] produced results consistent with a layer formulation of $(Si_{3.9}Al_{0.14})(Al_{1.35}Fe_{0.88}Mg_{0.59})O_{10}(OH)_2 K_{0.07} Na_{0.59}$ The cation exchange capacity (C.E.C.), determined by flame photometry, was found to be 68± 2 milliequivalents per 100g of clay (meq/100gclay).

3.2 THE INTERCALATION OF ORGANOMETALLIC CATIONS

The three organometallic cation exchanged montmorillonites forming the basis of these studies were prepared in the following manner [2] In order to produce the dimethyl tin, Me_2Sn^{2+}-montmorillonite system, 0.74g of dimethyl tin dichloride salt Me_2SnCl_2 was dissolved in $20cm^3$ distilled water, and rapidly mixed with an $80cm^3$ aqueous suspension of 2g of the $\leq 2\mu$m Na^+-montmorillonite base clay The resulting mixture exhibited a pH of 2.4. The dimeric $[Me_2SnOH]_2^{2+}$ exchanged system was produced in a similar manner except that the pH of the suspension was rapidly adjusted to 4.0 using an almost negligible quantity of NaOH. The mixtures prepared at both pH's were stirred continuously for 24 hours after which the clays were concentrated by centrifugation and the exchange procedure repeated. Following this second exchange the clays were washed and centrifuged until the supernatant was free of excess chloride.

centrifuged and dried at room temperature. This sodium exchanged clay is then ground with a mortar and pestle and stored, and for the purpose of this study will be referred to as the "base" clay

Chemical analysis of this sample by standard literature methods[1] produced results consistent with a layer formulation of $(Si_{3.9}Al_{0.14})(Al_{1.35}Fe_{0.88}Mg_{0.59})O_{10}(OH)_2 K_{0.07} Na_{0.59}$. The cation exchange capacity (C.E.C.), determined by flame photometry, was found to be 68± 2 milliequivalents per 100g of clay (meq/100gclay)

3.2 THE INTERCALATION OF ORGANOMETALLIC CATIONS

The three organometallic cation exchanged montmorillonites forming the basis of these studies were prepared in the following manner [2] In order to produce the dimethyl tin, Me_2Sn^{2+}-montmorillonite system, 0.74g of dimethyl tin dichloride salt Me_2SnCl_2 was dissolved in $20cm^3$ distilled water, and rapidly mixed with an $80cm^3$ aqueous suspension of 2g of the $\leq 2\mu m$ Na^+-montmorillonite base clay The resulting mixture exhibited a pH of 2.4. The dimeric $[Me_2SnOH]_2^{2+}$ exchanged system was produced in a similar manner except that the pH of the suspension was rapidly adjusted to 4.0 using an almost negligible quantity of NaOH. The mixtures prepared at both pH's were stirred continuously for 24 hours after which the clays were concentrated by centrifugation and the exchange procedure repeated. Following this second exchange the clays were washed and centrifuged until the supernatant was free of excess chloride.

The Me_3Sn^+-montmorillonite system was prepared by dissolving 2.66g Trimethyl Tin Chloride in $20cm^3$ distilled water and rapidly mixing it with an $90cm^3$ aqueous suspension of the $\leq 2\mu m$ montmorillonite clay The pH of the resulting mixture was 3.4. Again the mixture was stirred continuously for 24 hours, centrifuged and washed until the supernatant was chloride free.

In each of the above cases the clay sludge was spread on a clock glass, air dried, ground into fine powders and stored in stoppered glass sample bottles prior to further use. A summary of the experimental preparation parameters is given in Table 3.1

3 3 Quantifying the Exchanged Tin

This analysis was carried out on portions of the 120°C dried organometallic exchanged clays.[1] Solutions of each system were prepared by fusing weighed samples with sodium hydroxide. In each case the melt was decomposed with boiling water, the fused mass extracted with hydrochloric acid and diluted with distilled water Aliquots of each digestion solution were analysed for tin content with an IL-357 Atomic Absorption spectrophotometer, using a nitrous oxide flame and a detection wavelength of 235.5nm. A standard curve was plotted using a series of standard solutions. The tin content of each sample was determined by interpolation. The details of the instrument set-up procedures and running conditions are given in the appropriate manual.[3]

The Me_3Sn^+-montmorillonite system was prepared by dissolving 2.66g Trimethyl Tin Chloride in $20cm^3$ distilled water and rapidly mixing it with an $90cm^3$ aqueous suspension of the $\leq 2\mu$m montmorillonite clay. The pH of the resulting mixture was 3.4. Again the mixture was stirred continuously for 24 hours, centrifuged and washed until the supernatant was chloride free

In each of the above cases the clay sludge was spread on a clock glass, air dried, ground into fine powders and stored in stoppered glass sample bottles prior to further use A summary of the experimental preparation parameters is given in Table 3 1

3.3 Quantifying the Exchanged Tin

This analysis was carried out on portions of the 120°C dried organometallic exchanged clays.[1] Solutions of each system were prepared by fusing weighed samples with sodium hydroxide. In each case the melt was decomposed with boiling water, the fused mass extracted with hydrochloric acid and diluted with distilled water. Aliquots of each digestion solution were analysed for tin content with an IL-357 Atomic Absorption spectrophotometer, using a nitrous oxide flame and a detection wavelength of 235.5nm. A standard curve was plotted using a series of standard solutions. The tin content of each sample was determined by interpolation. The details of the instrument set-up procedures and running conditions are given in the appropriate manual.[3]

TABLE 3.1

PREPARATION OF ALKYLTIN EXCHANGED CLAYS

SALT	FINAL pH	MAJOR INTERLAYER SPECIES
$(CH_3)_2SnCl_2$	2.6	$(CH_3)_2Sn^{2+}$
$(CH_3)_2SnCl_2$	4 0	$[(CH_3)_2SnOH]_2^{2+}$
$(CH_3)_3SnCl$	3.4	$(CH_3)_3Sn^{+}$

TABLE 3.1

PREPARATION OF ALKYLTIN EXCHANGED CLAYS

SALT	FINAL pH	MAJOR INTERLAYER SPECIES
$(CH_3)_2SnCl_2$	2.6	$(CH_3)_2Sn^{2+}$
$(CH_3)_2SnCl_2$	4 0	$[(CH_3)_2SnOH]_2^{2+}$
$(CH_3)_3SnCl$	3 4	$(CH_3)_3Sn^{+}$

3 4 (i) Mössbauer Spectroscopy

The cation exchanged montmorillonite samples prepared as previously outlined in section 3 1 were used in all Mössbauer experiments described in this work. In a further pretreatment the exchanged clays were ground into fine powders using an agate mortar and pestle in order to minimize anomalous line assymetries associated with preferred orientations [4]

The Mössbauer spectrometer used was a constant acceleration MS-102 Microprocessor Mössbauer spectrometer consisting of an 8-bit high performance Motorola 68AOG microprocessor supplied by Cryophysics, U.K This instrument had sufficient read-write memory to store experimental spectra over 512 channels. The Mössbauer source used was a 5mCi calcium stannate - 119m source emitting γ-rays corresponding to an energy of 23 9keV This source was mounted on a Doppler drive system consisting of a moving coil drive vibrator coupled to a moving magnet velocity transducer. This ensured that the velocity of the Mössbauer source followed the velocity reference signal A standard X-Y oscilloscope was used to present a continuous display of each experimental spectrum as it was being collected. Each cation exchanged clay sample of about 0.2g was taken very quickly from a desiccator used to store the samples and mounted into a sample disc of approximately $0.75cm^2$ in area, covered in a thin film of aluminium foil and transferred to the Mössbauer cryostat.

Temperature control of each sample was achieved

3.4 (i) Mössbauer Spectroscopy

The cation exchanged montmorillonite samples prepared as previously outlined in section 3.1 were used in all Mössbauer experiments described in this work In a further pretreatment the exchanged clays were ground into fine powders using an agate mortar and pestle in order to minimize anomalous line assymetries associated with preferred orientations.[4]

The Mössbauer spectrometer used was a constant acceleration MS-102 Microprocessor Mössbauer spectrometer consisting of an 8-bit high performance Motorola 68AOG microprocessor supplied by Cryophysics, U.K This instrument had sufficient read-write memory to store experimental spectra over 512 channels The Mössbauer source used was a 5mCi calcium stannate - 119m source emitting γ-rays corresponding to an energy of 23.9keV This source was mounted on a Doppler drive system consisting of a moving coil drive vibrator coupled to a moving magnet velocity transducer. This ensured that the velocity of the Mössbauer source followed the velocity reference signal A standard X-Y oscilloscope was used to present a continuous display of each experimental spectrum as it was being collected. Each cation exchanged clay sample of about 0.2g was taken very quickly from a desiccator used to store the samples and mounted into a sample disc of approximately $0.75cm^2$ in area, covered in a thin film of aluminium foil and transferred to the Mössbauer cryostat.

Temperature control of each sample was achieved

using a DN-726M continuous flow liquid nitrogen cryostat, Fig 3.1 The cryostat was capable of operation between 77K and 300K and operated on the principle of a controlled continuous transfer of liquid nitrogen from a reservoir of 7 litres capacity to a heat exchanger surrounding the sample space. Each sample, locked in a sample holder was top-loaded into the cryostat and cooled by a static column of dry nitrogen exchange gas, thermally linking it to the heat exchanger The coolant liquid nitrogen flowed from the reservoir down the feed capillary and into the copper heat exchanger, and finally leaving the heat exchanger through an exhaust valve at the top plate The unit was fitted with two aluminised mylar windows through which the incident gamma rays interacted with the sample, and the resonant gamma rays were transmitted to the detector unit Temperature stability was maintained by a DTC-2 digital variable-temperature controller. Temperature stability was $\pm$ 0.1K of the desired temperature throughout the spectral measurement time. Both the cryostat and the variable temperature controller were supplied by Oxford Instruments Ltd

Count rates transduced in the proportional counter detector were amplified and sent to a multichannel analyser. A working data base was established by transferring each measured spectrum on to a VAX-785 mainframe computer via an RS232 interface. Velocity calibrations were based on the spectrum of natural iron incorporating a ^{57}Co source and β -tin.

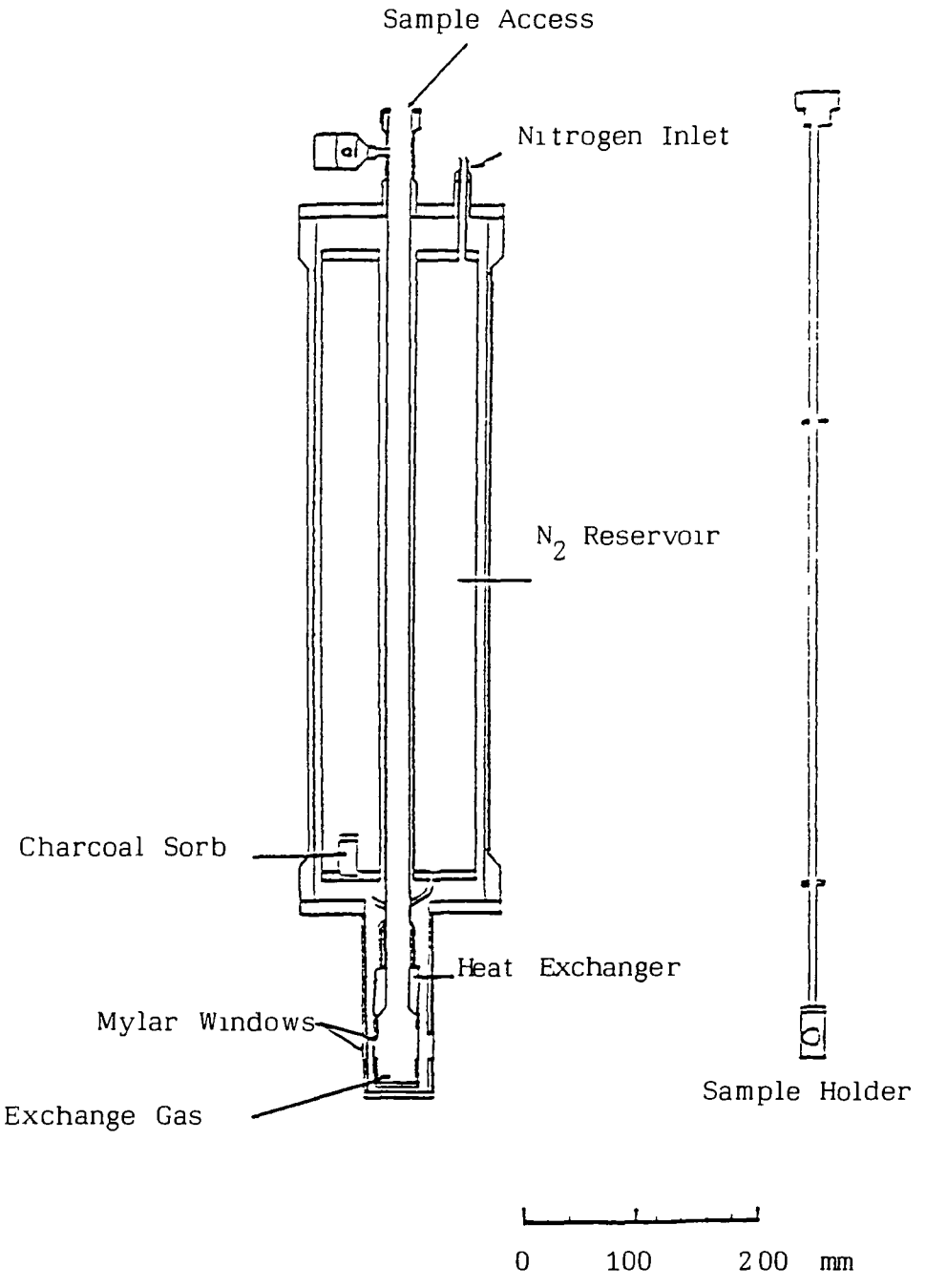

Fig 3 1 Liquid Nitrogen Mössbauer Cryostat DN726M

Each experimental spectrum was curve-fitted using conventional least-squares techniques to standard Lorentzian line-shapes, with prior data correction for parabolic background curvature The program minimised χ^2, printed the initial parameters, a history of the convergence process and the final values of the fitted parameters Details of the instrument set-up procedures and running conditions are given in the appropriate manuals.[5,6] A schematic diagram of the experimental system can be seen in Fig. 3.2.

3 4 (ii) **Experimental Curve Fitting**

After each experimental spectrum was collected it was transferred from the Mössbauer microprocessor unit to the VAX 785 mainframe computer system, and appropriately identified A computer printout of each spectrum was then obtained so that approximate values for the isomer shift (DI or δ), quadrupole splitting (QS or Δ) intensity, H1 and halfwidth, (GA or Γ) for each component of the theoretical spectrum could be calculated, Fig. 3.3.

An approximate value for each isomer shift in terms of the number of channels is calculated by adding together the channel numbers corresponding to the maximum positions of each wing in a theoretical component doublet, dividing the result by 2, and subtracting 256, the mid point channel from it. Multiplying this value by 2.8083×10^{-2}, the channel constant in mm s^{-1}, gives a preliminary isomer shift value.

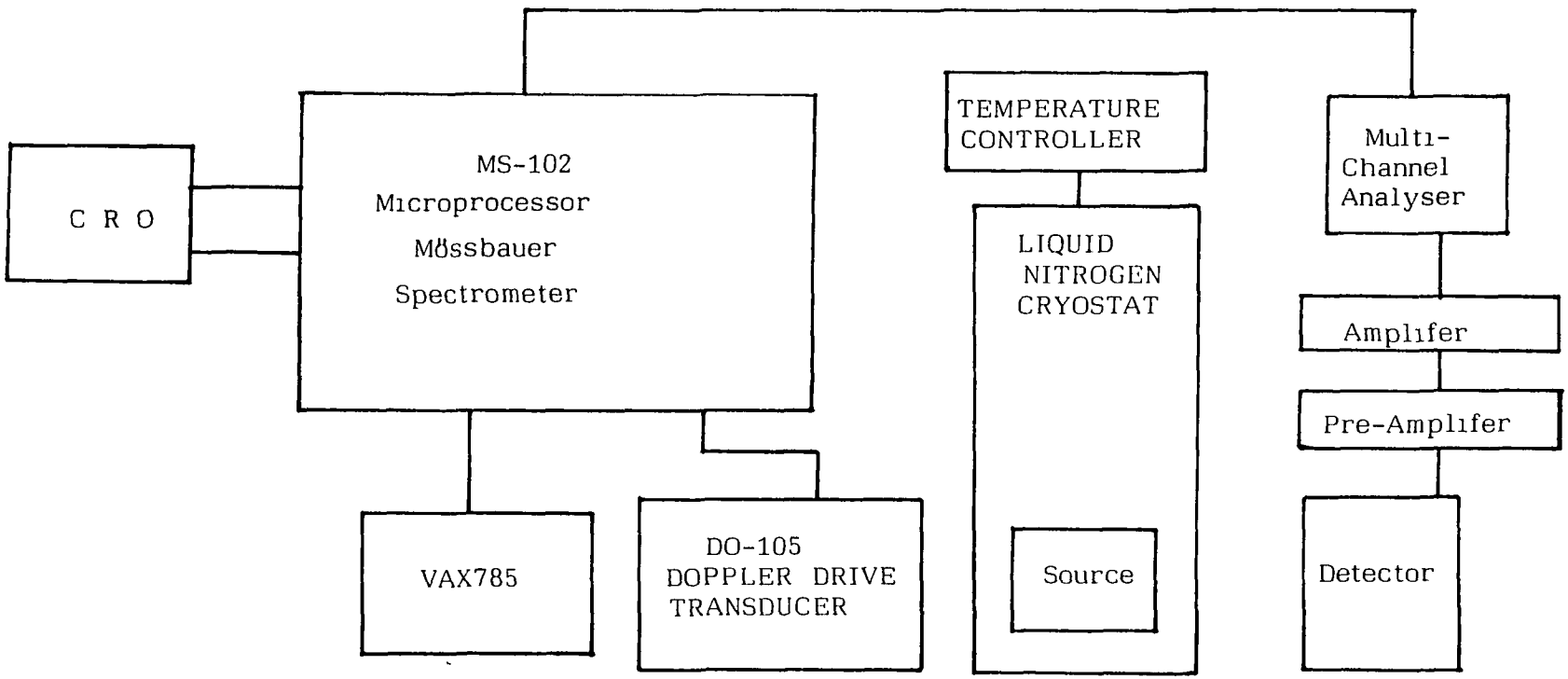

Fig 3 2 Schematic Diagram of Mössbauer Spectroscopy Experimental System

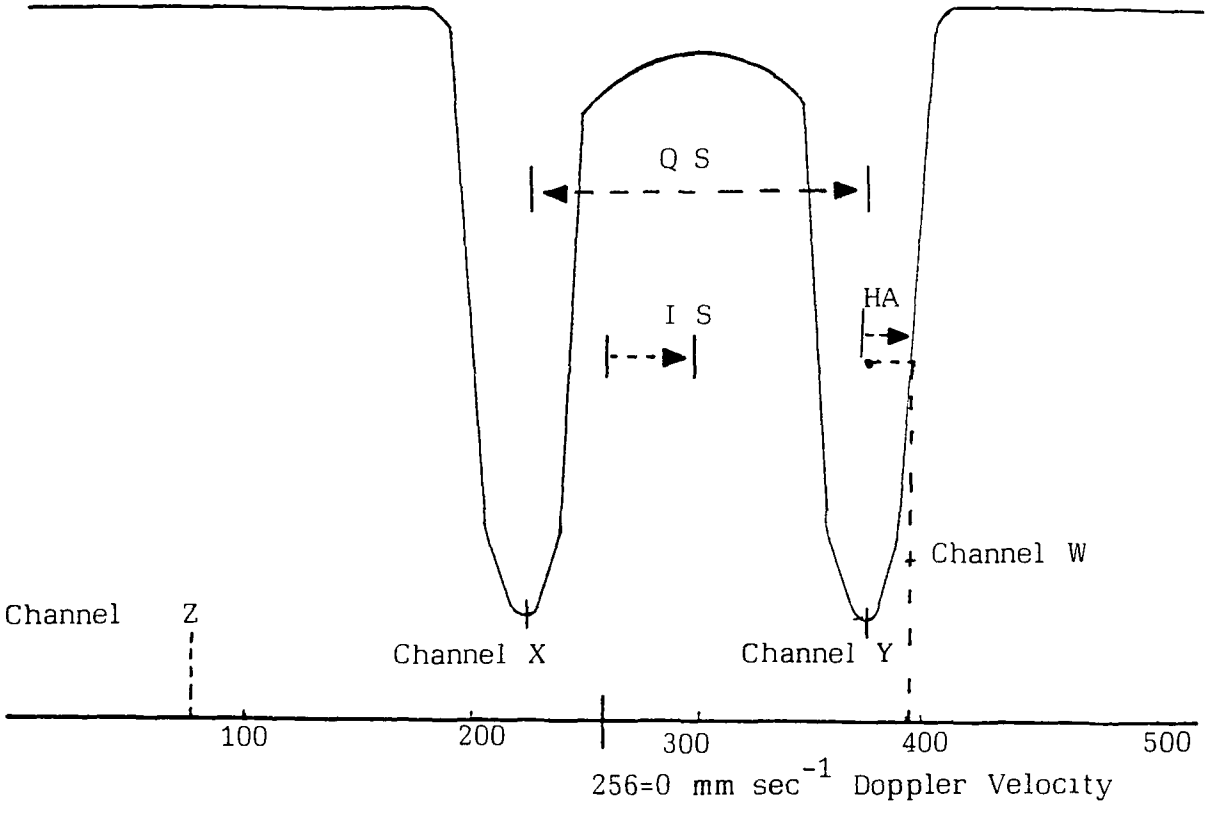

$$Q\ S = (Y-X)\ 28083\ E\text{-}2\ mm\ sec^{-1}$$

$$I\ S = \frac{(X+Y)}{2} - 256 \quad 2\ 8083\ E\text{-}2\ mm\ sec^{-1}$$

$$HA = (W-Y)\ 2\ 8083\ E\text{-}2\ mm\ sec^{-1}$$

Fig 3 3 Schematic Diagram of a recorded Mössbauer Spectrum Showing fitting regime and calculations for I S and Q S

The approximate quadrupole splitting, Δ , is calculated by subtracting the channel numbers corresponding to the maximum position of each wing of the doublet and multiplying by the channel constant. The approximate intensity is calculated by going to the digital block of each spectrum and subtracting the number of counts in a baseline channel, say channel Z from the counts corresponding to one for the peak position maxima of a experimental doublet and multiplying by 2. The half width, Γ , or "half width at half height" of each wing, in mm s^{-1} is calculated by subtracting the central channel of the wing from the channel representing the half height value, W and multiplying by the channel constant This value is generally 0.45 mm s^{-1} for tin

After each experimental spectrum had been corrected by removing the parabolic background using the REFORMAT program, a NAMELIST file was set up which allowed the nature and initial values of the variable parameters along with various other instructions and options to be entered Each NAMELIST file was then curve-fitted using the SPECFIT programme which compared theoretical spectra to experimental spectra by a least squares method. The output parameters for each fitted spectrum were used as refined input parameters in further runs until a reasonable set of output parameters were found corresponding to a best fit situation.

3.5 Thermogravimetric Analysis

The clays used for thermogravimetric analysis

were prepared as previously outlined in section 3.2. Before analysis, each exchanged clay was further ground with a mortar and pestle to $\leq 75\mu m$ The instrument used throughout this study was a Stanton-Redcroft TG-750 thermobalance. A schematic diagram of the system can be seen in Fig. 3.4.

In each analysis an $\sim$ 8mg sample of the exchanged clay was added to the sample pan and allowed to reach equilibrium in the N_2 gas flow The dry nitrogen gas passed through a drying column, consisting of a 4Å synthetic zeolite, followed by P_2O_5 with a visible moisture indicator which turned green on contact with water. The sample pan consisted of an inconel crucible suspended from one arm of an electronic microbalance enclosed in a glass balance head. In operation, the furnace was raised, forming a seal with the flange on the glass head and the temperature ramp initiated The purge gas, N_2, flowed into the right hand side of the balance chamber and over the sample preventing readsorption of the evolved vapours. An interesting feature of this instrument was that its water cooled furnace cooled from 1000°C to 100°C in less than 4 minutes at the end of each run, allowing a rapid instrument turn around. This instrument was designed to give a direct plot of weight versus temperature for any sample in the temperature range from ambient to 1000°C.

In order to convert the signal from the TG apparatus into its first derivative form a derivatising unit was connected between the thermobalance and the

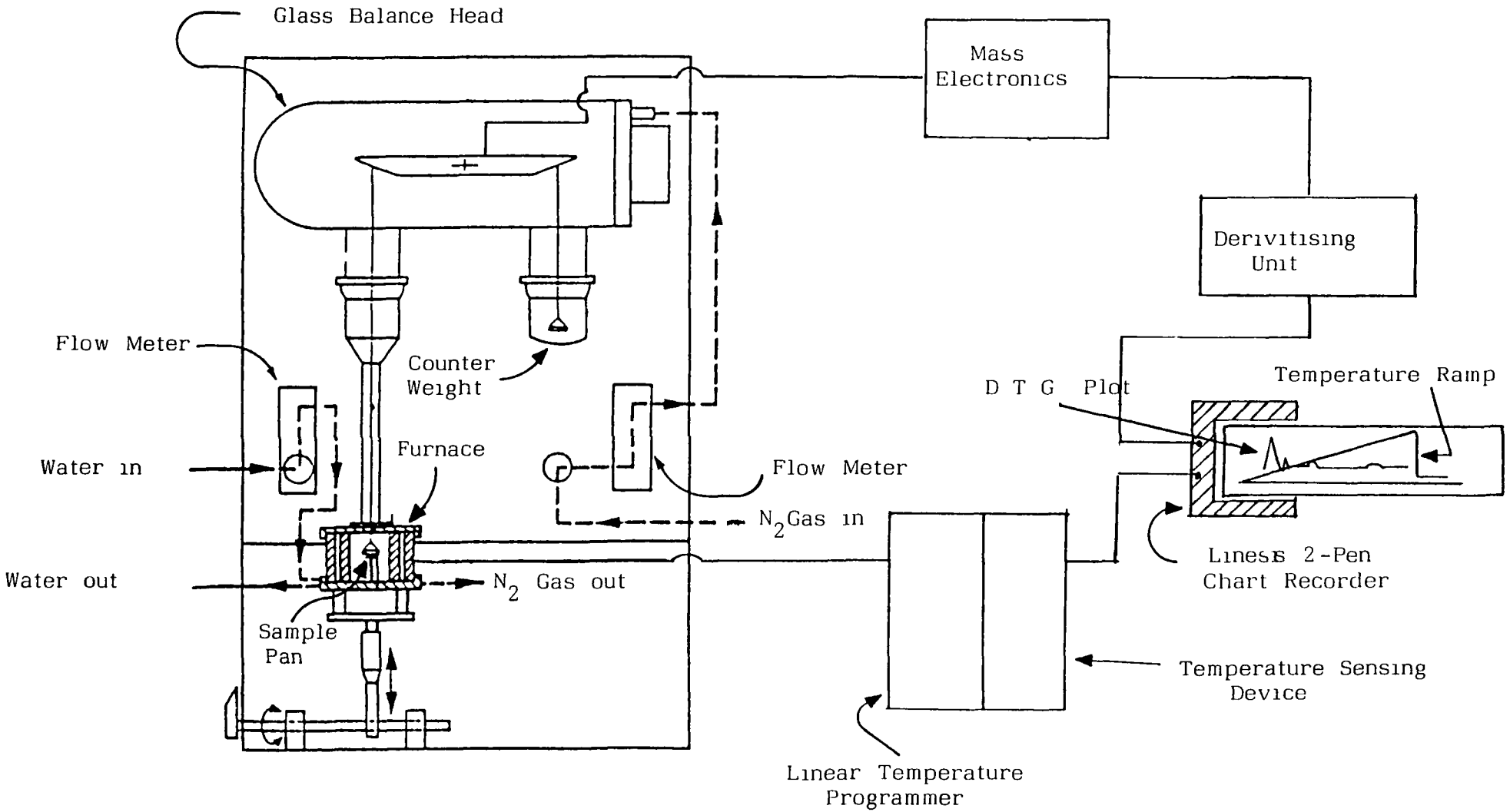

Fig 3 4 Schematic Diagram of the Stanton-Redcroft 750 TG/DTG System

chart recorder. This unit plotted the rate of weight loss versus temperature

This type of plot is referred to as the derivative thermogravimetric, or DTG curve. Examples of both TG and DTG curves recorded on the instrument can be seen in Fig 3.5

The experimental conditions used in each run were, purge gas, N_2, operating at a flow rate of $30cm^3$ per minute, a heating rate of 20°C per minute, and a chart speed of 20cm. per hour. Each sample was run between room temperature (20°C) and approximately 800°C, the latter of which is known to be above the dehydroxylation temperature of this clay mineral.[7] The general specifications of the Stanton-Redcroft thermobalance are given in Table 3.2

TABLE 3.2

SPECIFICATIONS OF THE STANTON-REDCROFT 750 THERMOBALANCE

Sample Size	0 1mg - 100mg
Balance Ranges	Between 0-1mg full scale deflection and 0-250mg Full scale deflection
Atmosphere Control	Flowing air or gas Static air or gas
Temperature Range.	Ambient to 1000°C
Temperture Measurement	Pt Vs Pt 13% Rh platform thermocouple
Heating Rate	1,2,3,5,10,15,20,30,50, 100°C/min
Programme Modes.	Heat-hold, heat-off, cool-hold, cool-off, isothermal.

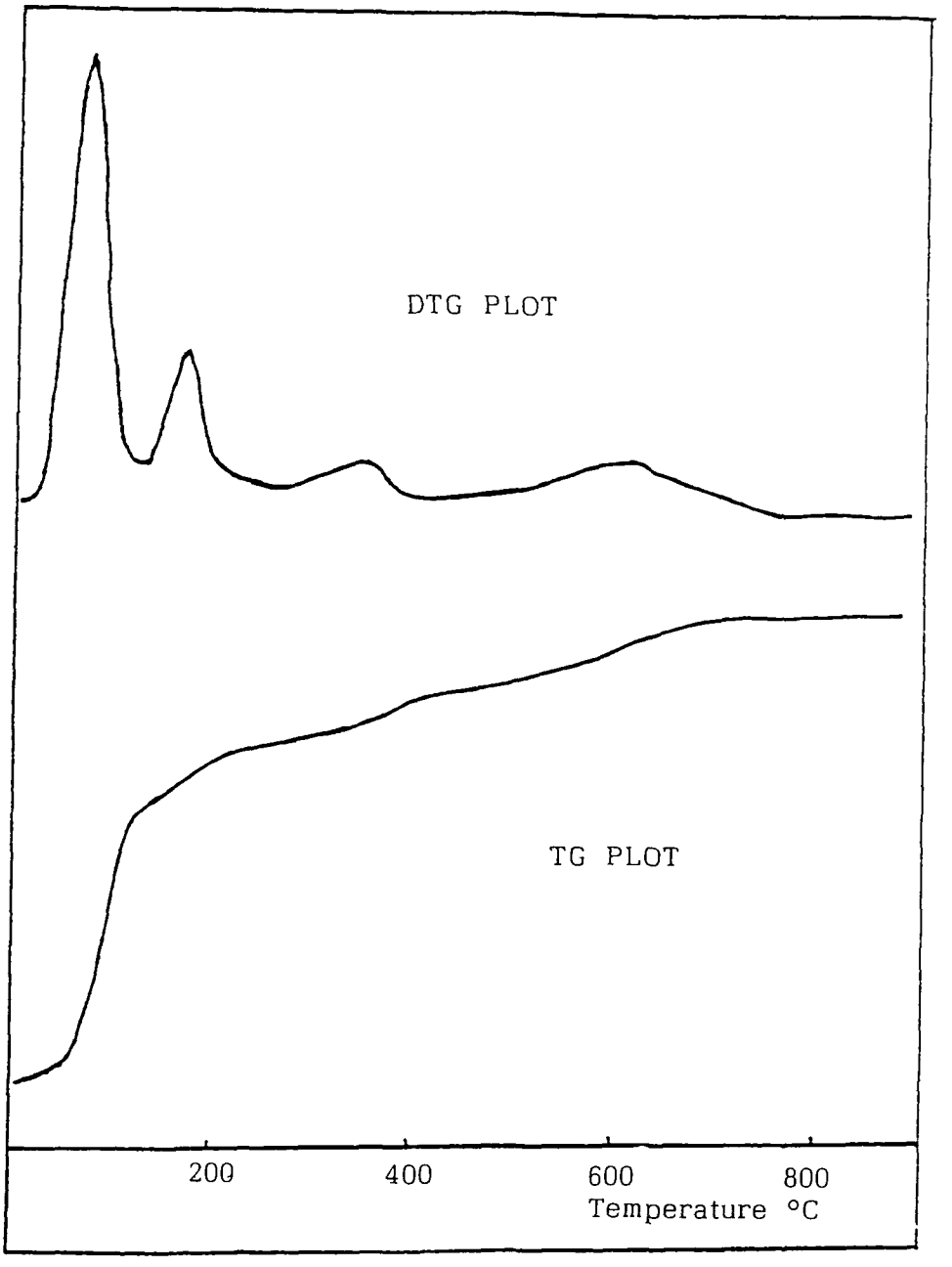

Fig 3 5 Schematic Diagram of recorded Thermogravimetric and derivative thermogravimetric plots

3 6 X-ray Diffraction

A Jeol JDS 8X diffractometer using Ni filtered Copper-K_{α} radiation (λ = 1.5418Å) at 40kV and 20mA was used in these studies to determine the basal spacing of clay samples presented as an oriented film on a glass slide. Samples of each cation exchanged clay were prepared by coating a layer of the clay slurry (prepared as in Section 3.2) on to a standard glass microscope slide The slides were then appropriately labelled and stored in a desiccator until required

The thermal stability of the basal spacings for each clay was determined by heating the clay coated slides in a muffle furnace at the desired temperatures for a period of 16 hours The samples were cooled in a desiccator and transferred to the diffractometer as quickly as possible in order to prevent rehydration of the interlayers.

3.7 Adsorption Isotherm Studies

Water adsorption isotherms were determined following the method of Branson and Newman.[8] Preweighed samples of each of the cation-exchanged clays were equilibrated at constant temperature, in desiccators containing salt solutions. The choice of salt was made by reference to published data,[9,10] and chosen to generate a range of relative partial pressures of water from 0.0 to 0.97. In general the finely ground samples, previously heated at 120°C required several days to reach constant weight before being transferred to the next partial pressure. It should be pointed out,

however, that samples stored over P_2O_5 and at humidities <90% required several weeks to reach constant weights. After the saturated weights of each clay had been recorded, desorption isotherms were measured by reversing the sequence of salt pastes, starting with $CuSO_4\ 5H_2O$ and finishing with P_2O_5. A standard hygrometer was used to record the actual humidity in each desiccator. The list of salt pastes and their relative humidities are given in Table 3.3. A schematic diagram of the apparatus used can be seen in Fig. 3.6 along with an example of an experimental B.E.T. Adsorption Isotherm plot.

TABLE 3.3

SATURATED SALT SOLUTIONS RECOMMENDED FOR HUMIDITY CONTROL AT 20°C

SALT	% RELATIVE HUMIDTY
P_2O_5	0
$LiCl.\ H_2O$	15
$CH_3COO.K$	24
$Ca\ Cl_2.6H_2O$	39
KSCN	52
$NaNO_2$	70
$H_2C_2O_4.2H_2O$	76
$Na\ C_2H_3O_2.3H_2O$	84
$Na_2CO_3.10H_2O$	94
$CuSO_4.5H_2O$	97

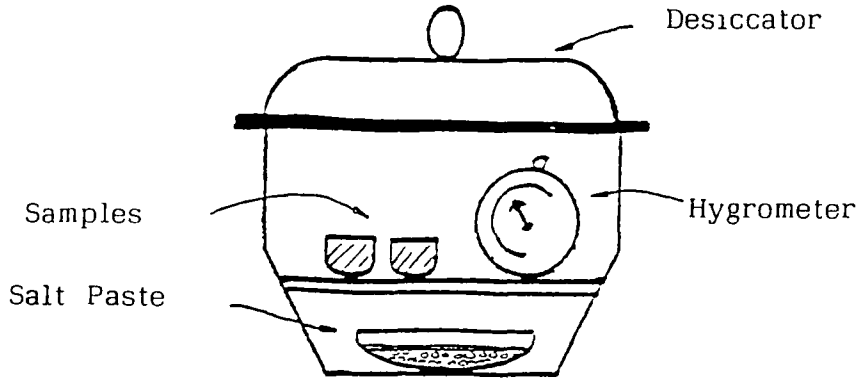

Fig 3 6 (i) System used to record water vapour isotherms on cation exchanged clays

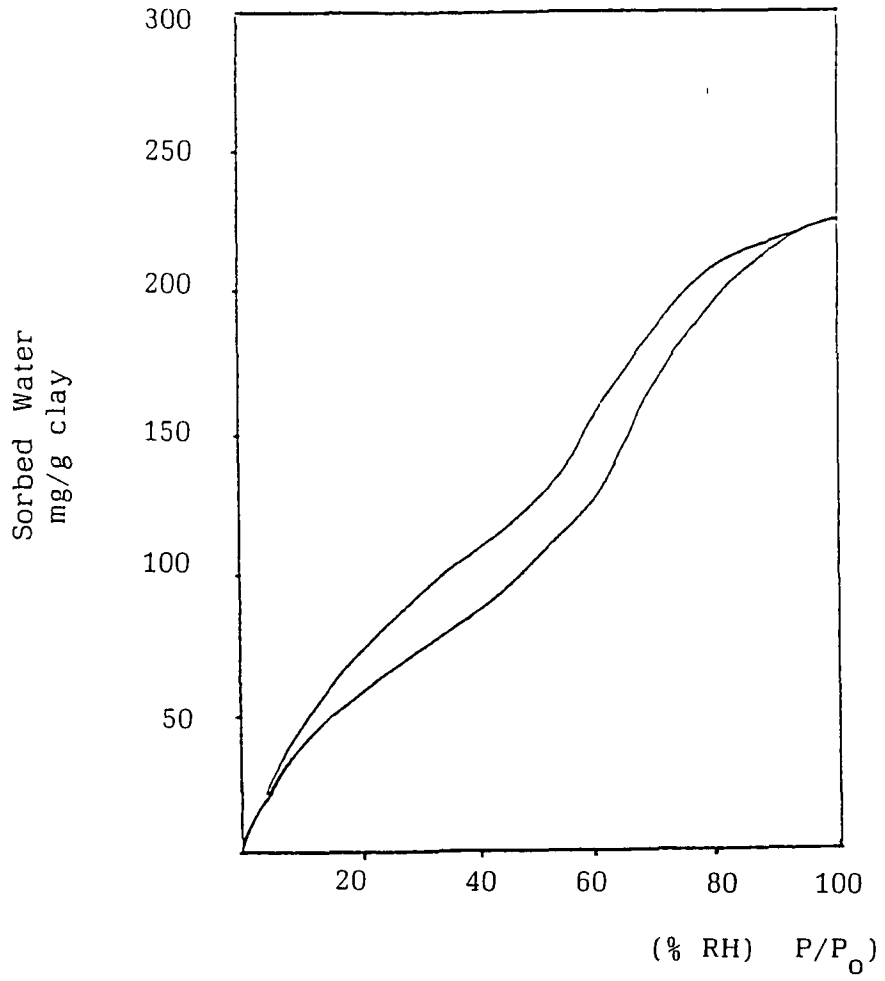

Fig 3 6 (ii) Example of a water vapour isotherm exhibiting hysteresis

CHAPTER 4

A MOSSBAUER STUDY OF ORGANOTIN EXCHANGED MONTMORILLONITES

CHAPTER 4

A MÖSSBAUER STUDY OF ORGANOTIN EXCHANGED MONTMORILLONITES

4.1 General Introduction

The emergence of Mössbauer spectroscopy as an important experimental technique for the study of solids has resulted in a wide range of applications in chemistry.[1] The technique has shown itself to be one of the most important methods for the microstructural analysis of materials,[2,3] particularly for its ability to identify different species of an isotope in several chemical forms in the same sample, and in determining their relative amounts.[4] However, as with most techniques, Mössbauer results can only be interpreted from corroborative evidence obtained from one or more ancillary techniques.

The purpose of the studies undertaken and reported here was to investigate the suitability and thermal stability of organotin exchanged montmorillonites as possible pillared acid catalysts in a range of novel and industrially significant processes. Furthermore, as organotin compounds are used in a wide variety of industrial applications such as agrochemicals anti-fouling agents and stablisers, the environmental fate of these compounds and their eventual degradation pathways to a non-toxic tin species is of obvious interest.[5] This current study may help clarify the nature and residence time of these species in clay bearing soils.

4 2 Mössbauer Spectroscopy

Although the phenomenon of atomic resonant fluorescence was predicted early this century, it was not until the late 1950s that Rudolph Mössbauer discovered the phenomenon of recoil-free nuclear resonance fluorescence [6] Mössbauer's solution was to eliminate the destructive effects of nuclear recoil and Doppler broadening (which had already been accurately identified[7]) and consider the behaviour of a recoiling nucleus when it was no longer isolated but instead fixed in a crystal lattice Under these circumstances, when the recoil energy is less than the lowest quantised lattice vibrational energy, there is a probability that the γ-ray is emitted without loss of energy due to the recoil of the nucleus This type of recoiless emission is optimised for low-energy γ-rays from nuclei which are strongly bound in a crystal lattice at low temperatures. Furthermore if these γ-rays are incident on another identical matrix containing the same isotope in the ground state, they will be resonantly absorbed and subsequently re-emitted in a random direction, e g by resonant fluorescence

In order to examine the energy states of any particular nucleus using the Mössbauer effect it is first necessary to have a source containing the same element in an already excited state. For example, after ^{57}Fe the most extensively investigated Mössbauer nuclide is ^{119}Sn, which decays from the first excited nuclear state, corresponding to a $\frac{3}{2} \longrightarrow \frac{1}{2}$ magnetic dipole

transition, (Fig. 4.1) releasing a cascade of γ-rays having an energy of 23.875 keV in the process. This γ-radiation is used in ^{119}Sn spectroscopy to investigate tin-bearing materials such as, in this instance, organotin exchanged montmorillonite, and involves the sample (called the absorber) being exposed to the radiation so that the γ-rays are absorbed by the organotin exchanged nuclei. However, as the energy states of nuclei depend on the interaction between the nuclei and their electronic environments, the energy transition between ground and excited states in the source and absorber nuclei are unlikely to coincide when the source and absorber are different compounds.

As such, the γ-ray energy has to be modified by the application of a Doppler velocity, generated by an electro-mechanical transducer and controlled by the Mössbauer microprocessor. Also, the range of Doppler velocities required is such that the much larger natural or Heisenberg linewidth for ^{119}Sn reduces the resolution of energy differences for tin. Note this theoretical natural or Heisenberg linewidth, Γ, for ^{119}Sn is 0.450 mms^{-1}. Mössbauer spectra are obtained by measuring resonance absorption as a function of γ-ray energy and are composed of a plot of γ-ray counts (ordinate), against the velocity of the source with respect to the absorber (abscissa), measured in mms^{-1}. The effective Debye temperature of most organotin coumpounds is low which means that measurements must be made at low temperatures, and the vast majority of the

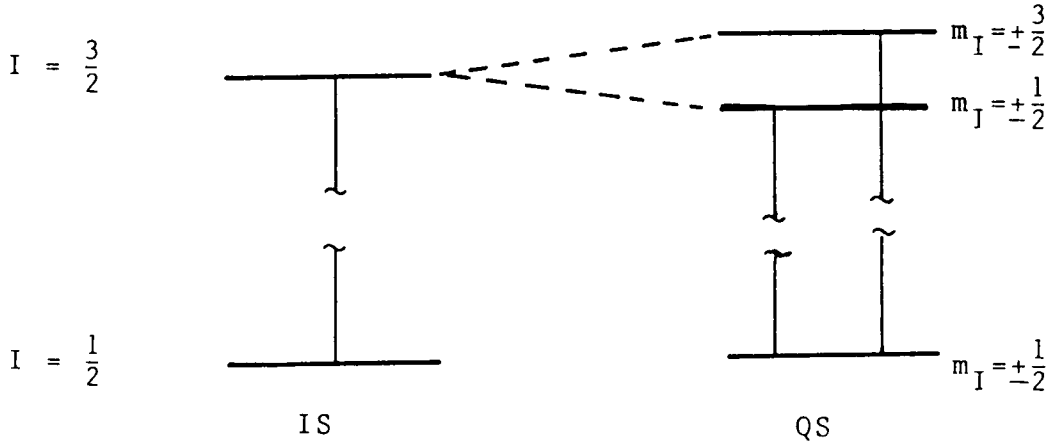

I = spin of the nucleus

m_I = magnetic spin quantum number

Fig 4 1 Origin of the isomer shift, δ , and quadrupole splitting, Δ

reported data, as with the work presently reported, refer to liquid nitrogen temperature (78K).

4.3 (i) **The Hyperfine Interactions**

The resonant absorption line of a Mössbauer spectrum has a Lorentzian shape having a width Γ, and is centered at zero relative velocity between the source and the absorber. The practical application of the Mössbauer effect would be limited except for the presence of static or hyperfine interactions due to the absorbing nuclear energy states being weakly influenced by their chemical environment. It is possible to detect these extremely small interactions because of the high monochromaticity, (which is better than 1 part in 10^{12}), of the γ-ray energy produced, and as such the Mössbauer effect can be used to probe the very small differences in energy separation between the nuclear ground and excited states associated with different chemical environments. Experimentally these small differences are seen as a shift in position of the observed resonance line.

The three main hyperfine interactions which can be observed by Mössbauer spectroscopy are the isomer shift, IS, (sometimes called the chemical isomer shift), the quadrupole splitting, QS, and the magnetic splitting, H. These interactions along with their temperature dependence produce large amounts of useful information. Further deductions can be made from linewidth data, the sign of the quadrupole interactions, and the influence of relaxation times on the above

parameters.

In the absence of an externally applied magnetic field the two most important quantities measured in a ^{119}Sn Mössbauer experiement at 78K are the isomer shift, IS, and the quadrupole splitting, QS. In order to obtain chemical information, the total interaction Hamiltonian for the atom containing terms relating to interactions between the nucleus and the electrons, (hence the chemical environment) is written as

$$H = H_0 + E_0 + M_1 + E_2 \qquad \text{Eq 4.1}$$

where H_0 represents all terms in the Hamiltonian except the isomer shift, quadrupole splitting and magnetic splitting; E_0 represents the experimental isomer shift and is related to the overlap of nuclear charge density with electron density; M_1 refers to the magnetic dipole hyperfine interactions; and E_2 represents the electric quadrupole interactions.

4.3 (ii) The Isomer Shift

The term E_0 presented in the total interaction Hamiltonian in the previous section alters the energy separation between the ground state and the excited state of the nucleus. This causes a slight shift in the position of the observed resonance line and is different in various chemical compounds. For this reason it is generally known as the isomer shift.

Essentially the isomer shift arises because the nucleus, which has a finite volume in the ground state, changes in an excited state. During the transition

between these two states the change in the positive charge density on the nucleus results in a change in the Coulombic interaction between the positive charge on the nucleus and the s-electron density, and, to a much lesser extent p-electron density. An expression for the isomer shift can be derived from electrostatic considerations.[8] Assuming that the nucleus is a uniformly charged sphere of radius R and that the s-electron density at the nucleus given by $[\psi(0)_s]^2$, is constant over nuclear dimensions, the isomer shift, IS, is given by

$$IS = K\left\{[\psi(0)_s]_A^2 - [\psi(0)_s]_S^2\right\}(R_e^2 - R_g^2) \quad \text{eq 4.2}$$

where K is a nuclear constant for ^{119}Sn, e and g refer to the first excited and ground nuclear states respectively, and A and S refer to the absorber and source of γ-radiation respectively. As the difference between R_e and R_g is very small, Eq 4 2 can be reduced to

$$IS = 2KR^2\left(\frac{\delta R}{R}\right)\left\{[\psi(0)_s]_A - C\right\} \quad \text{Eq 4 3}$$

where $\delta R = R_e - R_g$ and C is a constant characteristic of the source used. In these studies the source used was $Ca^{119m}SnO_3$, the numerical value of IS is zero with respect to this material. It can be seen then that IS for a compound is a product of a nuclear term δR and a chemical term $[\psi(0)_s]_A^2$. For ^{119}Sn, δR is a constant so that the IS is directly proportional to the s-electron density at the nucleus Also, as $\frac{\delta R}{R}$ is positive for ^{119}Sn, an increase in electron density at the nucleus gives rise to a more positive IS.

Mössbauer spectroscopy provides a method to monitor the s-electron density at the nucleus which is dependent on the p, d and f electron disposition. Hence, the IS is an important means by which atomic oxidation states can now be investigated.[9] Also, IS data can be used to quantitatively assess the electron-withdrawing power of substituent electronegative groups as well as the degree of π-bonding[10] and back donation from metal atoms to ligands in co-ordination complexes.

4.3 (iii) The Quadrupole Splitting, QS

The existance of an electric quadrupole interaction is one of the useful features of Mössbauer spectroscopy. the nuclear quadrupole moment, Q, is a measure of the deviation from spherical symmetry of the nuclear charge and can be expressed by

$$eQ = \int \rho r^2 (3 \cos^2\theta - 1) d\tau \qquad \text{Eq 4.4}$$

where +e is the charge on the proton and ρ is the charge density in the volume element $d\tau$ at a distance, r, from the centre of the nucleus at an angle θ to the axis of the nuclear spin. When the nucleus is flattened along the spin axis, Q is negative, when the nucleus is elongated along that axis, Q is positive. When the nuclear quadrupole moment experiences an assymetric electric field, an interaction occurs whereby the nuclear quadrupole moment aligns itself either with or accross the electric field gradient and gives rise to a splitting of the nuclear energy state. For example, in the very important γ-ray transition between the $I = \frac{3}{2}$

and $I = \frac{1}{2}$ states as occurs in ^{119}Sn, the nucleus can take on just two orientations, $m_I = \pm \frac{1}{2}$ and $\pm \frac{3}{2}$ when $I = \frac{3}{2}$. The $I = \frac{3}{2}$ state splits in two and a two line spectrum results, Fig. 4.1.

The energy separation between the two levels is called the quadrupole splitting, QS, and is proportional to the electric quadrupole moment and the z-component of the electric field gradient at the nucleus, q, and can be written

$$QS \quad x \; qQ \qquad \text{Eq 4.5}$$

This is a product of a nuclear factor Q, which is constant for the resonant nucleus, and q which depends on the chemical environment.

The interaction of the nuclear quadrupole moment with the electronic environment is given by the Hamiltonian

$$E_2 = \frac{1}{6} \; eQ.\nabla E \qquad \text{Eq 4.6}$$

where ∇E is the electric field gradient at the nucleus and is a tensor quantity and can be written as

$$\nabla_i \; E_j \; = \; - \frac{\partial^2 V}{\partial x_i \, \partial y_i} \; = - \; V_{ij} \qquad \text{Eq 4.7}$$

From this a Cartesian axis can be generated and a principal axis system defined such that all the V_{ij} terms with $i \neq j$ are zero, leaving the finite values V_{xx}, V_{yy}, V_{zz}. Furthermore as ∇E is a traceless tensor

$$V_{xx} + V_{yy} + V_{zz} \; = 0 \qquad \text{Eq 4.8}$$

As a result, in order to completely describe the electric field gradient tensor in its principal axis system, only two parameters need to be specified, and these are V_{zz} = eq being the largest value of V_{ii} and the asymetry parameter η , where

$$\eta = \frac{(V_{xx} - V_{yy})}{V_{zz}} \qquad \text{Eq 4.9}$$

and operate such that $|V_{zz}| \geq |V_{yy}| \geq |V_{xx}|$ and also $0 \leq \eta \leq 1$, where the Z axis is the major axis and the x axis the minor one.

The resulting Hamiltonian is given by

$$E_2 = \frac{eQ}{2I\ (2I-1)}[V_{zz}I_z^{\,2} + V_{yy}I_y^{\,2} + V_{xx}I_x^{\,2}] \qquad \text{Eq 4.10}$$

Although a completely general solution of this Hamiltonian is not possible, an exact expression can be given,[11] for example, if the electric field gradient has axial symmetry corresponding to η = 0, the energy levels are given by

$$E_2 = \frac{e^2q\,Q}{4I(2I-1)}\,[3I_z^{\,2} - I\ (I+1)] \qquad \text{Eq 4.11}$$

An important example in the case of ^{119}Sn is that $I = \frac{3}{2}$ which has two energy levels at $+\frac{e^2q\,Q}{4}$ for $I_z = \pm\frac{3}{2}$ and $-\frac{e^2q\,Q}{4}$ for $I_z = \pm\frac{1}{2}$

The QS therefore gives information about the symmetry of the site occupied by the resonant atom and also the electric field gradient at the nucleus. The QS

is also a very sensitive means of detecting small departures from ideal symmetry and determining the energy of separation between various orbital states.

4.3 (iv) The Recoil-Free Fraction

The interpretation of complex Mössbauer spectra can be simplified if the relative intensities of the components making up the composite spectrum are either known or can be estimated. The recoil-free fraction which determines the intensity of the spectrum is very important in organotin chemistry.

In order for the Mössbauer effect to occur, the nucleus emitting the γ-ray photon should be in an atom which is in a uniform vibrational state within the solid matrix. The vibrational energy of the lattice can only change by discrete amounts 0, $\pm \hbar w$, $\pm 2\hbar w$, etc., and if the recoil energy $Er < \hbar w$ then either 0, or $\hbar w$ units of vibrational energy will be transferred. If a fraction, f, of γ-ray photons are emitted without transfer of recoil energy to the vibrational states of the lattice (zero-phonon transitions), then a fraction (1-f) will transfer one photon, $\hbar w$. The size of the recoil-free fraction, f, is given by

$$f = \exp\left(\frac{-4\pi^2}{\lambda^2} \langle x^2 \rangle\right) = \exp\left(\frac{-E_\gamma^2}{hc^2} \langle x^2 \rangle\right) \quad \text{Eq 4.12}$$

where $\langle x^2 \rangle$ is the mean-square amplitude of vibration of the Mössbauer nucleus in the direction of the observed γ-ray, and E_γ is the energy of the γ-ray photon. This equation tells us that the displacement of

the nucleus must be small compared to the wavelength of the γ-ray photon. This also explains why the Mössbauer effect is not detected in gases and liquids.

4.4 The Chemistry of Organotin Cations in Aqueous Solution

In aqueous solution many organotin cations are subject to a variety of hydrolysis reactions, i.e. by proton transfer from co-ordinated water molecules, and by subsequent condensation reactions of the hydroxo complexes to form dimers and oligomers with several organotin cations.[12] The hydrolyses of alkyltin (IV) species are somewhat simpler than is characteristic of strongly hydrolysing monatomic metal species, because the alkyl groups effectly block co-ordination sites at the metal centre.[12]

Whereas the dipositve dialkyltin (IV) cations are much stronger aquo-acids than the monopositive trialkyltin (IV) species, and at concentrations above 10^{-5}M form significant fractions of polynuclear hydrolysis products,[13,14,15] the trialkyltin (IV) species behave as simple monoprotic acids,[13] and have acid strengths comparable to weak oxyacids. In general the acid strength shown by dialkyltin (IV) species is comparable to that of Sn^{2+}, and as such many solution properties of the R_2Sn^{2+} ions are similar to those of Sn^{2+}. The species distribution for both trialkyl-, and dialkyltin (IV) ions as a function of pH and concentration is shown in Fig. 4.2.[12] Note also that while a species distribution can be calculated for the

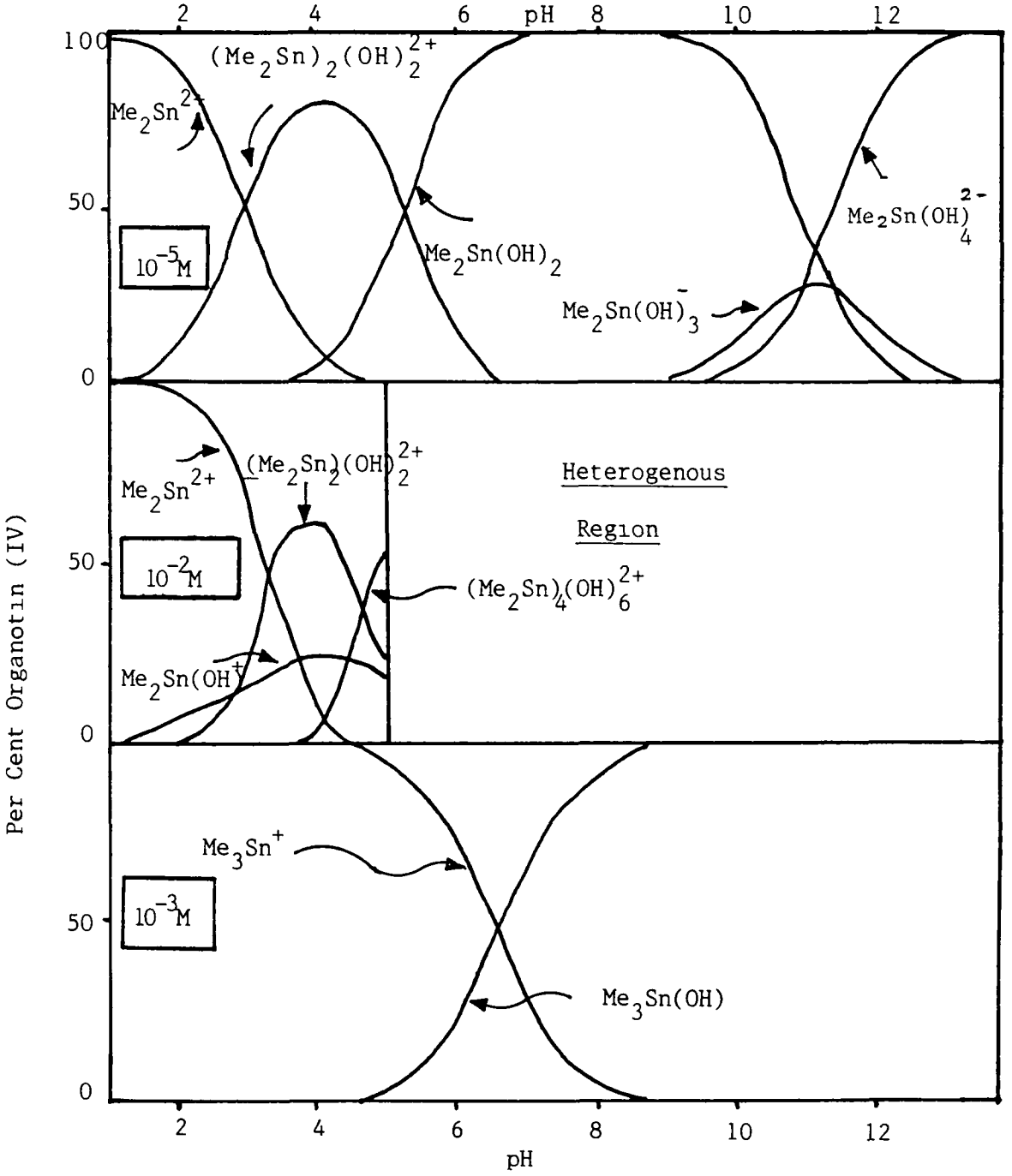

Fig 4 2 Species distribution as a function of pH for organotin (IV) cations used in these studies.

entire pH range, it will be meaningless at higher concentrations should precipitation occur. Fig. 4.2 shows the species formed in the 10^{-2}M dimethyltin dichloride system as being $(CH_3)_2Sn^{2+}$, $(CH_3)_2SnOH^+$, $[(CH_3)_2Sn]_2(OH)_2^{2+}$ and $[(CH_3)_2Sn]_4(OH)_6^{2+}$, and for the 10^{-5} trimethyltin chloride system as being $(CH_3)_3Sn^+$ and $(CH_3)_3SnOH^+$.

In order to interpret spectroscopic measurements, relevant information is required not only showing just what organotin species are present in solutions but also describing how these cations interact with water molecules in the first co-ordination sphere. It has been shown that the structures adopted by both the di- and trialkyltin (IV) ions in aqueous solutions appear to be those which minimize the energy of the organometallic moiety.[13] Furthermore, the dialkyltin (IV) ions have linear C-Sn-C, and the trialkyltin (IV) ions planar SnC_3 skeletons in aqueous solution.[16]

4.5 Experimental

The parent clay used in these studies was a <2 m fraction Wyoming montmorillonite which had been collected by sedimentation, cation-exchanged, washed free of excess salt, dried and stored. The initial centrifugation of the parent clay, cation exchange, and washing procedures, along with Mössbauer spectroscopy experimental details have already been discussed in Chapter 3, and only the pertinent experimental details will be given here.

In the case of three organotin exchanged montmorillonite

systems, finely powdered samples, each of which had been pretreated overnight (usually about 16 hours) at 20, 120, 150, 180, 200, 230, 260, 300, 350, 400, and 450°C, and cooled in a desicator were quickly loaded into a plastic sample disk, covered in aluminium foil and transferred to the Mössbauer cryostat. Air-dried dimethyltin (IV) exchanged montmorillonite samples prepared at pH 2.4 and 4.0 respectively were exposed to the organic bases pyridine, 2-picoline, 2,6-lutidine, and n-butylamine for a further 24 hours, loaded, covered and transferred into the Mössbauer cryostat in the same way. Spectra were then recorded over 512 channels at liquid nitrogen temperature, 78K. In order to obtain spectra of reasonable intensity each spectrum was collected for 24 hours. Recorded spectra were then transferred to the Vax 780 mainframe system via an RS-232 interface.

Experimental curve fitting of each spectrum was carried out using single, double and multi-component system models. Each model took cognisance of the number of different organotin species present in the exchange solution (Fig. 4.2) and also the number of possible exchange sites over which these species may have been distributed. Fig. 4.3 shows the recorded Mössbauer plots including parabolic background for the thermally pretreated dimethyltin (IV) samples prepared at pH 4.0. Fig. 4.4 shows the Mössbauer plots for the same sample series with the parabolic background removed. In the first part of the curve fitting regime, the initial

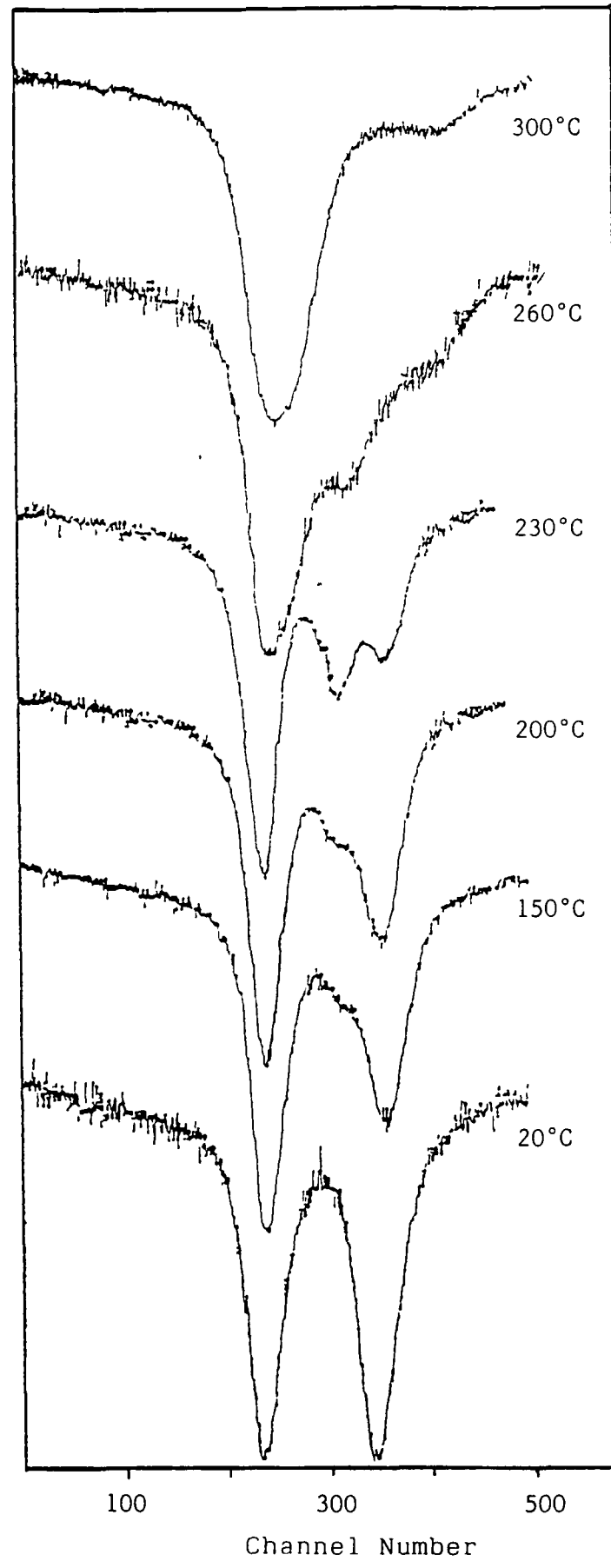

Fig 4.3 Mössbauer plots including parabolic background after thermal pretreatment for the dimethlyltin (IV) exchanged montmorillonite clays prepared at pH 4.0.

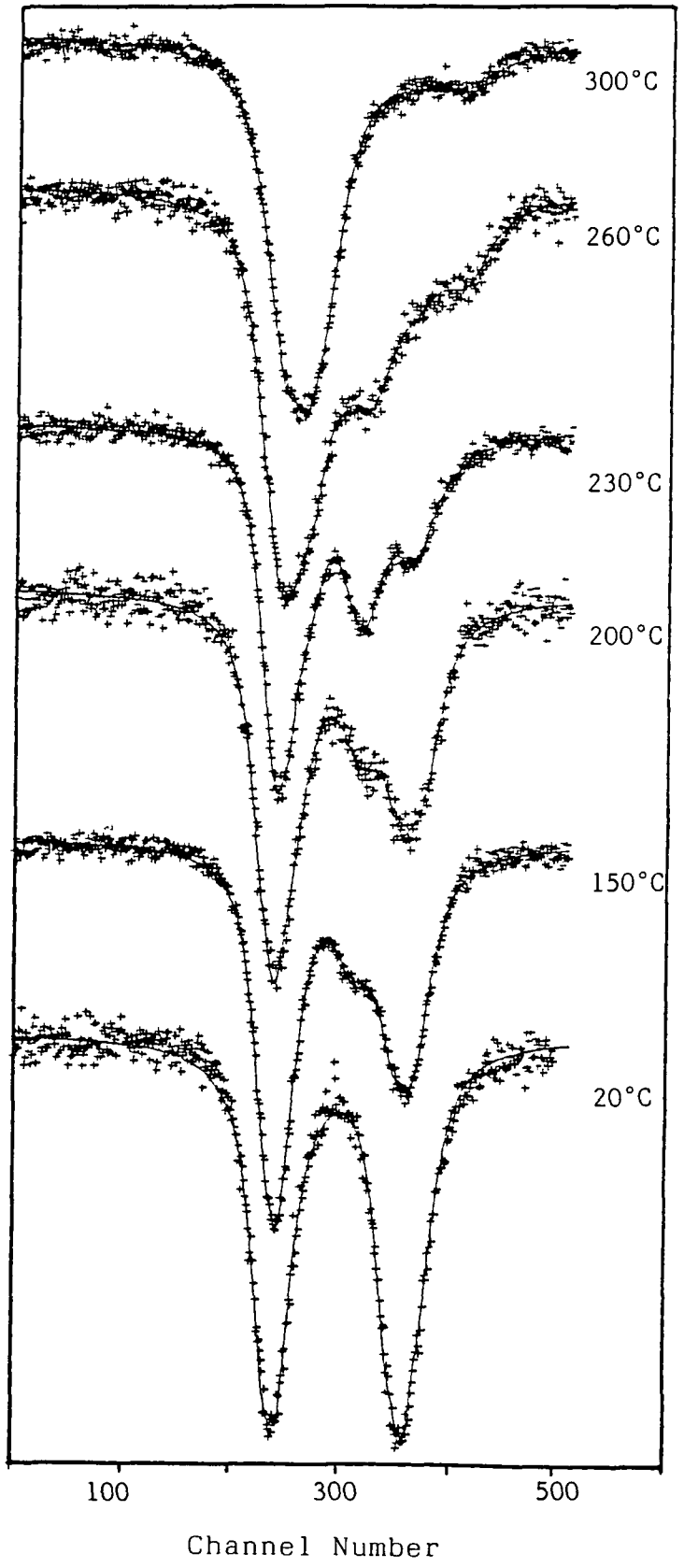

Fig. 4.4 Computer fitted Mössbauer plots after removal of the parabolic background for the thermally pretreated dimethyltin (IV) exchanged montmorillonite clays prepared at pH 4.0

input values of isomer shift, intensity, and quadrupole splitting obtained from existing data and also estimated (Fig. 3.3, Ch.3). were allowed to vary while keeping line half-width values, Γ, for each component fixed at the theoretical value of $0.45 mms^{-1}$. The output parameters from this iteration were then used as input parameters for the next part of the regime which further refined the isomer shift, intensity and quadrupole splitting, and this time also refining line half-width values. The final part of the regime used the output parameters from this second iteration as input parameters. These final output parameters included refined values for the intensity and half-width values for both the low velocity, Γ_L , and the high velocity, Γ_H , wings of each component doublet along with further refined values for isomer shift, quadrupole splitting. This output also included a χ^2 value which is a measure of the "goodness of fit" of the fitted curve to the original experimental one. Compatibility of these final output parameters for each spectrum with the proposed model was determined by visual inspection of the superimposed fitted and original experimental spectra. Where small inconsistancies in the superposition of the fitted and original experimental spectra existed, initial values of isomer shift and quadrupole splitting for some or all components generating the model were gently varied. In the event of this procedure resulting in incomplete superposition or the final output parameters being inconsistent with

interpretive integrity a new model was generated

4.6 RESULTS

Mössbauer spectra are presented as plots of the transmission of resonant -rays through an absorber as a function of Doppler velocity with respect to the source For all results presented here Doppler velocity calibration was based upon the spectrum of natural iron, and isomer shift data quoted are relative to $CaSnO_3$. Analysis of the tin content in the twice exchanged dimethyltin (IV) montmorillonite samples prepared at pH 2 4 and 4 0 respectively indicate that 87% and 64% of the exchange sites, respectively were satisfied by the dimethyltin (IV) species These figures are calculated assuming that the exchange sites are filled by monomeric $(CH_2)_2Sn^{2+}$ at pH 2 4 and dimeric $[(CH_3)_2Sn(OH)]_2^{2+}$ at pH 4 0. It will be seen later in Sec. 4.7 that there is evidence for the presence of other species at each pH. Analysis of the tin content in the $(CH_3)_3SnCl$ sample prepared at pH 3.4 indicated that only 22% of the exchange sites are filled with the monomeric $(CH_3)_3Sn^+$ species The distribution of alkyltin (IV) cations in each of the exchange solutions used throughout this work has already been presented in Fig 4 2 [12] Also, Table 4 1 outlines the pH of the experimental exchange solutions, compares the experimental Sn content for each exchanged clay, (as determined by Atomic Absorption spectrophotometry), with the calculated value for complete exchange.

Figs 4.3 - 4 4 illustrates the effect of

ORGANTIN SYSTEM	EXCHANGE SOLUTION pH	EXPECTED % Sn	EXPERIMENTAL % Sn	% EXCHANGE
Dimethyl Tin	2.4	3.9	3.4	87%
Dimethyl Tin Monohydroxy	4.0	7.8	5.0	64%
Trimethyl Tin 10 x CEC	3.4	7.9	1.7	22%

TABLE 4.1

pH's of experimental exchange systems before and after intercalation along with comparison of predicted and experimental tin content for each exchange system.

increasing the pretreatment temperature on the recorded spectra of the dimeric $[(CH_3)_2Sn]_2(OH)_2^{+2}$ - exchanged clay, each of which were recorded at 78K. In all cases the spectra consisted of several overlapping components which at best could only be partially resolved. Preliminary attempts at fitting the spectra from the three series of organotin (IV)-exchanged samples pretreated in the 120 to 260°C range yielded values for the half-width Γ, far in excess of the theoretical value of $0.45 mms^{-1}$, and generally resulted in unequal linewidths for the low and high velocity wings of the component doublets, Γ_L, and Γ_H respectively. From this then the number of contributing doublets was increased to try to reduce and stabilize these high linewidths. However, this resulted in an unworkable situation where the number of components outstripped the resolving power of the Mössbauer technique. Consequently, given that there are several possible organotin (IV) aquoions present in each of the exchange solutions, Fig. 4.2,[12] and that each of these may be distributed over a range of sites, it was considered expedient to keep the number of components to the minimum consistent with interpretive integrity while striving to minimise χ^2.

Isomer shift, δ ; quadrupole splitting, Δ ; high velocity, Γ_H and low velocity, Γ_L, linewidths; percentage component area; and χ^2 values derived from the recorded Mössbauer spectra within each organotin (IV) exchanged and thermally pretreated system are

collected and presented in Tables 4 2-4.4, while those derived from the recorded spectra of organotin (IV) exchanged samples prepared at pH 2 4 and 4 0 and exposed to the organic bases pyridine, 2-picoline, 2,6-lutidine, and n-butylamine are collected and presented in Tables 4.5 and 4 6.

For each of the thermally pretreated organotin (IV) exchanged systems, the fitting strategy resulted in the identification of up to five, temperature dependent components. Figs 4 5 - 4 10 illustrate how the isomer shift, and quadrupole splitting, of each of these subspectra vary with pretreatment temperature. However some difficulty was encountered in fitting the component with a contribution near 4 0 mms^{-1}, because the low velocity wing of the doublet lay under the main, broad absorption centréd around 0.124 mms^{-1}. The contribution to the area under the Mössbauer resonance from absorption due to the various components within each organotin (IV) system is presented in Figs. 4.11-4.13. For the organotin (IV) exchange samples prepared at pH 2 4 and 4 0 and exposed to the four organic bases, the fitting strategy was consistent in identifying a two component spectrum in each case Figs 4.14-4 15 illustrate how the isomer shift and quadrupole splitting varies with exposure to these bases.

Pretreatment Tempreature	Component	δ /mms^{-1}	Δ /mms^{-1}	Γ_L /mms^{-1}	Γ_H /mms^{-1}	Area %	χ^2
20	●	1.12	2.89	0.60	0.41	43	769
	□	1.26	3.66	0.52	0.49	57	
120	●	1.21	3.13	0.39	0.56	46	
	□	1.27	3.97	0.38	0.47	33	616
	■	0.83	1.67	0.51	0.62	21	
150	●	1.13	2.97	0.36	0.53	41	
	□	1.23	3.84	0.40	0.47	36	632
	■	0.79	1.55	0.47	0.54	23	
180	●	1.11	3.00	0.31	0.61	34	
	□	1.16	3.82	0.32	0.48	18	643
	■	0.78	1.61	0.52	0.59	48	
200	●	1.16	3.16	0.35	0.50	34	
	□	1.25	4.13	0.38	0.47	26	583
	■	0.85	1.74	0.54	0.73	40	
230	□	1.10	3.81	0.34	0.46	14	
	■	0.74	1.85	0.36	0.55	35	583
	○	-0.09	0.81	0.30	0.50	30	
	△	2.05	1.23	0.67	0.82	21	
260	□	1.10	3.87	0.40	0.81	18	
	■	0.95	1.95	0.45	0.69	39	555
	○	0.02	0.89	0.33	0.42	24	
	△	2.70	3.15	0.61	0.75	19	
300	○	-0.07	0.64	0.54	0.57	63	834
	△	2.32	3.09	0.61	1.67	37	
350	○	0.11	0.76	0.55	0.62	100	1400
400	○	0.12	0.81	0.60	0.67	100	2233
450	○	0.12	0.87	0.51	0.57	100	2034

TABLE 4.2

Parameters derived from Mössbauer fitting data for the dimeric $(Me_2Sn)_2(OH)_2^{2+}$-exchanged clay system.

Pretreatment Tempreature	Component	δ/mms^{-1}	$\triangle$/mms^{-1}	Γ_L/mms^{-1}	Γ_H/mms^{-1}	Area %	χ^2
20	●	1.11	3.12	0.54	0.52	49	619
	□	1.27	4.24	0.58	0.55	51	
120	●	1.26	3.27	0.52	0.67	71	538
	□	1.24	4.14	0.42	0.57	29	
150	●	1.13	2.95	0.42	0.53	41	
	□	1.23	3.82	0.40	0.48	36	632
	■	0.79	1.55	0.46	0.55	23	
260	□	1.36	4.47	0.40	0.83	12	
	■	1.00	2.18	0.44	0.89	44	557
	○	-0.04	0.85	0.32	0.34	18	
	△	2.59	3.69	0.59	0.60	26	
350	○	0.11	0.76	0.55	0.62	100	1399
450	○	0.12	0.87	0.51	0.57	100	2034

TABLE 4.3

Parameters derived from Mössbauer fitting data for the monomeric Me_2Sn^{2+}-exchanged clay system.

Pretreatment Tempreature	Component	δ /mms^{-1}	Δ /mms^{-1}	Γ_L /mms^{-1}	Γ_H /mms^{-1}	Area %	χ^2
20	◇	1.32	3.79	0.52	0.63	100	689
120	◇ ⬯	1.43 1.14	3.52 3.63	0.40 0.38	0.56 0.77	46 54	534
180	◇ ⬯ ■	1.45 1.18 0.61	3.17 3.95 2.21	0.43 0.38 0.31	0.79 0.44 0.70	41 27 31	472
220	⬯ ■ ○ △	1.21 0.83 0.03 3.45	3.88 1.85 0.90 1.82	0.38 0.41 0.26 0.40	0.59 0.52 0.48 0.39	31 40 21 8	535
300	○ △	0.06 3.22	0.76 2.15	0.51 0.99	0.60 0.72	66 34	521
400	○	0.15	0.80	0.57	0.67	100	1021

TABLE 4.4

Parameters derived from Mössbauer fitting data for the monomeric $(Me)_3Sn^+$-exchanged clay system.

Organic Base	Component	δ /mms^{-1}	$\triangle$ /mms^{-1}	Γ_L /mms^{-1}	Γ_H /mms^{-1}	Area %	χ^2
Pyridine	□	0.95	1.99	0.39	0.39	64	530
	○	1.06	2.91	0.38	0.57	36	
2-Picoline	□	0.94	2.06	0.42	0.43	65	613
	○	1.09	2.94	0.41	0.48	35	
2,6-Dimethyl pyridine	□	0.98	2.08	0.45	0.50	62	531
	○	1.07	3.02	0.42	0.49	38	
n-Butylamine	□	0.87	1.72	0.53	0.68	70	508
	○	0.55	2.56	0.45	0.43	30	

TABLE 4.5

Parameters derived from Mössbauer fitting data for the dimeric $(Me_2Sn)_2(OH)_2^{2+}$-exchanged clay prepared at pH 4.0 and exposed to the vapour of organic bases.

ORGANIC BASE	Ka	pKa
Pyridine	5.62×10^{-6}	5.25
2-Picoline	1.07×10^{-6}	5.97
2,6-Lutidine	1.02×10^{-7}	6.99
n-Butylamine	1.69×10^{-11}	10.77

TABLE 4.6

Acid dissociation and pKa values of organic bases

Organic Base	Component	δ /mms^{-1}	$\triangle$ /mms^{-1}	Γ_L /mms^{-1}	Γ_H /mms^{-1}	Area %	χ^2
Pyridine	□	1.00	2.26	0.42	0.47	53	623
	○	1.12	3.33	0.40	0.48	47	
2-Picoline	□	0.96	1.98	0.38	0.38	52	536
	○	1.07	2.86	2.39	0.53	48	
2,6-Dimethyl pyridine	□	0.96	2.11	0.45	0.56	61	666
	○	1.07	3.02	0.41	0.51	39	
n-Butylamine	□	0.96	1.74	0.41	0.54	49	545
	○	0.90	2.40	0.40	0.50	51	

TABLE 4.7

Parameters derived from Mössbauer fitting data for the monomeric Me_2Sn^{2+}-exchanged clay prepared at pH 2.4 and exposed to the vapour of organic bases.

4 7 Discussion

The observed range of chemical isomer shifts for the ^{119}Sn resonance in tin compounds falls within the range of between -0 5 and 4 5 mms^{-1} with respect to SnO_2. Shifts greater than 2 9 mms^{-1} are diagnostic for the Sn(II) oxidation state, whereas Sn(IV) compounds give rise to shifts between 0.55 and 2.20 mms^{-1}. However, although the isomer shift is useful in assigning the oxidation state of tin, it is the quadrupole splitting which yields an insight into the geometry of the complex For example, in R_2SnX_2 dialkyltin compounds, where R denotes the alkyl group, a Δ value near 4.0mms^{-1} indicates that the R groups are trans to the central tin atom Hence the quadrupole splitting is large when the angle, θ, between the alkyl groups is large, and reaches a minimum when θ is 90° and the alkyl groups are cis to the central tin

Recent partial quadrupole splitting calculations for Bu_2SnCl_2 dispersed in polyvinylchloride[17] at 1 2% (w/w) have shown that the Δ value for the butyl groups in trans configuration in an octahedral geometry is 3.54 mms^{-1} The quadrupole splitting resulting from butyl groups in cis configuration in trigonal bipyramidal co-ordination depends upon whether these groups are both in the equatorial plane ($\theta \simeq 120°$, Δ = 3.07 mms^{-1}) or one occupies an axial position ($\theta \simeq 90°$, Δ = 2.53 mms^{-1}).

The trends for the Mössbauer parameters within the three thermally pretreated organotin (IV) exchanged montmorillonites, along with those samples exposed to

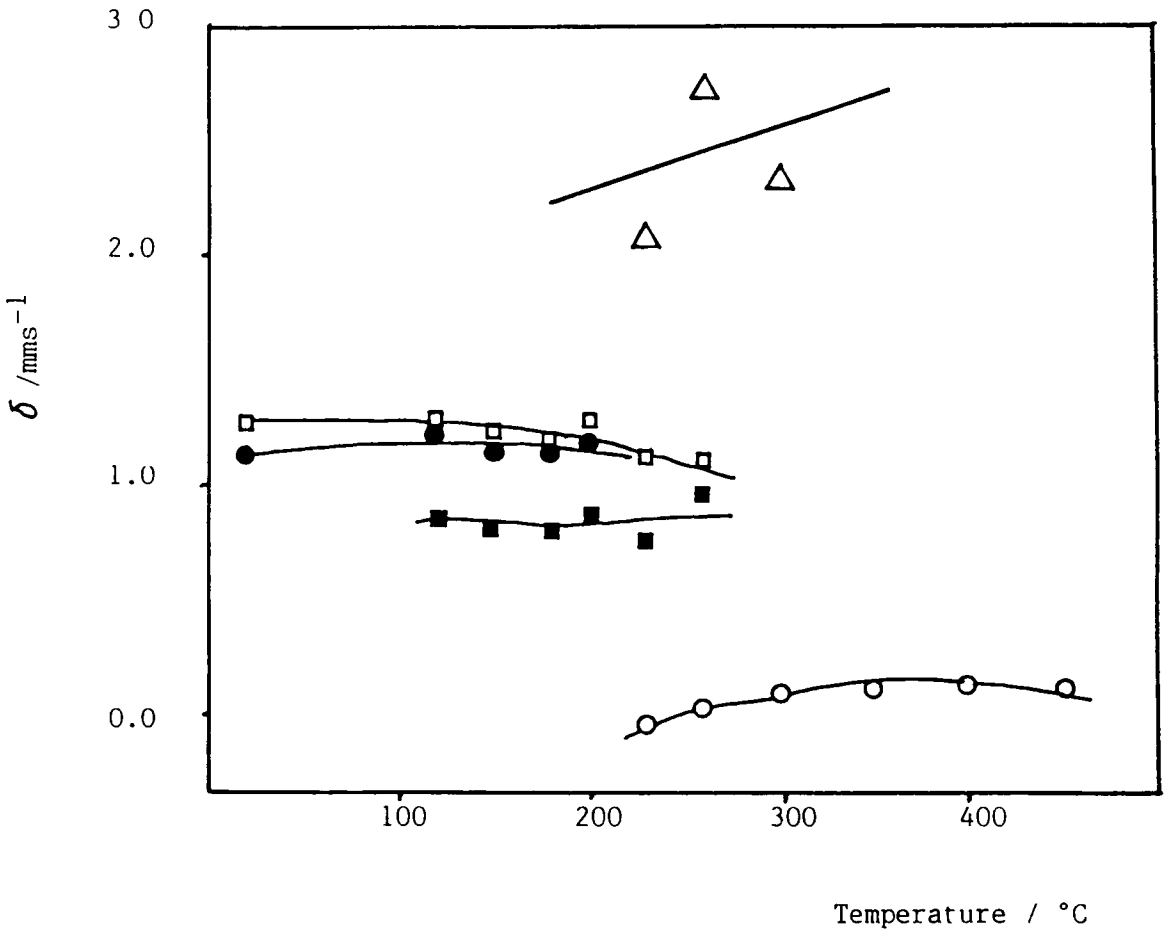

Fig 4.5 Temperature dependence of isomer shift, δ, for the dimethyltin (IV) exchanged montmorillonite prepared at pH 4.0. Symbols as in Table 4 2 (p 112)

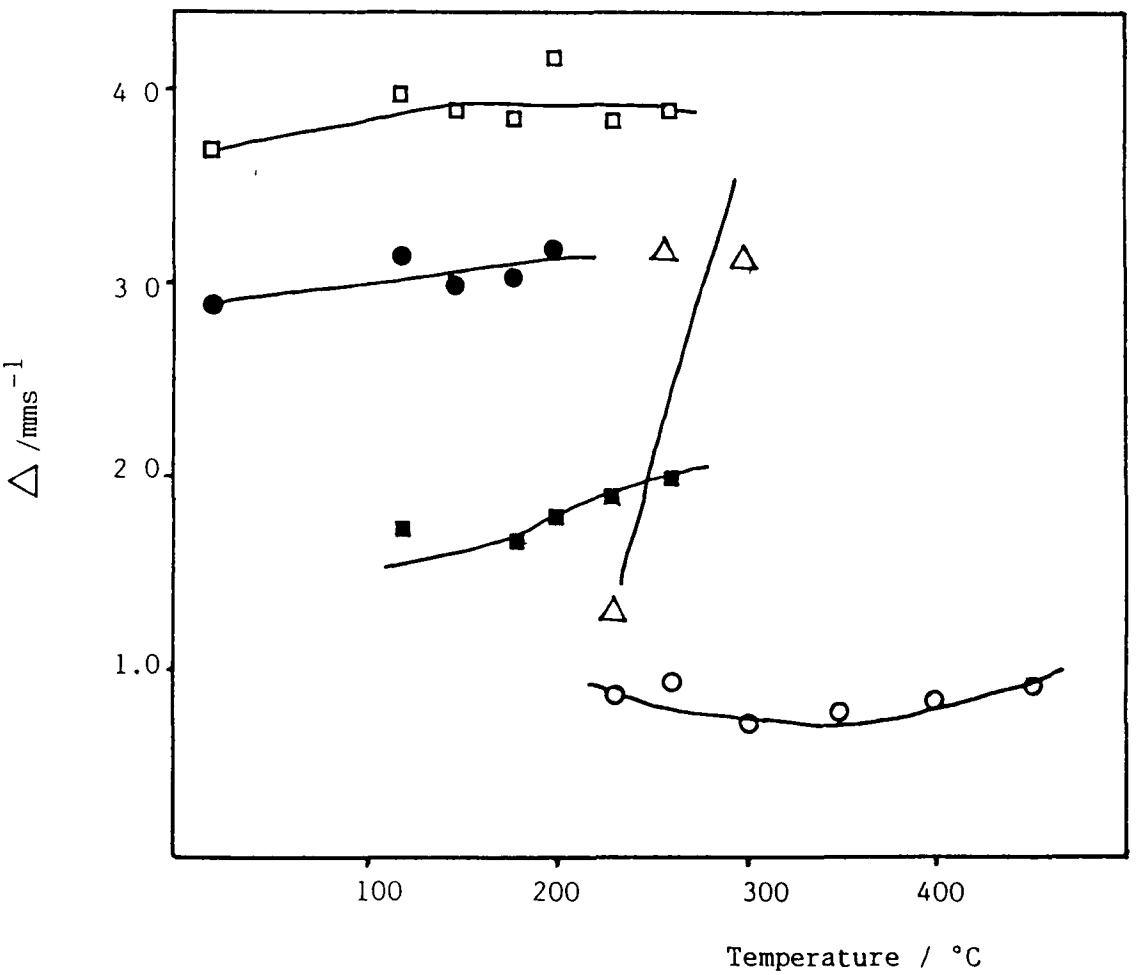

Fig 4.6 Temperature dependence of quadrupole splitting, Δ, for the dimethyltin (IV) exchanged montmorillonite prepared at pH 4.0.
Symbols as in Table 4 2 (p 112)

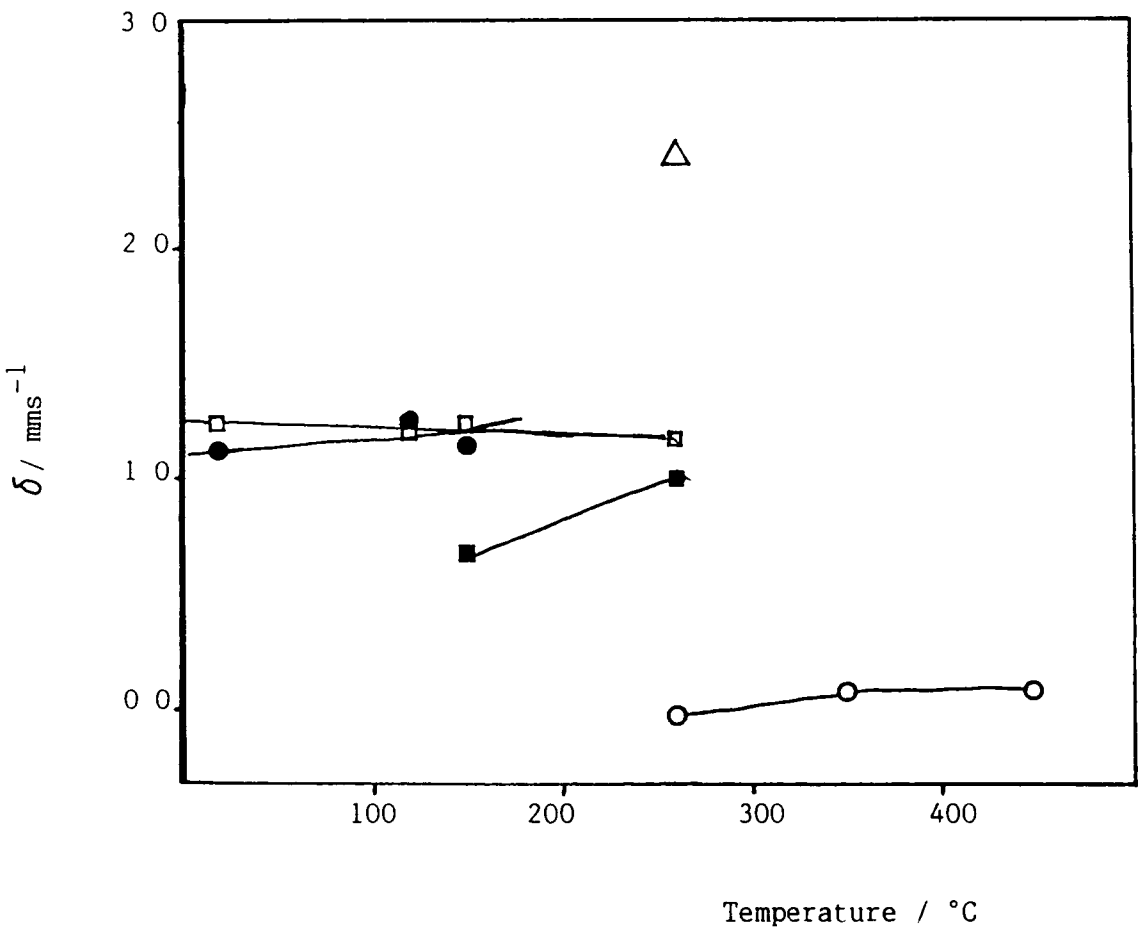

Fig. 4.7 Temperature dependence of isomer shift, δ , for the dimethyltin (IV) exchanged montmorillonite prepared at pH 2.4.

Symbols as in Table 4 3 (p 113)

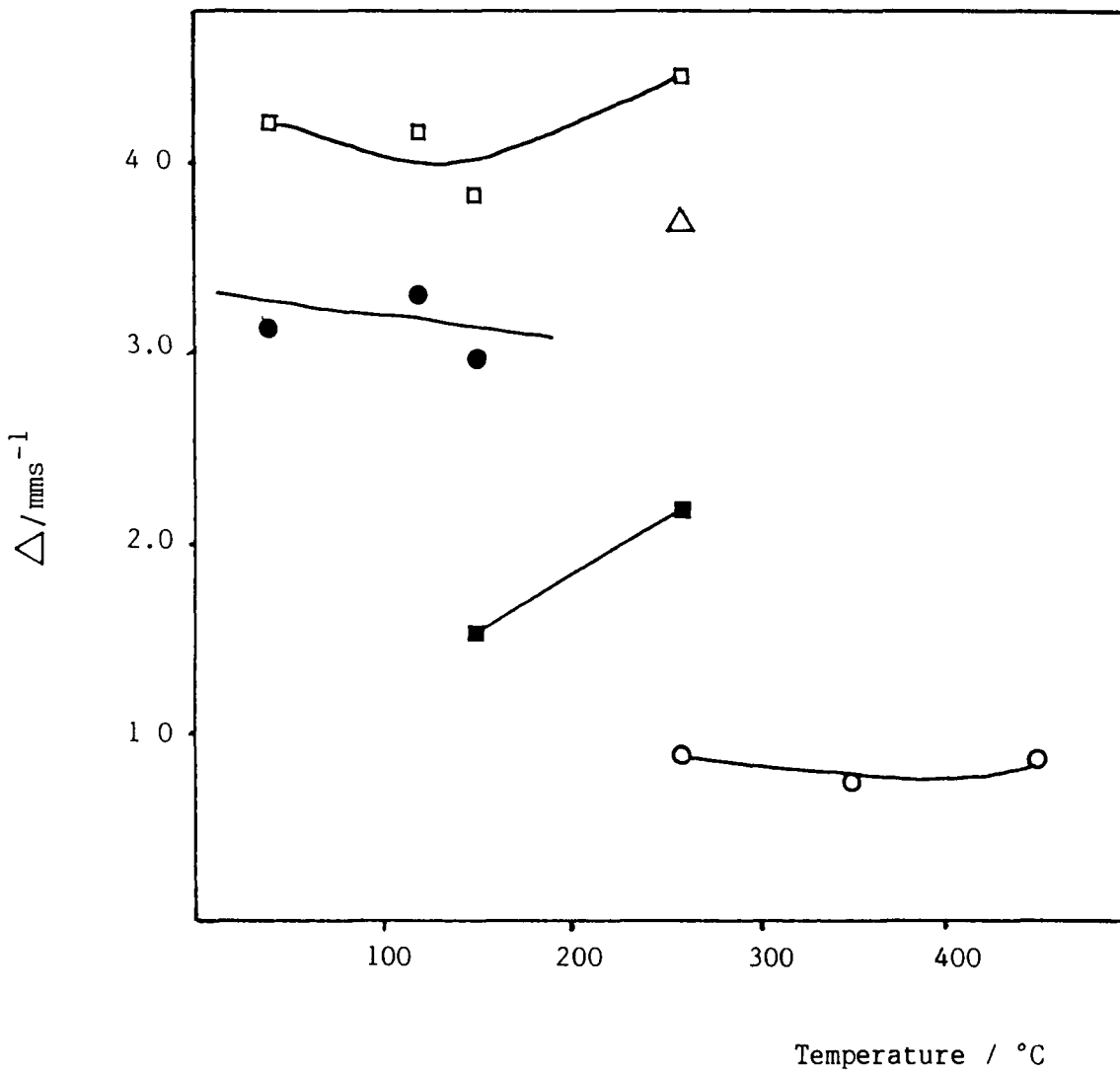

Fig 4 8 Temperature dependence of quadrupole splitting, △, for the dimethyltin (IV) exchanged montmorillonite prepared at pH 2.4.

Symbols as in Table 4 3 (p 113)

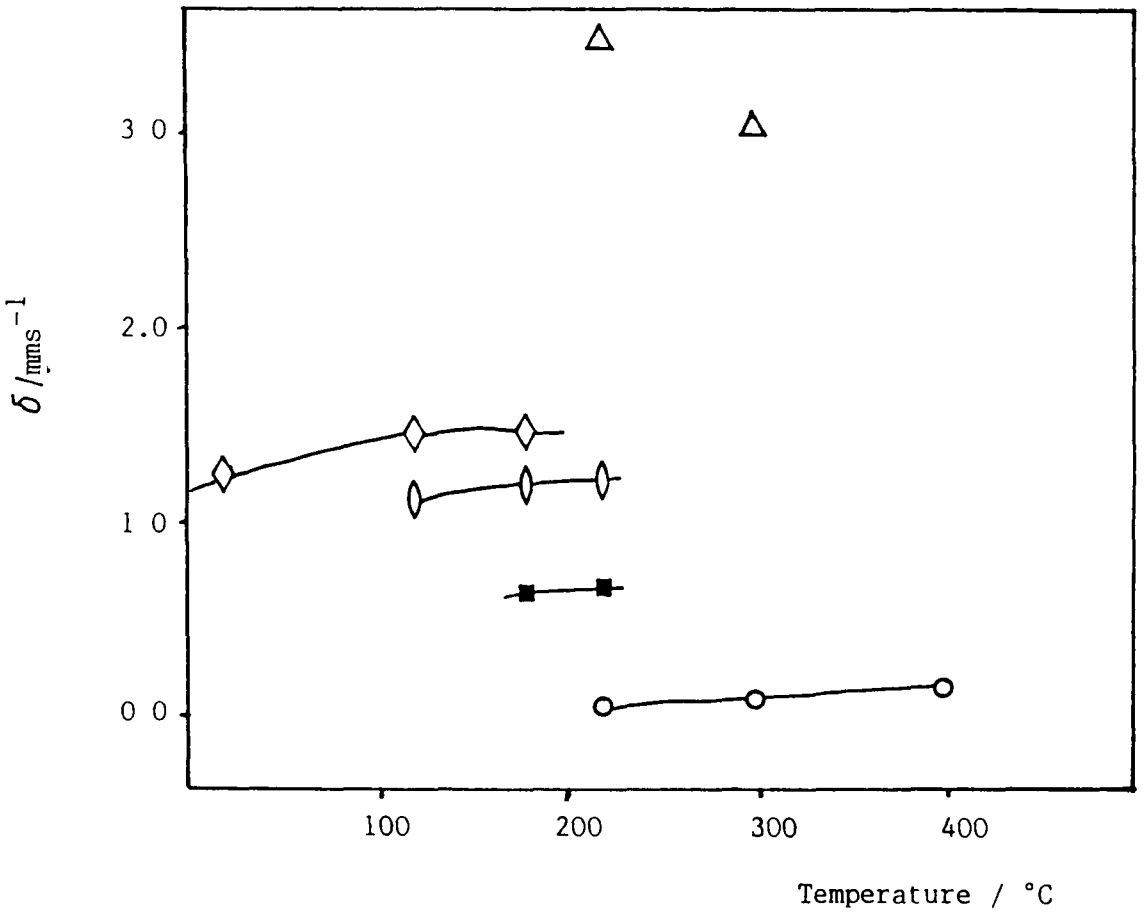

Fig 4 9 Temperature dependence of isomer shift, δ, for the Trimethyltin (IV) exchanged montmorillonite
Symbols as in Table 4 4 (p 114)

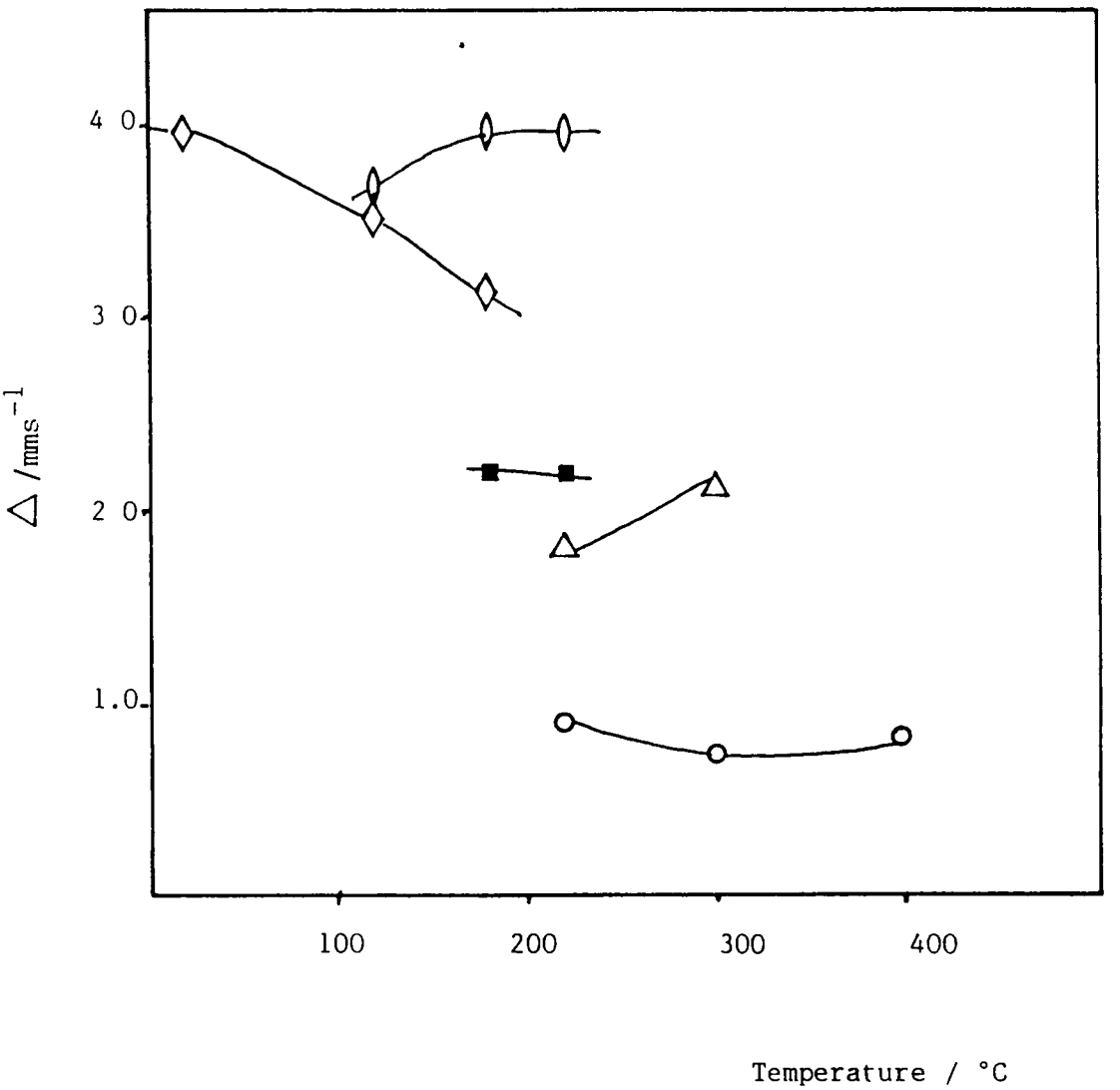

Fig. 4 10 Temperature dependence of quadrupole splitting , △, the trimethyltin (IV) exchanged montmorillonite.
Symbols as in Table 4 4 (p 114)

the organic bases, observed in these studies, provides considerable insight into the intramolecular changes taking place within the interlayer.

4.7 1 Dialkyltin (IV) Exchanged Montmorillonite Prepared at pH 4.0

Initial attempts to fit the Mössbauer spectrum of the dimethyltin (IV) exchanged air-dried sample prepared at pH 4 0, to one or three component doublets, as suggested by the number of organotin (IV) species existing at this pH (Fig 4.2), resulted in an unacceptably high χ^2 value for the one component fit, and unrealistic values for component line halfwidths, Γ, for the three component fit. However when the spectrum of this sample was fitted using only two component doublets, the spectrum revealed the presence of two components with Δ values averaging out near 3 0 and 3 8 mms^{-1}, (Table 4 2) Assuming that these values have physical significance, instead of signalling end members of a range of sites which the Mössbauer technique could not resolve, then the following interpretation may be made A Δ value of 3 66 mms^{-1} is indicative of a species in which the methyl groups are trans to the central tin atom in octahedral co-ordination. The other component, having a Δ value of 2.89 mms^{-1}, is consistent with a moiety in which the methyl groups are cis to the central tin atom in the equatorial plane of a five-co-ordinate structure.

Following thermal treatment for 16 hours at 120°C, a third component was resolved having δ , and Δ

values of 0 84 and 1 68 mms^{-1} respectively These values correlate well with the values reported by Parrish and Johnson[18] for dimethyl tin oxide, Me_2SnO and appears plausible given the environment in which the tin finds itself. However, caution must be observed with this interpretation because these parameters are for pure Me_2SnO which forms trimers in the solid state However, if Me_2SnO is present in the clay then it will almost certainly be oligomorised if not polymerised, and thus the local geometry at tin will be the same

For the sample thermally pretreated at 200°C, the same three components are resolved. The main transformation taking place was the conversion of the two components with isomer shift values of 1 1 and 1 2 mms^{-1}, respectively to Me_2SnO This is seen in Table 4.2 by the gradual increase in the percentage area of the Me_2SnO component, which has an average isomer shift near 0 8 mms^{-1}.

Thermal pretreatment up at 260°C, Fig 4 4, results in a dramatic decrease in intensity of the high velocity wing apparent in the air-dried sample. The emergence of a third wing, seen in the 150°C spectrum, which increases in intensity up to 260°C is thought to identify the presence of Me_2SnO. The fitting strategy found to be best suited to the samples pretreated at 230°C and 260°C respectively were based on four component models. Cross reference with Table 4.7, listing standard recognised values for organotin Mössbauer parameters, identifies the very characteristic

isomer shift and quadrupole splitting values for the two components resolved by the computer program at 230°C and 260°C as SnO[19] and SnO_2 [19] An interesting feature of the recorded spectra of samples treated in this temperature range is that the trans species, having isomer shift and quadrupole splitting values of 1.1 and and 3.8 mms^{-1} respectively, is still present

On thermal pretreatment, at 300°C, computer fits based on models comprised of three and four component doublets were rejected In most cases computer fits were rejected on the basis that the computed component line widths were either too narrow or too broad. However, the best fit decided on for the 300°C pretreated sample was based on a two component doublet model. the components were identified as SnO and SnO_2, via cross reference with Table 4.7.

After thermal pretreatment at 450°C the fitting strategy resulted in computer fits based on one component models. The poor χ^2 values associated with these fits (Table 4 2) were attributed to the presence of small quantities of unidentified phases which could not be resolved using models based on more than one component

Reference to Fig. 4 5 demonstrates the very close agreement for the isomer shift values of the cis and trans components seen at lower temperatures. However, Fig. 4.6 confirms by the consistent separation of quadrupole splitting values of these components that they are different and independent of each other. The

COMPOUND	δ /mms^{-1} ±0.02	$\triangle$ /mms^{-1} ±0.02	REFERENCE No
SnO_2	0.00	0.00	8
SnO (black)	2.71	1.45	19
SnO (Red)	2.60	2.20	19
Me_2SnCl_2	1.52	3.62	21
Me_2SnO	0.92	1.82	18
$Me_2SnCl_2.py_2$	1.27	3.83	26
Bu_2SnCl_2	1.60 1.50	3.25 3.02	17 PVC @2%
Me_3SnCl	1.43 1.57	3.32 3.55	22 in graplite
Me_3SnOH	1.07	2.71	23
$Me_2Sn.oxin_2$*	0.88	1.98	27

TABLE 4.8

Mössbauer parameters and cited reference sources for compounds cross-referenced in this work.

*oxin = 8-Hydroxyquinoline.

temperature dependence of the percentage areas of each component, seen in Fig 4 11 outlines the interconversion between components occurring throughout the thermal pretreatment regime.

Overall, by assuming that the recoil-free fraction of all resolved components are equal, Figs. 4.4 and 4.11 together with the data in Table 4.2 suggest the following trends - (1) Both the cis and trans components are unstable with respect to increased pretreatment temperature but the contribution from the trans species can be identified to higher temperatures, (2) Both the cis and trans species convert to Me_2SnO, (3) At temperatures greater than 200°C both the remaining trans species, and Me_2SnO convert to oxides of Tin. Further evidence for this interpretation has been reported very recently by Petridis et al.,[20] for a dimethyltin (IV)-exchanged montmorillonite prepared at pH5 5, and thermally pretreated up to 300°C However, the computer fitting strategy used was constrained in that the reported line widths referred to each component as a whole and not to the low and high velocity wings of each component doublet. This may account for a component due to SnO not being reported as is in the case of this present work.

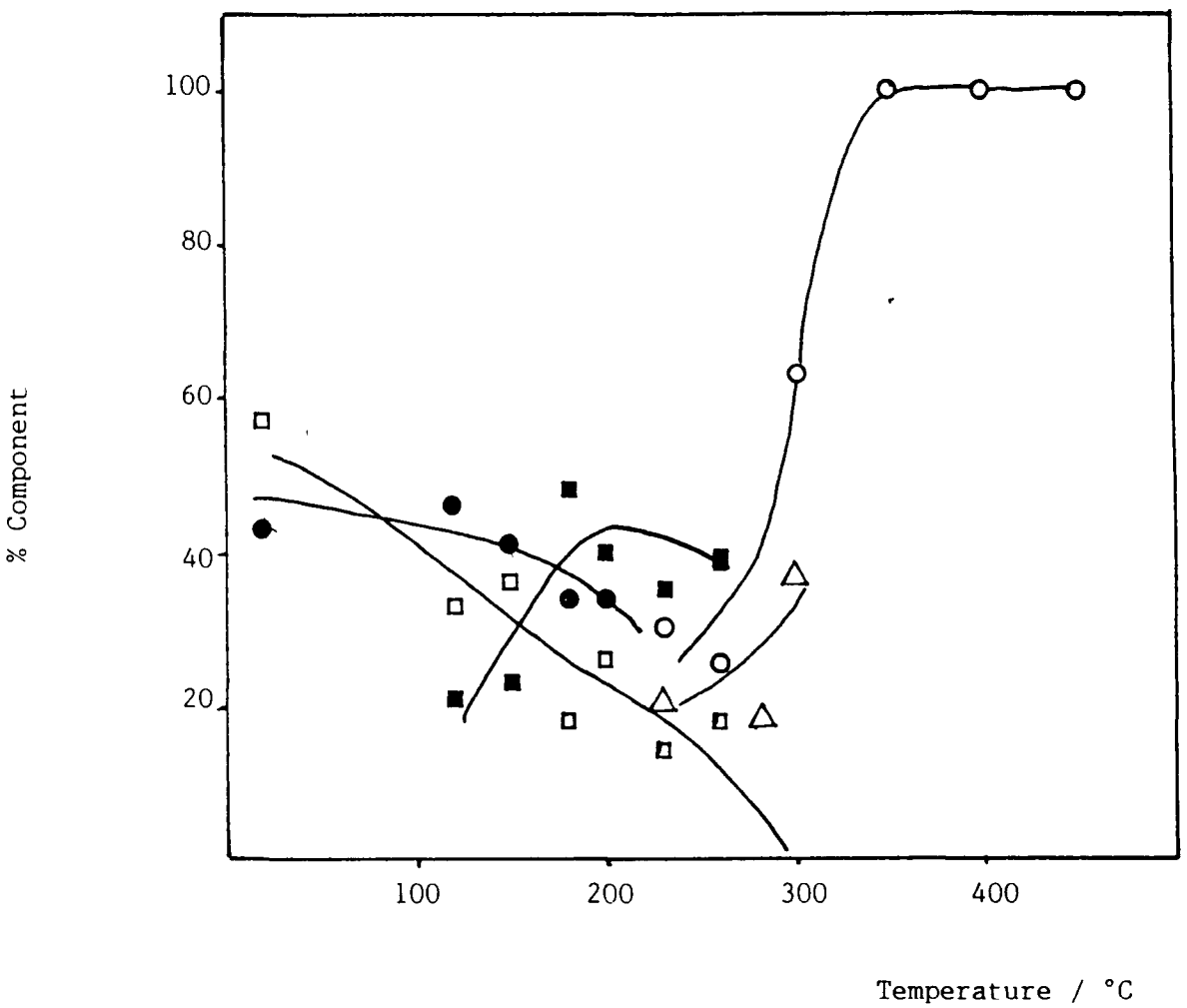

Fig 4 11 Temperature dependence of component (%) areas for the dimethyltin (IV) exchanged montmorillonite prepared at pH 4.0.
Symbols as in Table 4 2 (p 112)

4 7 2 Dialkyltin (IV) Exchanged Montmorillonite Prepared at pH 2.4

In the case of the air-dried dimethyltin (IV) exchanged montmorillonite system prepared at pH 2.4, a fitting strategy comprising a two component doublet model as suggested by the number of organotin (IV) species existing at this pH, (Fig 4 2) was deemed most suitable The output results for this spectrum demonstrates the presence of two component doublets (Table 4 3), corresponding to the cis and trans species previously seen in the sample prepared at pH 4.0. However the trans species shows a quadrupole splitting somewhat larger than that seen in the sample prepared at pH 4.0 Both the isomer shift and quadrupole splitting for this component are also larger than those seen for Me_2SnCl_2, which exhibits a considerably distorted trans octahedral geometry in the solid state.[21] It is also seen that the low velocity line widths, Γ_L , of the component doublets in the air-dried samples prepared at pH 2.4 and 4 0 agree closely but the high velocity wings, Γ_H , in the sample prepared at pH 2.4 are larger than those in the corresponding sample prepared at pH 4 0. This is not surprising given the range of environments the cations may find themselves in. For example, there are both interlayer and edge sites. However, at the exchange levels used in this work, it is assumed that the cations are predominantly held in the interlayer region. Furthermore, the spatial distribution of these cations within the interlayer may

reflect the different isomorphous substitution patterns within the layers

Initial attempts to fit the sample prepared at pH 2 4 and pretreated at 120°C to a three component doublet model as used in the 120°C pretreated sample prepared at pH 4.0, resulted in unacceptably low values for the low velocity line widths for the components seen in the air-dried sample Although a two component fitting strategy produced acceptable values for isomer shifts, quadrupole splittings, line widths and χ^2 value, the distortion of the percentage peak areas may be due to system resolving difficulties

Thermal pretreatment to 150°C using a three component fitting strategy identifies Me_2SnO having an isomer shift of approximately 0 8 mms^{-1} and a percentage peak area of 23%, identical to the 150°C pretreated sample prepared at pH 4 0

For the sample pretreated at 260°C, the fitting strategy found to produce the most acceptable and reasonable results was again based on a four component model. Table 4.3 suggests that it is the trans isomer and Me_2SnO that converts to oxides of tin. Both components are readily identified by their characteristic isomer shifts and quadrupole splittings (Table 4.8).

Further thermal pretreatment at 350°C and 450°C respectively demonstrates that a fitting strategy based on a single component doublet resolved the most meaningful output parameters. These output parameters represents SnO_2 suggesting that above 260°C the

remaining trans species along with Me_2SnO are converted to SnO_2.

Reference to Fig 4.7 and 4 8 and to Table 4.3 clearly identifies the presence of five discreet components, resolved by the computer fitting program for samples prepared at pH 2 4, and thermally pretreated in steps up to 450°C. Although the isomer shift values, Fig. 4.7, for the cis and trans components seen at lower temperatures agree closely, the quadrupole splitting values, Fig 4.8, for each component confirms that they are indeed different species The temperature dependence of the component percentage areas for the samples prepared at pH 2.4 seen in Fig. 4 12, suggests that the interconversion processes to SnO_2 agree closely with those occurring in the thermally pretreated samples prepared at pH 4.0. Essentially the increase in percentage component area of the Me_2SnO species with increasing pretreatment temperature occurs at the expense of the decreasing percentage component areas of the cis and trans components

4 7 3 Trimethyltin (IV) Exchanged Montmorillonite Prepared at pH 3.4

Analysis of the Mössbauer fitted data for the monomeric $(CH_3)_3Sn^+$-exchanged montmorillonite sample at pH 3.4 shows the air dried sample to consist solely of a single component doublet. This in turn is consitent with the number of species expected,[12] (Fig. 4.2). In view of the parameters in Table 4.8, the parameters for tin in this montmorillonite sample are not

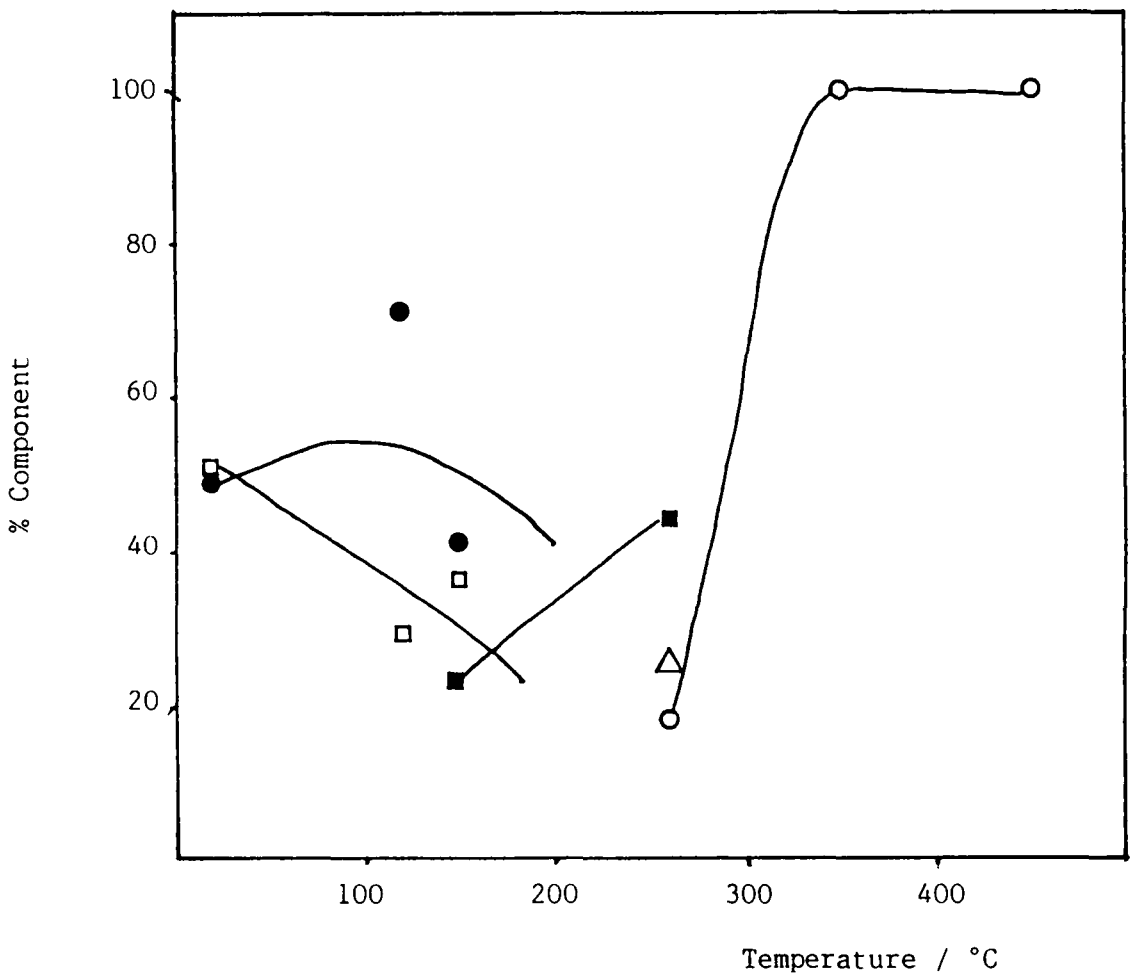

Fig 4 12 Temperature dependence of component (%) areas for the dimethyltin (IV) exchanged montmorillonite prepared at pH 2.4.
Symbols as in Table 4 3 (p 113)

inconsistent with the presence of a trimethyl tin cation. It can also be seen from Table 4 4 that the widths of both the low velocity and high velocity wings of this single component doublet are somewhat broader than expected This may be interpreted as a mean value of isomer shift and quadrupole splittings associated with a range of exchange sites that this species may find itself in, and for which the computer program could only resolve a single component. Although two and three component models having very similar isomer shift and quadrupole splitting input parameters were used to try and tease out this possible narrow range of sites, the computed output parameters were seen to be unrealistic. It should also be pointed out that the very low exchange level for this system, (Table 4 1), may also explain the inability of the program to resolve more than one component having similar isomer shifts and/or quadrupole splittings.

After thermal pretreatment at 120°C a second component doublet is resolved As the pH of the exchange solution was 3 4, and the interlayer environment is quite acidic,[20] it is reasonable to assume that this species is not $(CH_3)_3SnOH$,[23] which is seen to be formed in solution at pH 5.5 (Fig. 4.2).[12] Of the two other possibilities, i.e. partial demethylation or internal rearrangement of exchange environments, it is thought that the latter may be more plausible given that the Sn-C bond is 193 $kJmol^{-1}$.[24]

Further thermal pretreatment at 180°C, resolved

a third component having isomer shift and quadrupole splitting values of 0 62 and 2 22 mms^{-1} respectively These values closely agree with those reported for Me_2SnO[18] and also seen in both of the organotin (IV) exchanged samples prepared at pH 2 4 and 4 0 and thermally pretreated to 180°C. The transformation to, and growth of this component up to~31% takes place at the expense of the component, having isomer shift and quadrupole splitting output parameters of 1 14 and 3.63 mms^{-1} respectively, which was resolved at 120°C (Table 4.4)

Thermal pretreatment at 220°C indicated that a four component model comprising a component similar to that seen in the air-dried sample, Me_2SnO, SnO and SnO_2 produced the most reasonable set of output parameters. As in the earlier cases of dialkyltin (IV) spectra in this temperature region, the output parameters for three and five component model fits produced unequal widths for both the low velocity and high velocity wings of component doublets and thus were rejected Furthermore, the component exhibiting values of isomer shift and quadrupole splitting of 1.45 and 3.17 mms^{-1} at 180°C has disappeared and SnO_2 and SnO, evidenced by their very characteristic isomer shift and quadrupole splitting values, have appeared together with a component with Δ equal to 3.9mms^{-1}.

At pretreatment temperatures above 220°C, the remaining fraction of the component having isomer shift and quadrupole splitting values of 1.20 and 3.90 mms^{-1}

and evident at 180°C is converted to SnO_2 at 300°C. Above 300°C Table 4.4 shows that the SnO species is transformed to SnO_2

Reference to Figs 4 9 and 4 10 and to Table 4.4 identifies the presence of five discreet components resolved by the computer program for the trimethyltin (IV) exchanged montmorillonite sample prepared at pH 3.4 and thermally pretreated in steps up to 400°C. Once again assuming that the recoil free fraction of each resolved component was the same the following thermal transformation trend is suggested by reference to Fig. 4.13. (1) the trimethyltin (IV) exchanged species is unstable with respect to pretreatment temperature, (2) below 220°C, this species seen to occupy more than one exchange site and is partially demethylated to Me_2SnO, (3) at higher temperatures, above 300°C all the components remaining along with Me_2SnO are transformed to SnO_2

4 7 4 **Dialkyltin (IV) Exchanged Montmorillonites Exposed to Organic Bases.**

The Mössbauer spectral analysis of the air-dried dialkyltin (IV) exchanged montmorillonite samples prepared at pH 4 0 and exposed to vapour of the organic bases pyridine, 2-picoline, 2,6-Lutidine, and n-butylamine gave rise to a set of output parameters which were quite dramatic across the series. In each case a model consisting of two component doublets resulted in the most acceptable output parameters, (Table 4.5). Cross reference between Tables 4.2 and 4.5 shows that the formation of the room temperature exchanged

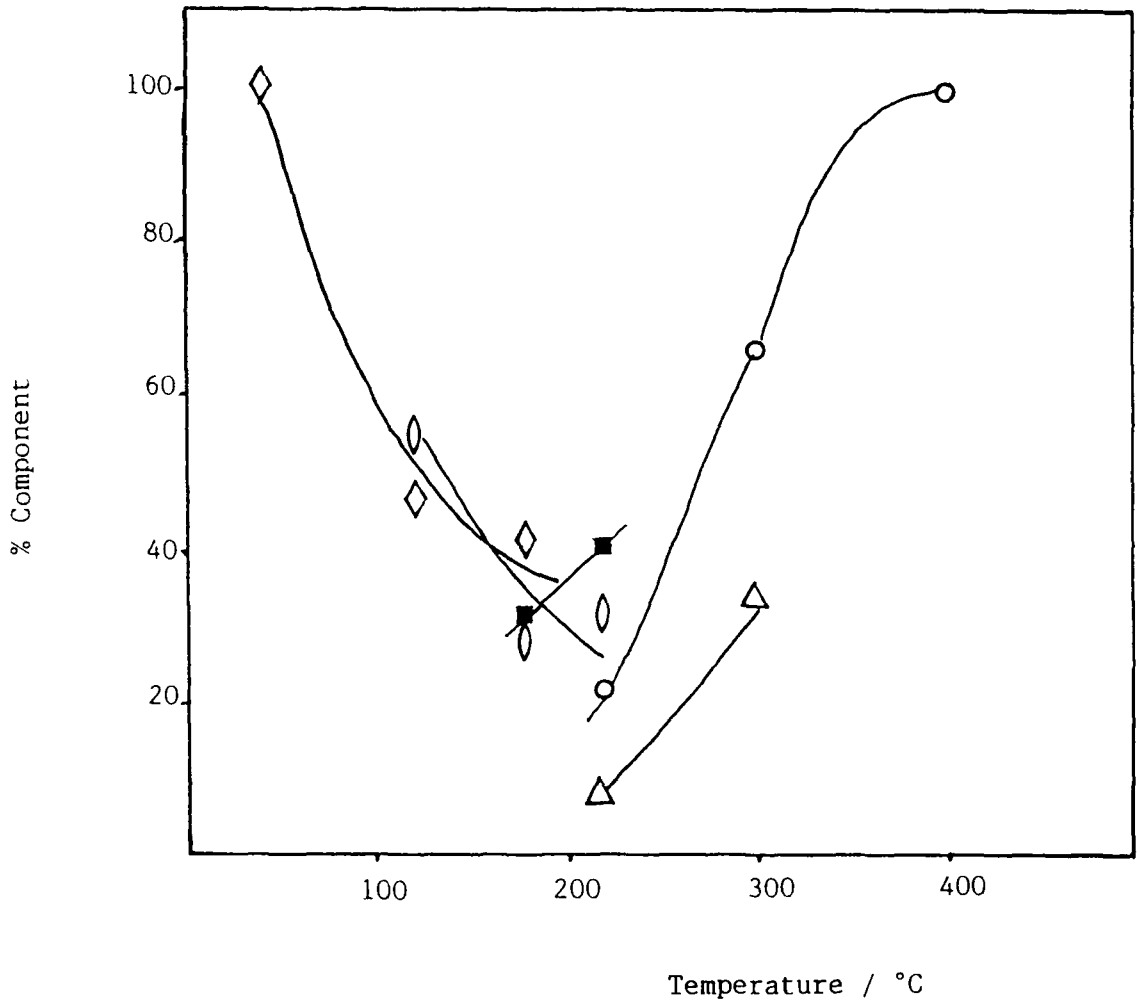

Fig. 4 13 Temperature dependence of component (%) areas for the trimethyltin (IV) exchanged montmorillonite. Symbols as in Table 4 4 (p 114)

dialkyltin (IV)-organic base adduct leads to a lowering of both isomer shift and quadrupole splitting output parameters for both components compared to the non-organic base exposed system. This effect is even more pronounced following exposure to the straight chained aliphatic base, n-butylamine. Considering the range of acid dissociation constants and pK_a values of the organic bases used in this study (Table 4.6),[25] the lower isomer shift and quadrupole splitting values seen for both components in the air dried sample exposed to n-butylamine vapour may be explained in terms of n-butylamine being a weaker acid (stronger base) than pyridine and each of the substituted alkylpyridines. In addition, n-butylamine being a linear molecule and smaller than the substituted alkyl pyridines is less likely to be affected by steric hinderance in forming adducts with the intercalated dialkyltin (IV) species. Furthermore it is interesting to note the close agreement in isomer shift and quadrupole splitting values for each resolved spectral component in the air dried samples exposed to the vapour of pyridine, 2-picoline, and 2,6-lutidine, (Fig.4.14). Reference to Tables 4.5 and 4.6 and Fig. 4.14 suggests that although there is an increase in pK_a values for these organic bases (as expected with increasing substitution of electron-releasing and ring activating alkyl groups), the effect of exposure to each base seems to be limited to the formation of two component adducts whose isomer shift and quadrupole splitting values are similar across

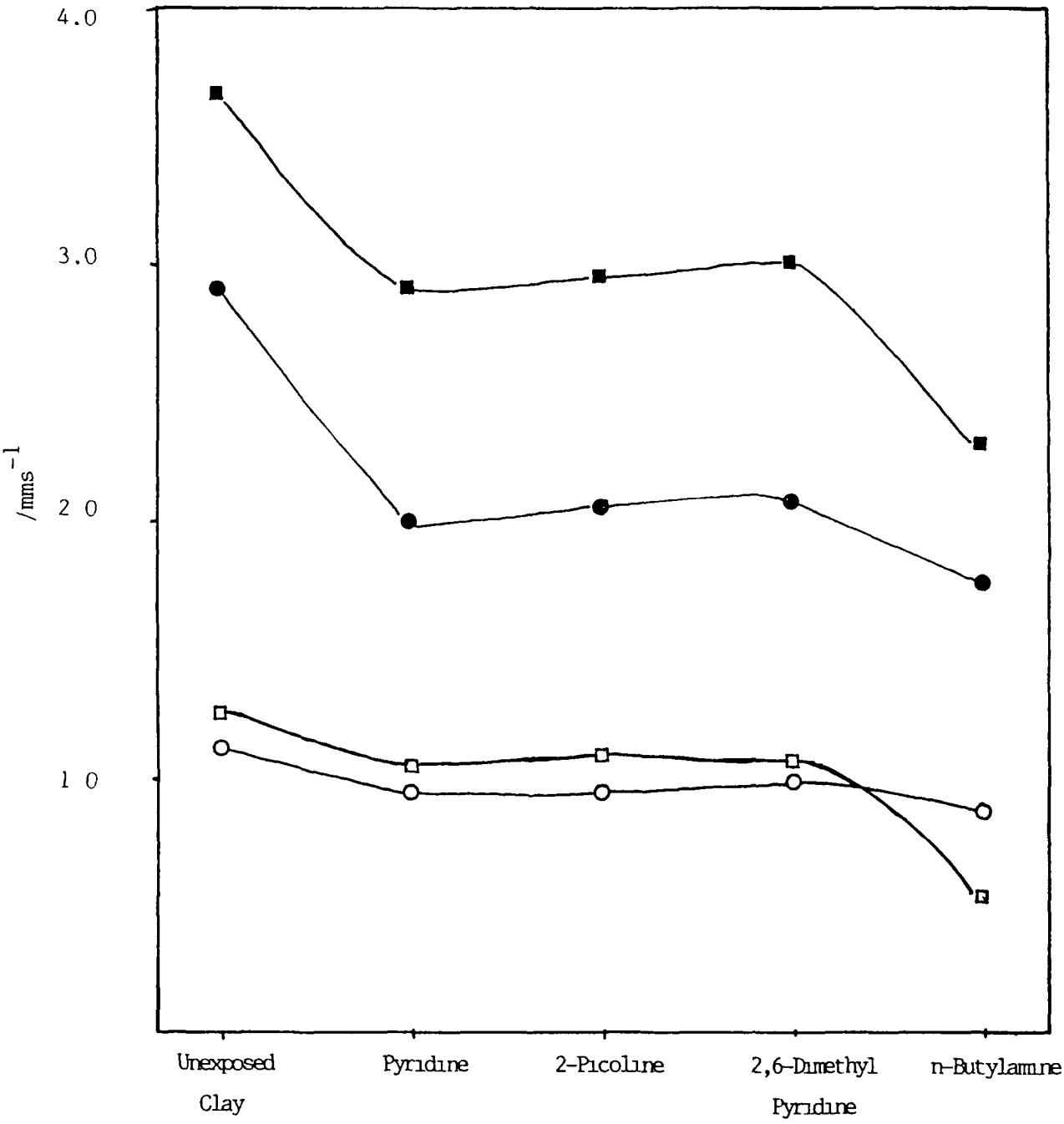

Fig. 4 14 Resolved isomer shift and quadrupole splitting parameters for the $(Me_2Sn)_2(OH)_2^{2+}$-exchanged montmorillonite prepared at pH 4.0 and exposed to the vapour of organic bases. Symbols as in Table 4 5 (p 115)

the series. Also possible effects due to steric hinderance on the hyperfine parameters as a result of the increasing number of alkyl substituents was seen to be negligible in these systems. Further reference to Tables 4.5 and 4.8 suggests that the component having isomer shifts and quadrupole splittings of 0.95 and 2.0 mms^{-1} respectively across pyridine and substitued alkylpyridine series has a similar stereochemistry to $Me_2Sn.oxin_2$ in which the Me groups are known to be cis to each other.[27]

The Mössbauer spectral analysis of the air dried dialkyltin (IV) exchanged montmorillonite samples prepared at pH 2.4 and exposed to the vapour of the same series of organic bases as the samples prepared at pH 4.0 gave rise to an equally dramatic series of resolved hyperfine parameters, Table 4.7. Once again a model consisting of two component doublets resulted in the most acceptable output values of output parameters for each exposed system, with the straight chained adduct components exhibiting values for isomer shift and quadrupole splitting somewhat lower than the alkylpyridine exposed systems, Fig. 4.15.

If it is assumed that the number of alkyltin (IV) species formed in the exchange systems prepared at pH 2.4 and 4.0 respectively remain the same after exposure to each organic base, as evidenced by the number of resolved components, then reference to Tables 4.5 and 4.7 suggests that the adducts formed at each pH have very similar structures.

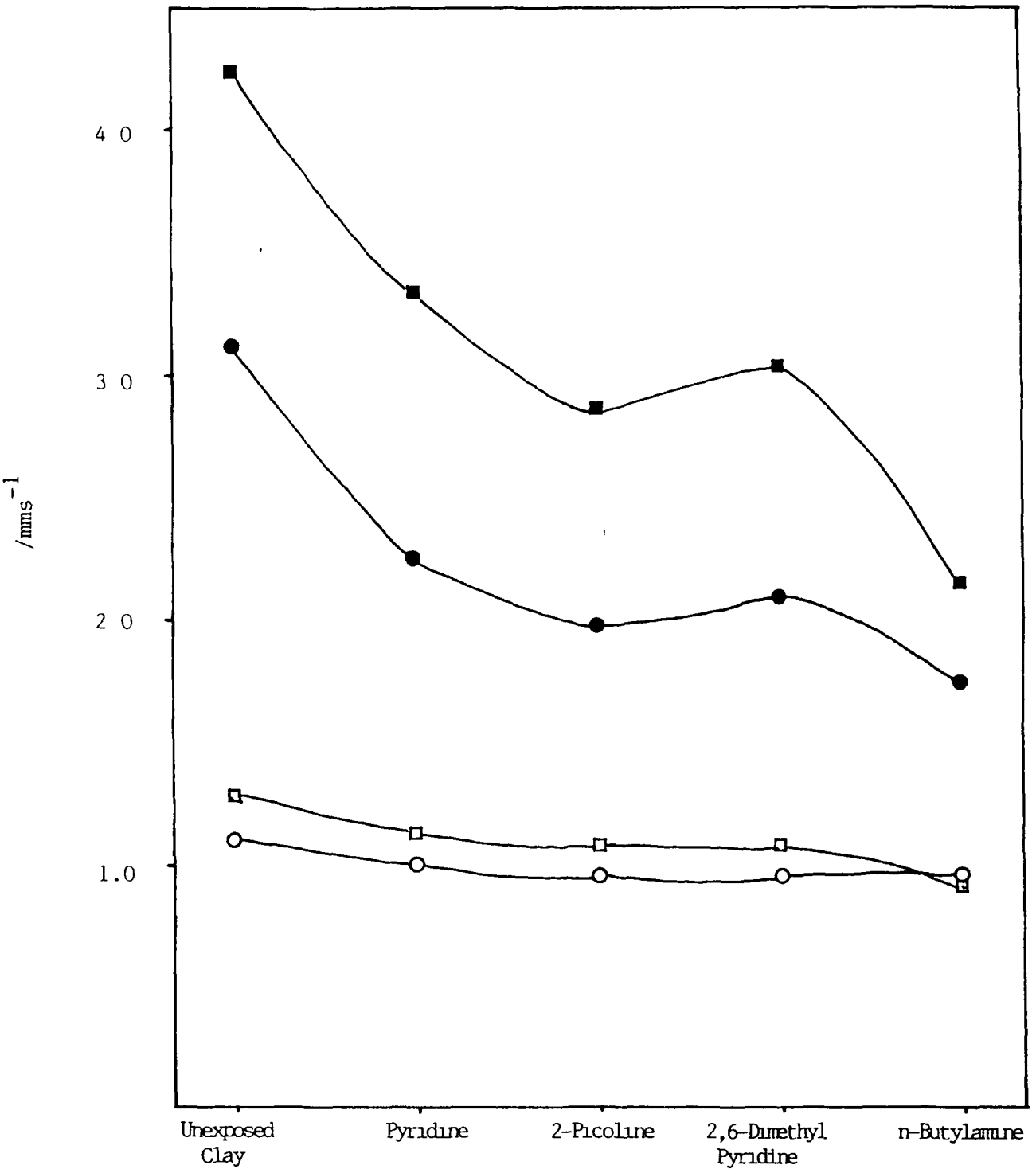

Fig. 4.15 Resolved isomer shift and quadrupole splitting parameters for the Me_2Sn^{2+}-exchanged montmorillonite prepared at pH 2.4 and exposed to the vapour of organic bases. Symbols as in Table 4.7 (p 117)

4.8 Conclusions

Within each of the three thermally pretreated organotin (IV) exchanged montmorillonite systems it is seen that the intercalated species are unstable with respect to increasing pretreatment temperature. In the system prepared at pH 4 0, the contribution from the trans species to the formation of Sn(IV) oxide was easily discerned at temperatures above 230°C. The cis and trans species however, were seen to convert to Me_2SnO between 20 and 230°C. In addition, at temperatures above 200°C both the Me_2SnO, and the remaining trans species converted to oxides of tin

The thermolysis pattern of the intercalated organotin (IV) molecular props in the interlamellar space of the exchanged montmorillonite prepared at pH 2 4 is quite similar to the sample prepared at pH 4 0. At temperatures below $\sim$ 200°C both the cis and trans species decrease resulting in an increasing contribution from Me_2SnO At temperatures greater than 200°C conversion of Me_2SnO and the remaining trans species to oxides of tin takes place.

The monomeric Me_3Sn^+-exchanged system behaves in an almost identical fashion where a low isomer shift component, corresponding to an organotin (IV) oxide is preferentially formed, albeit at a somewhat higher pretreatment temperature than the dimethyltin (IV) systems prepared at pH 4.0 and 2 4 respectively. Furthermore any remaining methylated components at temperatures $\geqslant$ 200°C are similarly converted to Sn(IV) oxide.

It is gratifying to see a uniform organotin oxide conversion process for the three exchanged systems. This is not surprising however, as it may be expected that the demethylationn process should be almost the same in molecules of similar structure. This is evidenced in both dimethyltin ($\mathring{I}V$) exchanged systems and occurs at a slightly higher temperature in the trimethyltin (IV) system.

It is interesting to note the formation of similar dimethyltin (IV) adducts in the exchanged systems prepared at pH 4.0 and 2.4 after exposure to the same series of organic bases. The effect of exposure to the straight chained n-butylamine at each pH is readily discerned by the dramatic reduction in isomer shift and quadrupole splitting parameters compared to exposure to pyridine and the substituted alkylpyridines. This may be explained in terms of the relative basicities of these compounds.

However, in order to substantiate the interpretation of the processes causing the relatively low temperature degradation of the organotin (IV) intercalated complexes, further corroborative evidence using X-ray diffraction, thermogravimetric analysis and water adsorption isotherms will be presented in later chapter.

In addition, it has been reported[20] that when a glycerol-solvated organotin (IV)-exchanged montmorillonite complex was thermally pretreated in successive steps, the intercalated tin moieties did not

disintegrate up to 500°C, the interlayer opening remaining at 3.0A at this temperature. However, it was not possible to verify if the same phenomenon occurred in organotin (IV) systems reported in this work as a result of time constraints at the time of submission.

However, the investigation outlined in this work indicates the possiblity of obtaining information about the interactions between stable Sn(IV) oxide pillars and other intercalated molecules using ^{119}Sn Mössbauer spectroscopy.

CHAPTER 5

A CORROBORATIVE INVESTIGATION OF ORGANOTIN EXCHANGED MONTMORILLONITE

CHAPTER 5

5.1 Introduction

The growth in the application of intercalated clay minerals in clay catalytic reactions[1,2,3] outlines the increasing importance of the precise characterisation of the intercalated clay and also their exchanged cations Properties such as basal spacing,[4] and cation exchange capacity[5] help to determine individual properties of layered silicates It is important that these properties should be determined for each intercalated clay system so that data concerning the hydration states of the exchanged cations, derived from other techniques, can be significantly compared

The work reported in this chapter uses thermogravimetric analysis and X-ray diffraction coupled with water adsorption/desorption isotherms to help corroborate the results obtained from Mössbauer spectroscopy in the characterisation of the organotin (IV)-montmorillonite exchange complexes discussed in the previous chapter.

5.2 General Theory

For many years the main methods of identification and characterisation of both clay minerals and their intercalants were through the techniques of classical "wet" chemical analysis.[6] The introduction of x-ray diffraction allowed major advances to be made in the classification of clay minerals [7] Furthermore x-ray diffraction studies have been used to

show the effect of temperature on the conversion of high spacing intercalates to low spacing ones [8] In addition, thermogravimetry along with differential thermogravimetric analysis have been frequently used in the characterisation of intercalated clay minerals.[9,10] Indeed, water vapour isotherms for cation-exchanged montmorillonites have been used to characterise these materials as sorbents and also to indicate their useful limits for the separation of molecular species by selective intercalation [11,12,13,14]

5 2 ,1 Thermogravimetry

Thermogravimetric analysis is based on the change in mass recorded as a function of increasing temperature. The resulting mass-change versus temperature curve is called a thermogram and provides information concerning the thermal stability and composition of the initial sample, and any intermediates formed along with residues remaining following heating

In conventional thermogravimetry (TG), the mass of a sample, m, is continuously recorded as a function of temperature, T, or time, t, i.e

$$m = f(T,t) \qquad \text{Eq 5.1}$$

By determining the distance between points of interest on the mass axis of the curve, quantitative measurements can be obtained. A second method of displaying TG data is to record the first derivative of the mass change, m, with respect to time, t, i.e.

$$\frac{dm}{dt} = f(T \text{ or } t) \qquad \text{Eq. 5.2}$$

This curve may be obtained by electronic differentiation of the T.G curve, and is called derivative thermogravimetry (DTG)

As with any instrumental technique, the results derived from thermogravimetry can be affected by a number of factors. For example, factors such as heating rate, furnace geometry and balance sensitivity are fixed for any given thermobalance However, other factors such as particle size, sample packing and solubility of evolved gases are difficult to repeat continuously. Although much work has been done on such parameters[15] no uniform standard sample is available to compare any given apparatus with another.

5 2 2 X-ray Diffraction [4]

X-rays are electromagnetic waves and as such are governed by quantum relations in their interaction with matter Two distinct processes are involved in X-ray emission In the first of these processes, X-rays characteristic of the target material are produced when rapidly moving electrons which have been accelerated through potential differences of the order of 10^3 to 10^6 volts, bombard atoms in a metal target such as copper, ejecting an electron from the innermost K shell. In losing an electron, the atom becomes "ionised" resulting in an increase in it's overall energy. However, the transfer of another electron into this vacancy from the L shell serves to decrease the energy of the atom by an amount ΔE, where

$$\Delta E = h\nu = \frac{hc}{\lambda} \qquad \text{Eq 5 3}$$

This energy is released as an X-ray photon of frequency ν, h, being Planck's constant, c, the velocity of light and λ, the wavelength of the emitted x-ray photon. X-ray wavelengths are generally of the order of 10^{-10}m. The vacancy left in the L shell can now be filled by another electron from the M shell giving rise to an energy change having a different value. By a continuation of this process a"spectrum" of discrete X-ray wavelengths is built up for the atom, and all atoms of a given target material have the same set of characteristic X-rays. The X-ray spectra of different metals are similar in appearance and generally show two sharp characteristic peaks called the K_α and K_β lines, the wavelengths of which are independent of the potential difference. Due to the multiplicity of energy levels in the L shell, the K_α line being the most intense and having the longest wavelength is essentially a close doublet $K_{\alpha 1}$, $K_{\alpha 2}$

In the second process, a continuous spectrum known as "white X-rays" is superimposed on the line spectrum of the target. This continuous spectrum is generated by the sudden deceleration of bombarding electrons which do not eject an electron from an inner shell. Also, the shape of the continuous spectrum is independent of the target material, extending indefinitely towards the long wavelength end, and being cut off sharply at the short wavelength end. The cut-off wavelength can be explained by considering an electron giving up all it's energy to an atom on

collision If all of this energy is absorbed by the atom, then the X-ray quantum produced will also have a maximum energy corresponding to a minimum wavelength.

In cation exchanged layered silicates, the layers are arranged symmetrically and form planes or groups of planes having a constant separation between them[7] as a result of the size and hydration state of the exchanged cations. When a collimated beam of monochromatic X-radiaton is focussed on a clay sample at an incident angle, θ, constructive interference occurs and an intense X-ray beam is reflected when the crystal planes are oriented so as to satisfy Bragg's relation,

$$n \lambda = 2d \sin \theta \qquad \text{Eq 5 4}$$

where d represents basal spacing, n, the order of diffraction and λ, the wavelength of the X-radiation

5 2 3 Water Adsorption Isotherms

The adsorption of water molecules by cation exchanged layered silicates is based on mass changes recorded as a function of the relative vapour pressure under controlled conditions The resulting mass-change versus relative vapour pressure curve is called a water adsorption isotherm, and provides information relating to the hydration characteristics of both the clay[11,16] and its intercalated cations [12,13]

The general shape of these physical adsorption isotherms, of which five different types have been distinguished[17], can be used to determine the type and number of physically adsorbed layers of adsorbate

and also to determine if condensation of adsorbate occurs in the small pores, capillaries or interlayer space of the adsorbent material The hysteresis phenomenon associated with these isotherms is considered to be expected for porous type adsorbents[18] in which the adsorption-desorption process causes a change in pore volume shape, and rearrangement of the surface of the sample. Hysteresis has also been explained as being associated with the late development of adsorbate-rich and poor phases in the interlayer region and related to the true equilibrium between the adsorbate vapour and the separated montmorillonite layers with or without interlayer adsorbate.[12]

The adsorption of water vapour on montmorillonite is a very complex process and as such it is difficult to associate the phenomena to one single model of physical adsorption [19] For multimolecular adsorption on a free surface using relative vapour pressures the B.E.T. equation[20] was developed by applying the Langmuir model to the concept of multilayer physical adsorption. The B.E T. equation is written as

$$\frac{P}{V(P_o-P)} = \frac{1}{V_m C} + \frac{C-1}{V_m C}\ (P/P_0) \qquad \text{Eq 5.5}$$

where V is the volume of water adsorbed per gramme of clay at pressure p, p_o is the saturation vapour pressure, and V_m is the monolayer volume of adsorbed water. C is a constant given by

$$C = e^{(E_1-E_L)/RT} \qquad \text{Eq 5.6}$$

where T is temperature, R is the molar gas constant, E_1 is the heat of adsorption of the first layer and E_L is the heat of condensation of water vapour, given as 43.88 kJmol^{-1} for water at 25°C [13] The ratio (P/p_o) represents Relative Humidity.

According to Eq. 5 5 a plot of $(P/P_o)/V(1-P/P_o)$ against (P/P_o) should give a straight line with a slope given by $\frac{(C-1)}{V_m C}$ and an intercept of $\frac{1}{V_m C}$ A value for the slope and intercept, V_m and C respectively, is easily calculated.

5 3 Experimental

The parent clay used in the following studies was a Wyoming montmorillonite with the $< 2\mu$ m fraction collected by sedimentation The sedimentation, cation-exchange, thermal analysis, X-ray diffraction and water uptake procedures have been described in detail in Chapter 3, and only the pertinent experimental details will be given here

The thermobalance used in the dynamic thermogravimetric studies was a Stanton-Redcroft TG 750. The flow rate of the nitrogen gas, which was dried by passing it through a 4Å molecular sieve and P_2O_5, was calibrated using an external bubble flow meter. Thermograms were obtained using a heating rate of 20°C min^{-1}, and a flow rate of nitrogen purge gas of 25cm^3 min^{-1}, and were recorded using a dual pen Linseis chart-recorder at a recording speed of 20 cm hr^{-1}.

X-ray slides were thermally pretreated for 16

hrs prior to x-ray diffraction studies. The diffraction traces were recorded at $2°(2\theta)min^{-1}$ between $2°(2\theta)$ and $10°(2\theta)$ on a Jeol JDS 8X diffractometer using Ni filtered copper K_α radiation (λ = 1 5418Å) operating at 40kV at 30mA.

Finely ground pre-weighed clay samples were pretreated at 120°C for 16 hours, and equilibrated at constant temperature, in desiccators containing saturated salt solutions chosen to generate relative partial pressures of water from 0.0 to 0 97. Both adsorptions and desorption cycles were recorded

5.4 Results

The basal spacings for each of the three organotin (IV) exchanged montmorillonites as a function of pretreatment temperature are collected together in Tables 5 1 - 5.3. Fig. 5 1 clearly shows that the basal spacing of approximately 15 85Å corresponding to the dimethyltin sample prepared at pH4 0 was nearly 2 0Å larger than that of the sample prepared at pH 2 6. Furthermore, after thermal pretreatment at 120°C for about 16 hours, the sample prepared at pH 4 0 continued to exhibit a larger basal spacing over the sample prepared at pH 2.6, this time by about 2.5Å. This difference continues up to 300°C after which both clays collapse to approximately 10Å, after thermal pretreatment at 300°C.

The air-dried trimethyl tin exchanged clay on the other hand exhibited a basal spacing of 13.80Å, some 2.0Å lower than the dimethyl tin sample prepared at

SAMPLE PRETREATMENT TEMPERATURE	2θ	d/Å
20	5.57	15.85
120	5.70	15 50
200	5.70	15.50
300	8 77	10 08
200 + 5 mins Air	5.79	15 27
200 + 50 mins Air	5 73	15.51
300 + 22 mins Air	8.68	10.19
300 + 32 mins Air	8.78	10.07

TABLE 5.1 Temperature Dependence of the d_{001} Basal Spacings for the $Me_2Sn(IV)$-montmorillonite sample prepared at pH 4.0.

SAMPLE PRETREATMENT TEMPERATURE	2θ	d/Å
20	6.40	13.80
120	6 80	13.00
200	7.89	11 20
300	9 21	9.60
200 + 5 mins Air	7 89	11.20
200 + 34 mins Air	6.99	12.65
300 + 6 mins Air	9.27	9.54

TABLE 5.2 Temperature Dependence of the d_{001} Basal Spacings for the $Me_2Sn(IV)$-montmorillonite sample prepared at pH 2.6.

SAMPLE PRETREATMENT TEMPERATURE	2θ	d/Å
20	6 40	13.80
120	6.75	13 10
200	6.80	13 00
300	8.75	10.10
300 + 20 mins Air	8.35	10.59

TABLE 5.3 Temperature Dependence of the d_{001} Basal Spacings for the $Me_3Sn(IV)$-montmorillonite sample prepared at pH 3.4

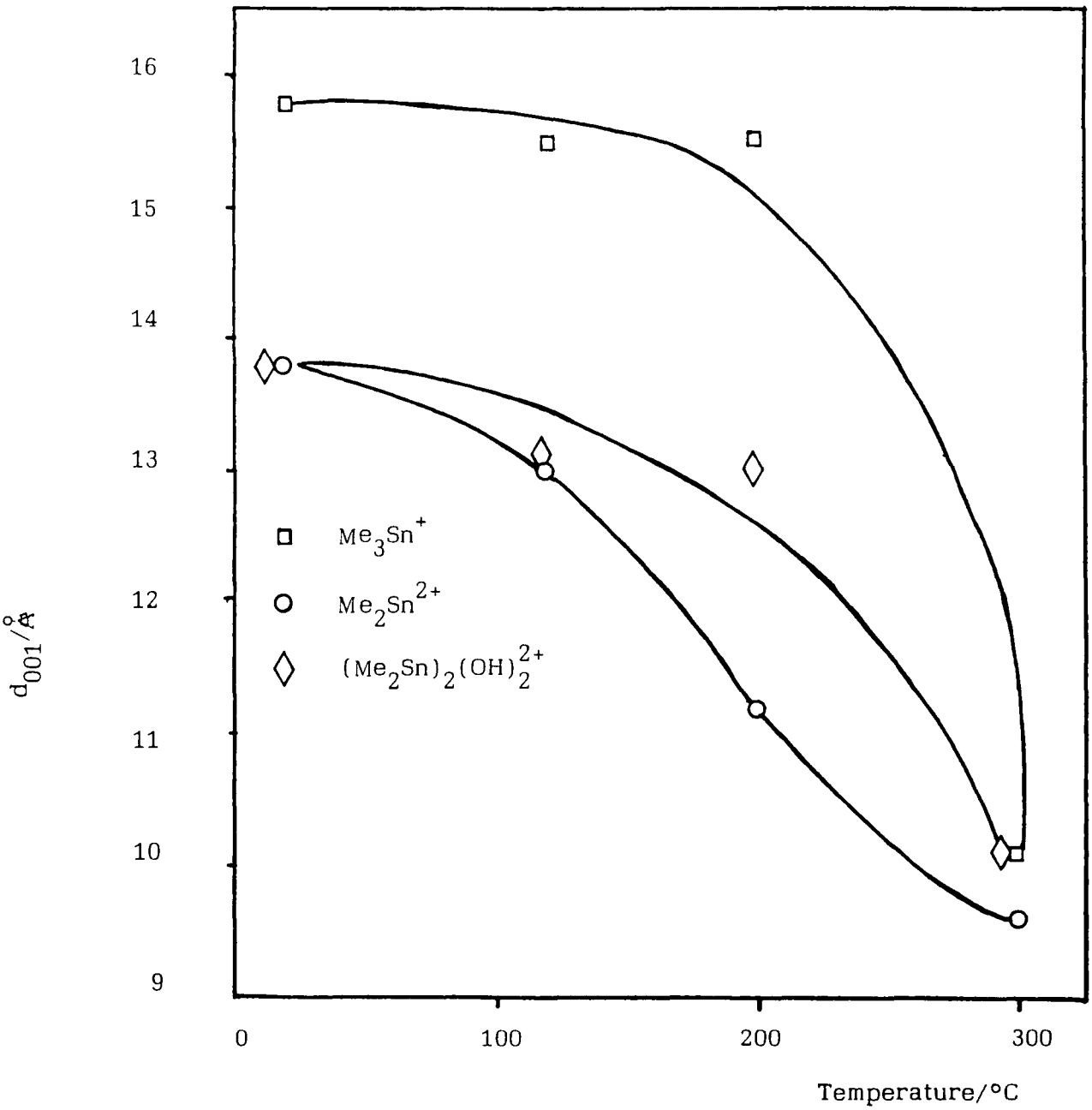

Fig 5 1 Temperature dependence of the d_{001} basal spacing for the dimethyltin (IV)-montmorillonite clays prepared at pH 2.6 and 4 0 respectively, and the trimethyltin (IV)-montmorillonite clay prepared at pH 3.4

pH 4 0 and similar to the sample prepared at pH 2 6 Heating this clay to 120°C for a period of 16 hours results in a reduced basal spacing of 13 10Å In continuing thermal pretreatment to 200°C the basal spacing remains at about 13 00Å, reducing to 10 10Å after thermal pretreatment at 300°C

It can be seen from the shape of the curves in Fig 5 1, corresponding to each of the organotin (IV) exchanged clays, that both of the dimethyltin exchange forms show a similar thermal stability over the pretreatment temperature range In addition, it can also be seen from Fig 5 1 that the thermal stabilty of the trimethyltin exchanged clay is comparable to the exhibited by both dimethyltin exchanged forms

Fig 5 2 shows the basal spacings of the heated organotin (IV) clays plotted as a function of their re-exposure time to the atmosphere This shows that only the dimethyl tin clay prepared a pH 2 6 displayed rehydration after thermal pretreatment at 200°C This is seen in a d-spacing increase of 2 4Å after 34 minutes exposure to the atmosphere

Since many of the X-ray diffraction, Mössbauer and water adsorption experiments carried out in this work involved heating the different organotin (IV) clays between 120°-450°C, the results in Table 5 4 also indicate the amount of water lost by 120°C as a percentage of the total water lost by the clay, as derived from the thermogravimetric profiles This data assumes that the organotin (IV) exchange levels used

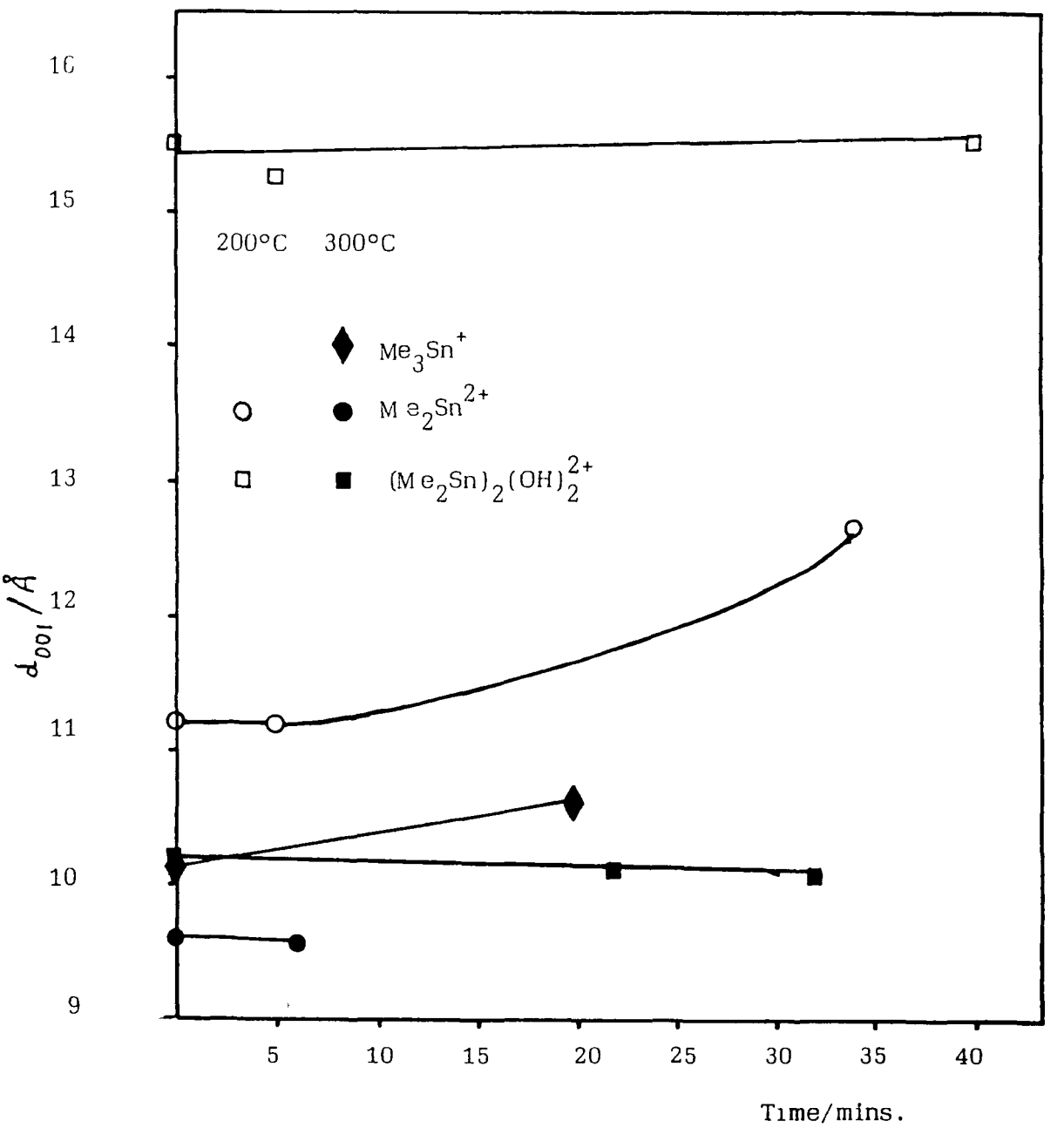

Fig 5 2 d_{001} basal spacing of the rehydrated dimethyltin (IV)-montmorillonite clays prepared at pH 2.6 and 4.0 respectively and the trimethyltin (IV) montmorillonite clay prepared at pH 3 4, as a function of time.

Major Species in Solution	pH	C E C	% H_2O lost by 120°C
$(Me_2Sn)_2(OH)_2^{2+}$-	4.0	1	70
$(Me_2Sn)_2(OH)_2^{2+}$-	4 0	2	71
Me_2Sn^{2+}-	2 6	1	74
Me_2Sn^{2+}-	2.6	2	76
Me_3Sn^{+}-	3.4	10	66

TABLE 5.4 Data derived from the Thermogravimetric curves for the organotin (IV) exchanged montmorillonite clays.

throughout these studies, most of the weight loss is due to water. These data shows that the % water lost by 120°C in each organotin (IV) exchanged system was lowest for the trimethyl tin sample and highest for the dimethyl tin (IV) sample prepared at pH 2 6

Fig. 5 3 displays the derivative thermogravimetric profiles for the three organotin (IV)-exchanged montmorillonite clays. Fig. 5.4 compares the derivative thermogravimetric profiles for the exchanged dimethyltin (IV) exchanged montmorillonites prepared at pH 4 0 and pH 2 6 Respectively, with those prepared at the same pH values but at twice their exchange capacities

Water adsorption and desorption data for both the dimethyltin (IV) samples prepared at pH 4.0 and pH 2 6 are tabulated in Tables 5.5 and 5 6 respectively, and plotted in Fig. 5.5. The water adsorption and desorption isotherms for both samples are of type IV in the Brunauer-Emmet-Teller classification.[17,20] Fig. 5 5 shows that the sample prepared at pH 2.6 exhibits a larger sorption capacity for water. Type IV isotherms, which are characterised by the termination of further sorption near P/P_o = 1.0 are indicative of capilliary condensation in a defined pore network, i.e. sorption ceases when the pore volume is filled. This represents a behaviour pattern more associated with zeolites[21] than layered silicates. The hysteresis seen in the desorption cycle for the sample prepared at pH 4.0 was less marked, and closed sooner than the sample prepared

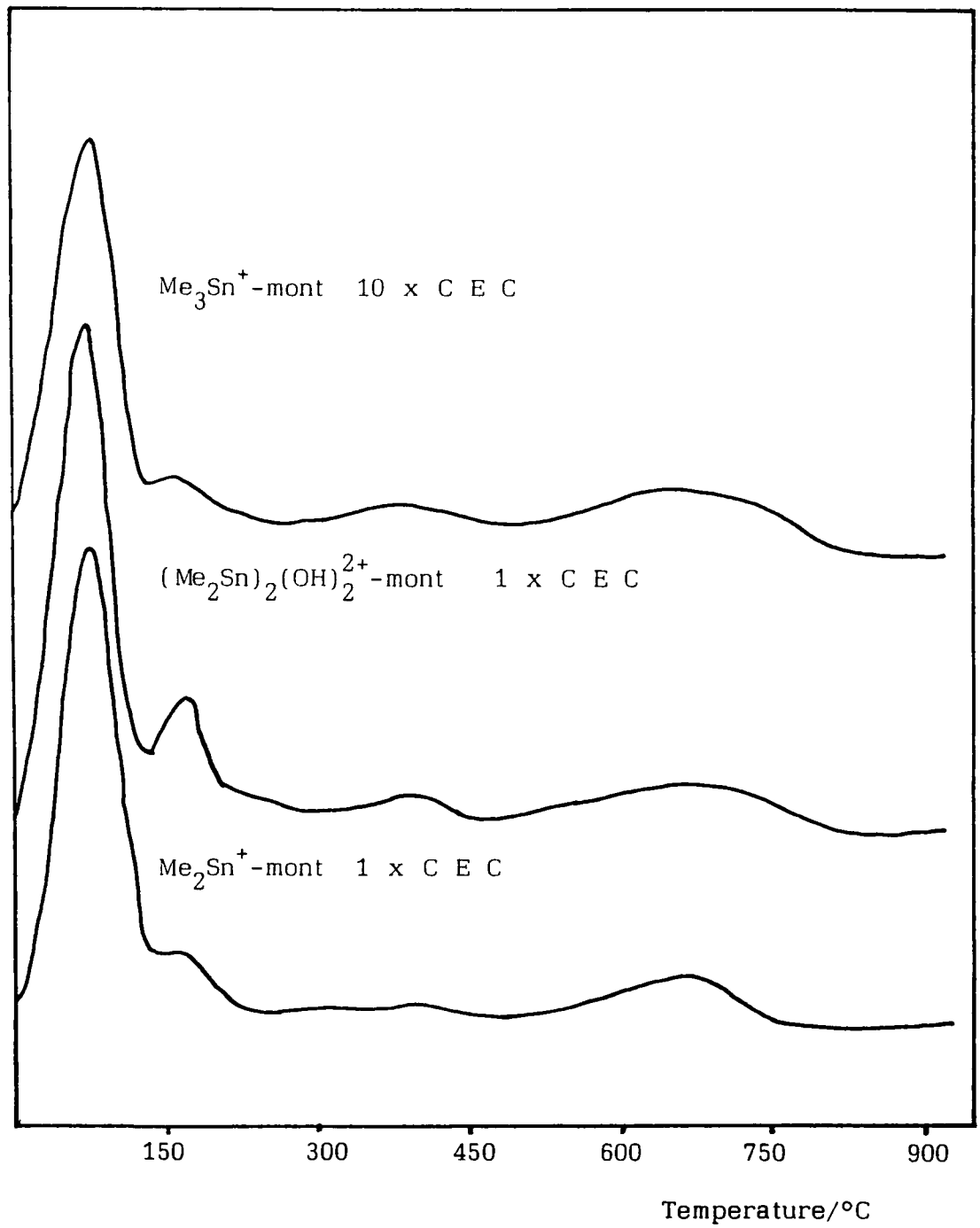

Fig 5 3 D T G profiles for the organotin (IV)-montmorillonite clays.

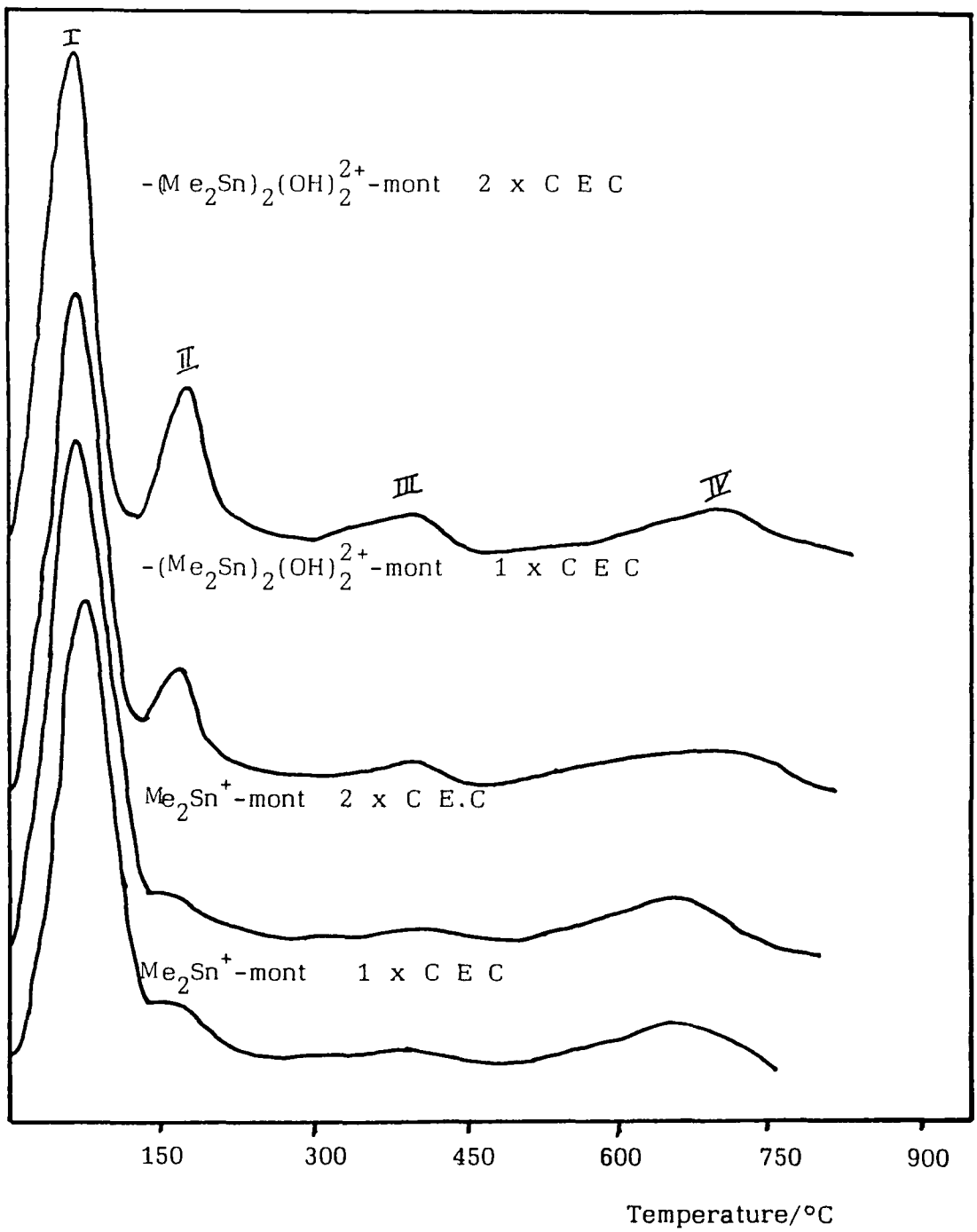

Fig 5 4 Comparison of the D T G profiles for the organotin (IV)-montmorillonite clays prepared at pH 2 6 and 4.0 respectively at once and twice exchange capacities.

SORPTION CYCLE		DESORPTION CYCLE	
P/Po	mg $H_2O/(g\,clay)^{-1}$	P/Po	mg $H_2O/(g\,clay)^{-1}$
0 06	19 94	0.94	182 31
0.15	28.76	0.73	151.92
0.24	61.73	0.65	128 15
0.39	81.28	0.47	107.35
0.52	104 38	0.36	85 59
0.70	124.44	0 24	73 04
0 84	136.97	0.12	32.40
0.94	188.50	0.06	19.24
0.97	192.90		

TABLE 5.5 Water sorption and desorption data for the $(Me_2Sn)_2(OH)_2^{2+}$-montmorillonite clay system prepared at pH 4.0.

SORPTION CYCLE		DESORPTION CYCLE	
P/Po	mg $H_2O/(g\,clay)^{-1}$	P/Po	mg $H_2O/(g clay)^{-1}$
0 06	18 26	0.94	226 18
0.15	32.99	0 73	188 77
0.24	65.69	0.65	163.09
0 39	92.08	0 47	140.22
0.52	127 22	0.36	113.74
0.70	154.40	0 24	97.99
0.84	174.10	0 12	58.68
0.94	232.80	0.06	22 36
0.97	233.40		

TABLE 5.6 Water sorption and desorption data for the Me_2Sn^+-montmorillonite clay system prepared at pH 2.6.

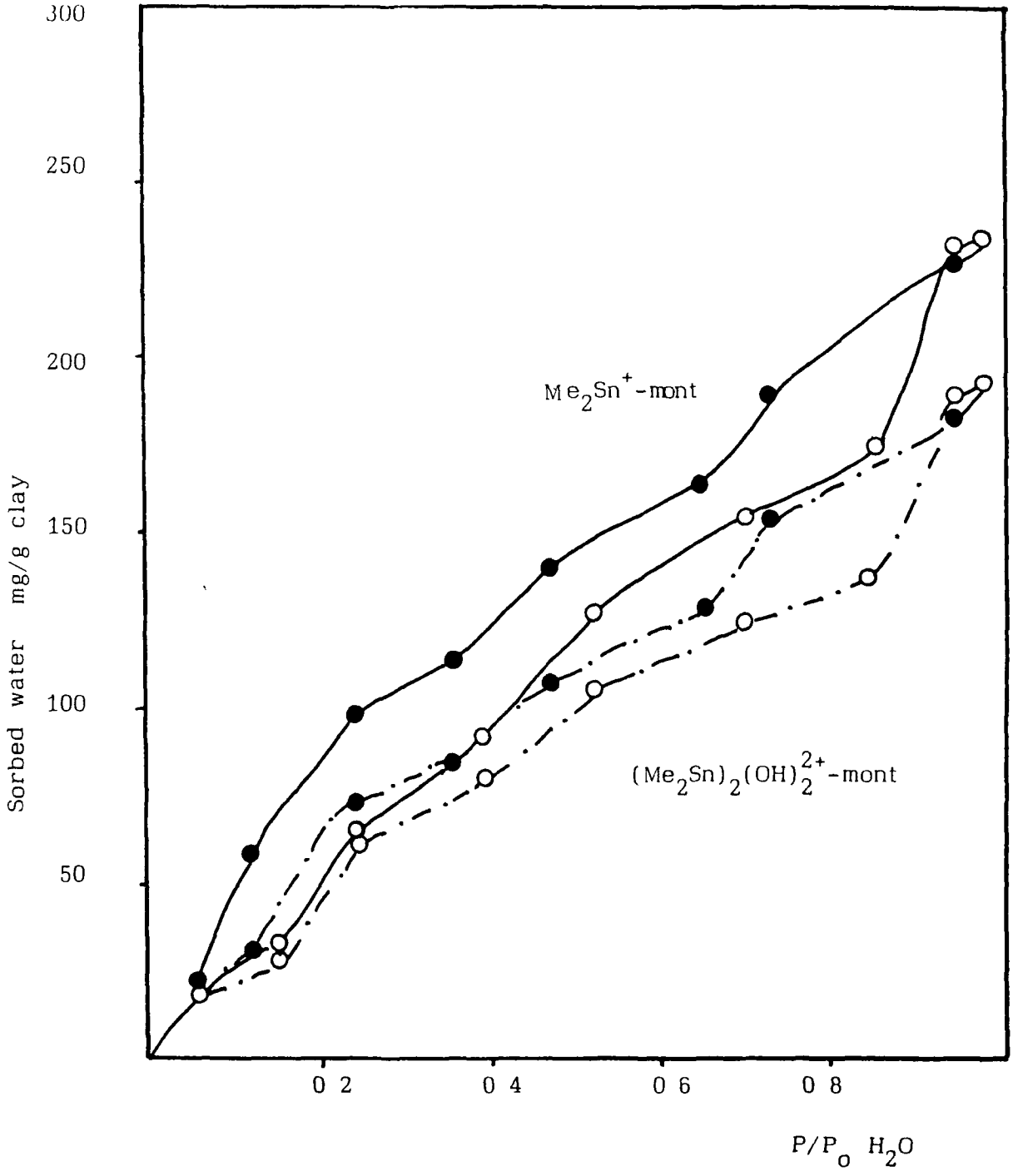

Fig 5 5 Water vapour sorption O, and desorption ● isotherms for the organotin (IV)-montmorillonite clays prepared at pH 2 6 and 4.0 respectively.

at pH 2 6. Corresponding B E.T water sorption and desorption data for both monomeric and dimeric dimethyltin (IV) clays within the range of $0 > p/p_0 > 0.6$, are collected in Tables 5 7 and 5.8 respectively and plotted in Fig 5 6 Table 5 9 collects the calculated slopes and intercepts for the adsorption cycles of both clays in the plotted range and also compares the calculated heats of adsorption of water and mass of water required to form a monomolecular layer for each clay

5 5 DISCUSSION

5 5 1 Discussion of X-ray Diffraction Studies

The Mössbauer investigations previously discussed in Chapter 4 established that both cis and trans dimethyltin (IV) species were present in samples prepared at pH 2.6 and pH 4 0, up to temperatures of 200°C.

X-ray diffraction results for both dimthyltin (IV) systems given in Tables 5 1-5.2 and plotted in Fig 5 1 indicate the different basal spacings associated with each clay system These data can also demonstrate the nature and orientation of the different intercalated species within the interlamellar space of each clay system.

The size of each proposed intercalated species can be determined using a combination of the normal covalent radii[22] and the non-bonded Van der Waal's radii[22,23] of atoms making up the species.

SORPTION		DESORPTION	
P/Po	P/Po/V(1-P/Po)	P/Po	P/Po/V(1-P/Po)
0 06	3 21	0.47	8.29
0 15	6 11	0.36	6.44
0 24	5.11	0 24	4.33
0 39	7 85	0.12	4.22
0.52	10 36	0.06	3.82

TABLE 5.7 B.E.T. water sorption and desorption data between $0 < P/Po < 0.6$ for the $(MeSn)_2(OH)_2^{2+}$-montmorillonite clay system prepared at pH4.0.

SORPTION		DESORPTION	
P/Po	P/Po/V(1-P/Po)	P/Po	P/Po/V(1-P/Po)
0.06	3 49	0.47	6 33
0.15	5.28	0.36	4.84
0 24	4.80	0.24	3 23
0.39	6.93	0.12	2.33
0.52	8.50	0.06	2.78

TABLE 5.8 B.E.T. water sorption and desorption data between $0 < P/Po < 0.6$ for the Me_2Sn^{2+}-montmorillonite clay system prepared at pH 2.6.

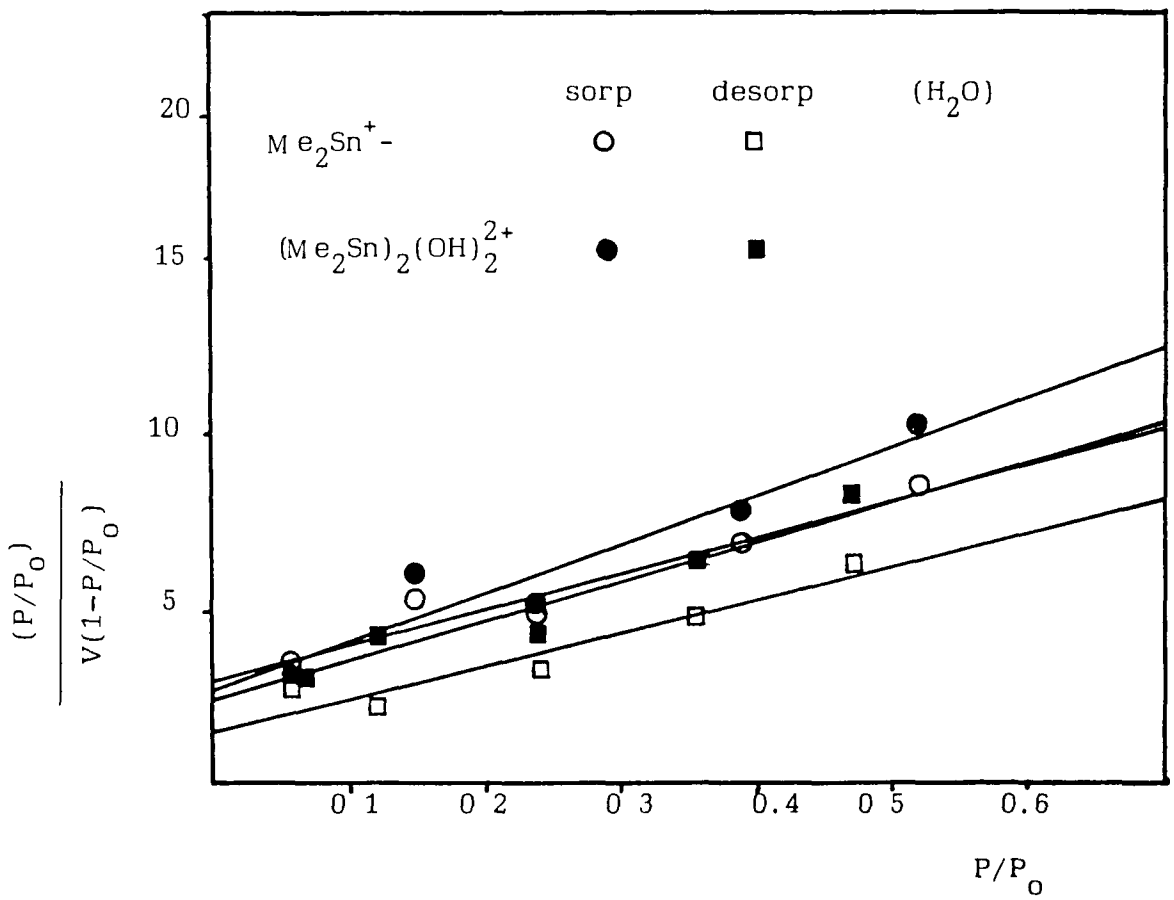

Fig 5 6 B E T plots of the sorption and desorption isotherms for the organotin (IV)-montmorillonite clays prepared at pH 2 6 and 4 0 respectively, in the range $0 < P/P_o < 0.6$.

Intercalated Cation	Vm = Mm mgH_2O/g clay	C	E_1-E_L kJ/mol	E_1 kJ/mol
Me_2Sn^{2+}-	76	4.36	3 65	47
$(Me_2Sn)_2(OH)_2^{2+}$-	60	6.14	4.5	48

TABLE 5.9 B.E.T. parameters including heats of adsorption and adsorbed water calculated, using Eqn 55 for dimethyltin (IV) exchanged clay systems prepared at pH 2.6 and 4.0

In making reference to Table 5.10, consideration of the structure for $(Me_2Sn)_2(OH)_2^{2+}$, drawn schematically in Fig 5.7 (a) shows that in the air dried sample prepared at pH 4.0, this five co-ordinate structure has one axial ligand position on each tin atom which is satisfied by a silicate oxygen in the basal plane of the silicate sheet This results in any possible interaction between the basal surface and the methyl groups being minimised. Assuming that keying of tin atoms into the basal surface does not occur, this orientation would result in a d_{001} basal spacing of 16 4Å Assuming a d_{001} basal spacing of 9 6Å for montmorillonite in the absence of interlayer polar molecules, this is in very close agreement to the observed basal spacing of 15.85Å for the dimethyltin (IV) sample prepared at pH 4 0, Fig. 5.7 (a). Alternative structures for this species, Fig. 5.7 (b) and (c), in which the methyl groups are directed towards the layers result in spacings which are too high. Thermal pretreatment of this sample up to 200°C maintains a spacing up to 15 5Å, indicating a reasonable pillaring effect which can be explained by the presence of both a trans dimethyltin (IV) species, Fig. 5.8 (c), and dimethyltin (IV) oxide, Fig. 5.8 (d). The C-Sn-C axis of each species being parallel to the basal surface in each case. Further thermal pretreatment of this sample to 300°C results in a basal spacing of 10.08Å. This suggests complete demethylation of the organotin (IV) cations to SnO_2 which may have diffused out into edge

ELEMENT	COVALENT RADIUS (Å)	Van der Waals Radius (Å)
Sn	1.37	2 20
C	0.77	1 7
H	0.37	1.22
O	0 74	1 40

TABLE 5.10 Standard covalent, and Van der Waals radii for elements contained in the organotin (IV) species used throughout this work

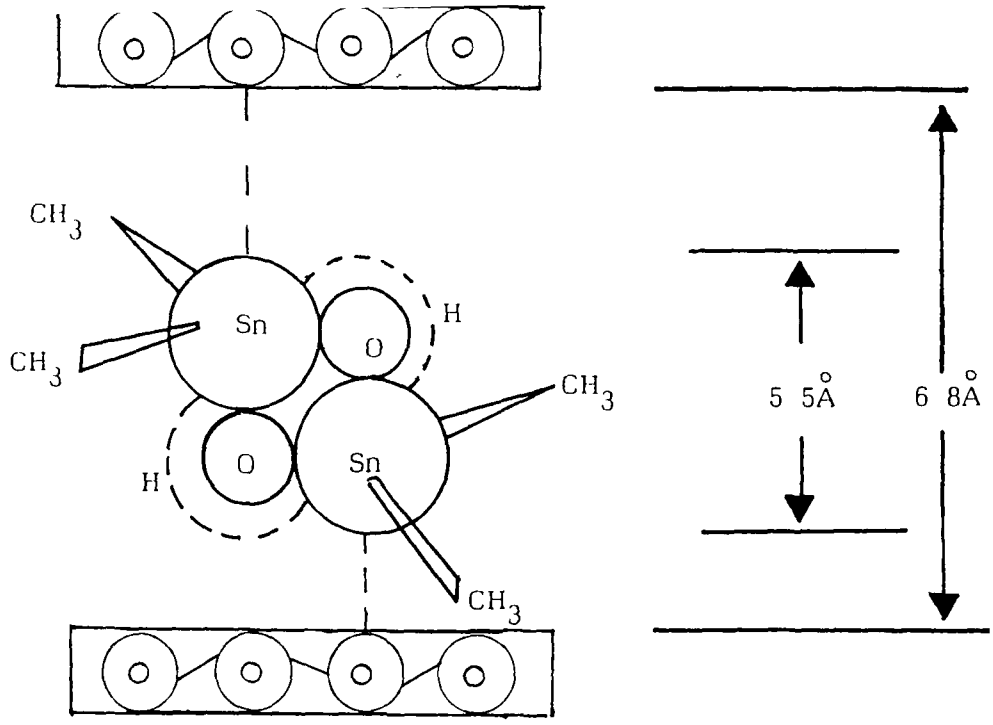

(a)

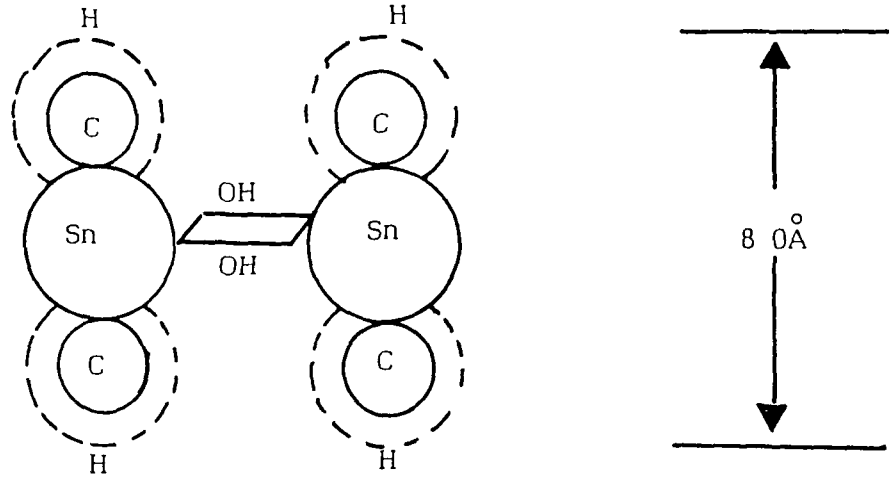

(b)

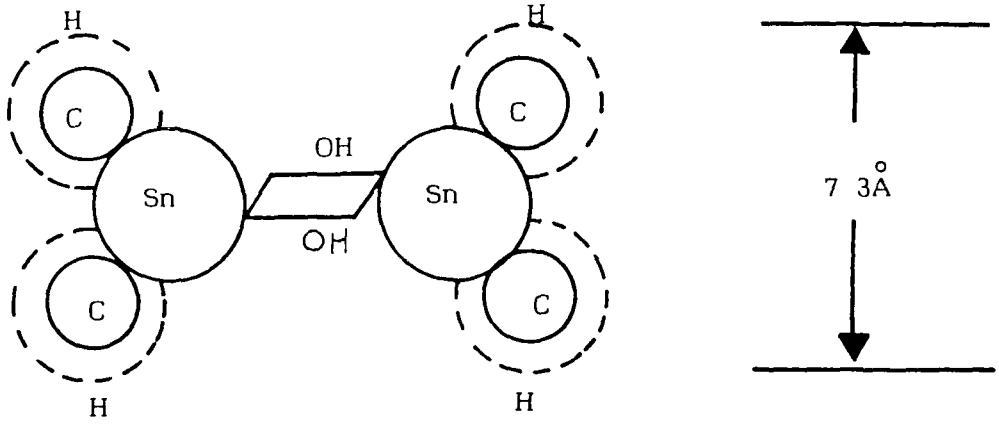

(c)

Fig 5.7 Schematic diagram depicting possible structural orientations for the $(me_2Sn)_2(OH)_2^{2+}$ species.

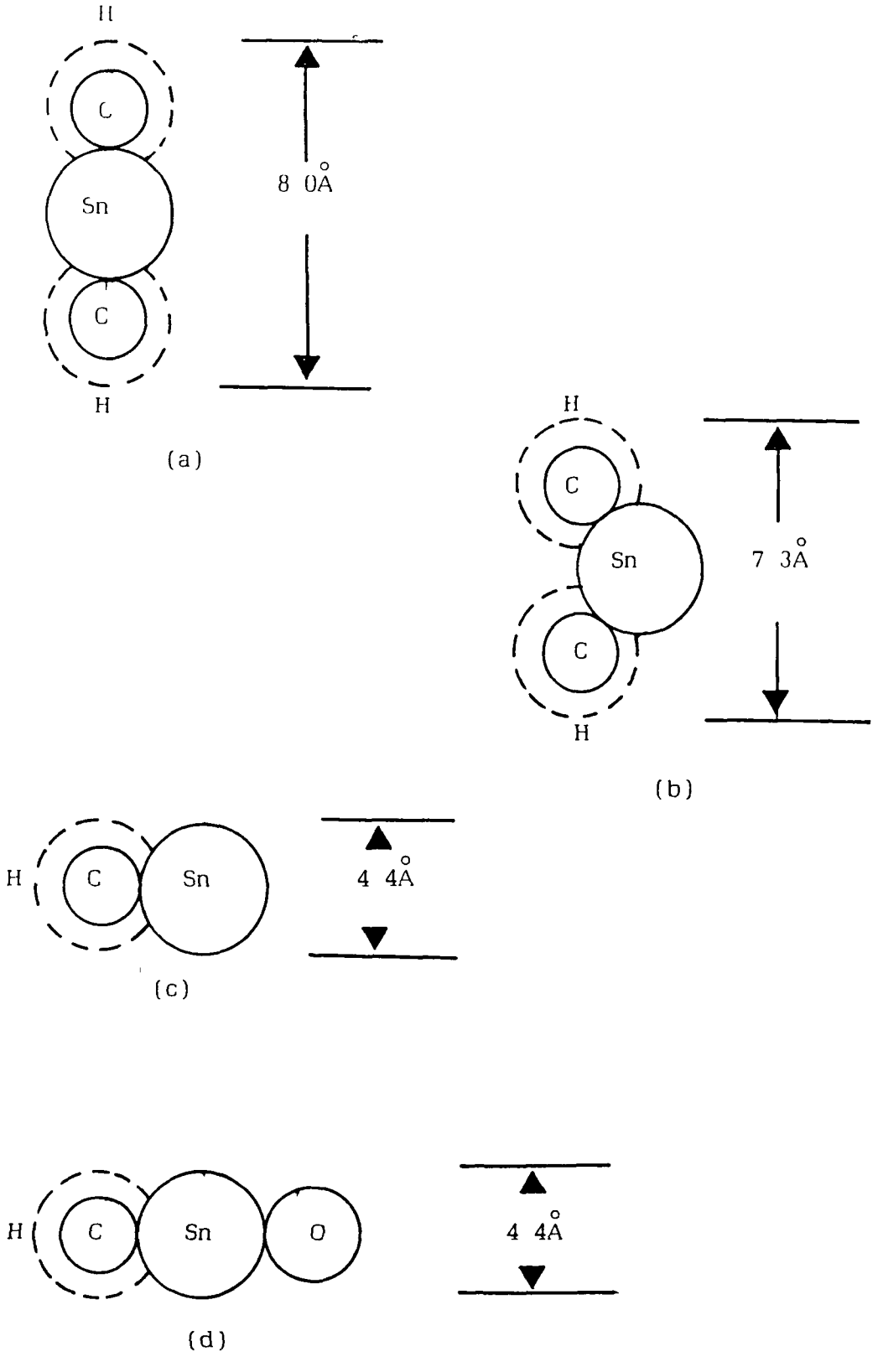

Fig 5.8 Schematic diagram depicting possible structural orientations for the me_2Sn^{2+}- and me_2SnO^{+} species

sites, rather than having become trapped in hexagonal holes

For the dimethyltin (IV) air dried clay prepared at pH 2 6, X-ray diffraction data collected in Table 5 2 and plotted in Fig. 5 1, indicates that the 13.8Å basal spacing is in very close agreement to a predicted 14.0Å spacing for a monomeric dimethyl (IV) species whose C-Sn-C axis is parallel to the basal surface Clearly, the orientation of the cis species in the sample prepared at pH 2 6 is different from that for the sample prepared at pH 4 0 On thermal pretreatment of this sample up to 200°C the reduction of the basal spacing to 11 2Å indicates that some demethylation of the intercalated species had taken place The reduced thermal stability of the sample prepared at pH 2.6 probably reflects the increased acidity which reduces the stability of the dimethyl tin species as suggested by Petridis et al.[27] However, considering Fig. 5.8 (c) and (d), a basal spacing of about 13 0Å would be expected to be maintained during this transformation process This may be explained by possible keying-in of partially demethylated species into hexagonal holes during diffusion to external edge sites Further thermal pretreatment up to temperatures of 300°C resulting in a basal spacing of 9 6Å indicate that all of the intercalated tin species have migrated out of the interlayer space, leaving the silicate layers practically in contact.

The X-ray diffraction data for the air dried,

trimethyltin (IV) exchanged clay prepared a pH 3.4, which is collected in Table 5.3 and plotted in Fig 5 1 suggests that a basal spacing of 13 8Å is indicative of an intercalated planar trimethyltin (IV) species, whose SnC_3 axis is parallel to the basal surface, Fig 5.9(c) An alternative orientation of this species, Fig 5 9 (a), within the interlayer space would have resulted in a basal spacing close to 17Å.

On thermal pretreatment of this sample up to 200°C, a basal spcing of 13.0Å is maintained, thus reflecting an internal pillar stability intermediate between both dimethyltin (IV)-exchanged clays prepared at pH 4 0 and 2.6 respectively. continuing thermal pretreatment up to 300°C results in a basal spacing of 10 1Å, once again indicating the disintegration of the organotin (IV) species and subsequent diffusion of the various tin oxide species out of the interlayer region and into edge sites

The range of basal spacings seen on thermal pretreatment of the three organotin (IV) exchanged montmorillonite samples up to 200°C suggests in each case a dehydration of the interlayer space, along with desorption of physically bound surface water. This dehydration may limit the amount of interlayer water to the most tightly bound water associated with the first hydration shell of the intercalated species, restricting mobility of intercalated species. Above 200°C a high Brønstead acidity develops in the interlayer[24,25] due to the dissociation of co-ordinated water as well as

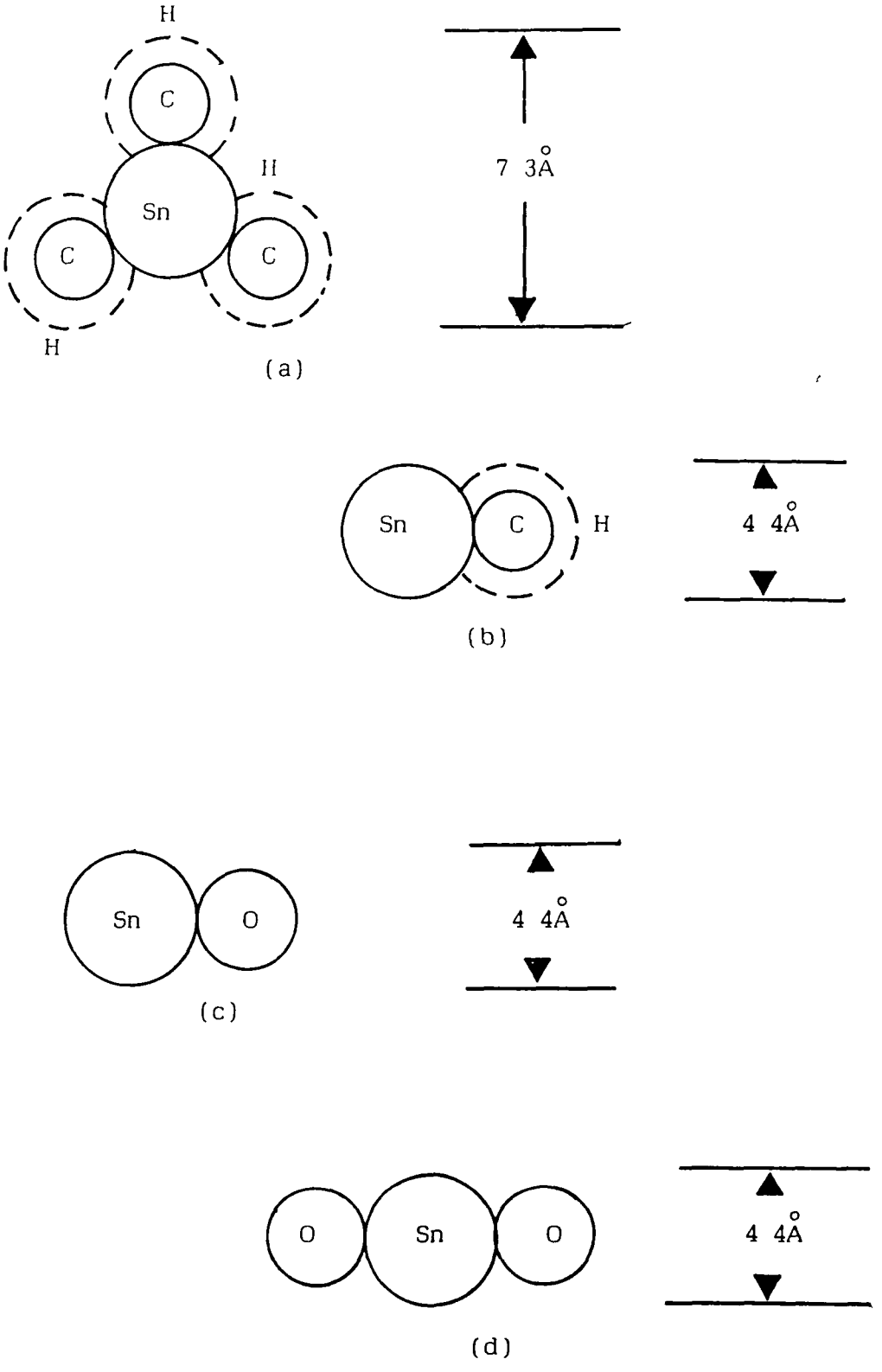

Fig. 5 9 Schematic diagram depicting possible structural orientations for the me_3Sn-, $Sn^{II}O$, and SnO_2 species.

condensation of hydroxyls belonging either to the intercalated species or to the clay lattice This high interlayer acidity probably induces the dissolution of the intercalated organotin cations, dispersing them in the interlayer. In addition, these organotin cations disintegrate, and after transformation to SnO_2 migrate out of the interlamellar space The above picture is supported by Christiano et al ,[26] in that further dehydration of their PILC precursor at 130°C under vacuum for 24 hours led to the formation of pillars stable up to 350°C, while direct thermal pretreatment of the room-temperature dried precursor at 250°C resulted in the collapse of the interlayer Furthermore, Petridis et al.,[27] demonstrated basal spacings for their air-dried organotin (IV) exchanged montmorillonite clay prepared at pH 5 3, and thermally pretreated up to 200°C, which were consistent with those reported in this present work. On thermal pretreatment above 200°C, their intercalated species disintegrated, and after further thermal pretreatment at 300°C, the disintegrated species had migrated out of the interlayer space leaving the silicate layers practically intact.

Data collected in Tables 5 1-5 3 and plotted in Fig. 5.2 indicate that the rehydration of thermally pretreated organotin (IV) exchanged clays only occurs in the dimethyltin (IV) clay prepared at pH 2.6, which had been heated at 200°C. The increase in basal spacing from 11.20Å to 12.65Å after exposure to the atmosphere for 34 minutes may well be attributable to the

rehydration of Na^+ ions remaining in this partly exchanged clay.

5.5 2 Discussion of Thermogravimentric Analysis Results

Thermogravimetric curves recorded for the three organotin (IV) cation exchanged montmorillonites can be used to determine the number of major thermal events associated with each clay as a function of increasing temperature To this end the shape of these profiles including their length and steepness can be related to the number of water molecules liberated along with their respective binding energy which holds them to the interlayer cation or onto the clay surface.[10] These water molecules can be classified into three types, namely (1) "Free water" which is found in the case of pastes and gels and can easily be removed at temperatures slightly above room temperature (2) "Surface water" which is physically bound to the clay surface and requires slightly higher energy to be removed. (3) The water molecules which are in the primary co-ordination sphere of positively charged cations and are electrostatically bound to them These molecules require the highest energy to overcome these attractive forces.[10]

Below 100°C the thermogravimetric curves for each of the three organotin (IV) clays were found to be almost identical to each other, each having very steep slopes Both "free" and "surface" water are expected to be desorbed in this temperature range This is

evidenced by the size of the first peak in each DTG curve seen in Fig. 5 3 This figure also shows that the dimethyltin (IV) sample prepared at pH 4 0 is different to both the dimethyltin (IV) sample prepared at pH 2.6 and also the trimethyltin (IV) sample by virtue of the peak near 175°C In addition, the shape of these profiles at $\sim$170°C suggests the presence of some hydroxy species in the dimethyltin (IV) exchanged clay prepared at pH 2 6 and also an hydroxy species in the trimethyltin (IV) clay However, given the formation constants of these species this is not surprising Examination of the DTG profiles for the once and twice exchanged clays in Fig. 5 4, shows that this peak is somewhat more intense in the twice exchanged clay prepared at pH 4.0 confirming this interpretation A marked deviation from the baseline between 360°C and 420°C can also be seen in the DTG profiles in Fig 5 3 This concurs with Mössbauer data indicating the presence of SnO_2. Demethylation would also be expected to occur in this region.

As many of the experiments carried out in this work involved predrying the different cation exchanged clays to 120°C, (particularly the water adsorption/ desorption isotherms discussed in section 5 5 (iii)), consequently the amount of water removed by this thermal pretreatment is relevant Data collected in Table 5.4 shows that the amount of water lost up to 120°C by the once exchanged sample prepared at pH 2.6 is 74% of the total amount lost by 550°C This assumes that at the working exchange levels, water is the primary interlayer

component present When this clay is exchanged for a second time the water lost is 76% This contrasts with 70% and 71% for the once and twice exchanged samples prepared at pH 4.0, and 66% for the trimethyltin (IV) prepared sample, and is probably related to the hydrophbic nature of the organotin (IV) species which is present to the lesser extent in the clays prepared at pH 2 6, and as such allowing greater access to water molecules diffusing through the interlayer regions. However, a more plausible explanation may lie in the fact that the dimethyltin (IV) clays prepared at pH 2.6 may still contain unexchanged interlayer sodium ions Alternatively, experimental parameters such as the clays prepared at pH 2.6 remaining in the N_2 flow for a longer period of time, or that the furnace was at 35°C and not 25°C when loading the samples may have been contributing factors

5 5 3 Discussion of Water Vapour Isotherm Results

Water sorption and desorption isotherms for both dimethyltin (IV) exchanged montmorillonites are plotted in Fig. 5.5 from data collected in Tables 5 5 and 5.6 Comparison of these profiles indicate a similar sorption pattern up to P/Po $\sim$ 0.35 after which the extent of sorption is seen to be much greater in the clay prepared at pH 2.6. Both isotherms close below P/P_o = 1.00. Hysteresis is associated with both exchanged clays but to a much greater extent in the clay prepared at pH 2.6. The desorption isotherms of both clays close at $\sim P/P_o$ = 0 06. The difference in sorption/desorption phenomena

for both clays can be explained by fewer hydrophobic methyl groups available to oppose water sorption when exchange sites are occupied by the monomeric divalent Me_2Sn^{2+} cations in the clay prepared at pH 2 6 This has the effect of making more space available for water sorption Also desorption of water from the clay prepared at pH 2.6 is more difficult as the gallery height of 4 4Å maintained by the Me_2Sn^{2+} cations is much less than 6 4Å maintained by the $(Me_2Sn)_2(OH)_2^{2+}$ cations in the sample prepared at pH 4 0, and as such effectively traps the adsorbed water.

Evidence for condensation and evaporation of water vapour in both systems resulting in the filling and emptying of pore volumes is clearly seen in the B E T plots depicted in Fig 5 6 An approximately linear relationship for adsorption and desorption cycles exists in the region $0 < P/P_o < 0\ 6$, although the regression of the data to the equation was not very good It can be seen from Table 5.9 that the heat of adsorption, E_1, for the first water layer in each of the dimethyltin (IV) clays is approximately the same. Also the mass of water required for a monomolecular water layer, V_m, is greater in the Me_2Sn^{2+}- clay prepared at pH 2 6 as would be expected on the basis of there bein gless hydrophobic methylgroups present in this clay than in the clay prepared at pH 4 0 In addition, the small C-constants, derived from each plot indicates that the interaction between the surfaces of the pillared clays and water is very weak [29]

5 6 Conclusions

When air-dried samples of both dimethyltin (IV)-exchanged montmorillonite prepared at pH 2 6 and 4 0, along with trimethyl tin (IV)-exchanged montmorillonite prepared at pH 3 4, are thermally pretreated in a series of steps up to 300°C, their respective basal spacings are seen to decrease with increasing pretreatment temperature

For each clay system this decrease in basal spacing is indicative of the interconversion and subsequent disintegration of the respective intercalated organotin (IV) species to SnO_2 At 300°C, most of the SnO_2 in each system has migrated out of the interlayer leaving the silicate layers practically in contact This interpretation is consistent with Mössbauer evidence presented and discussed in Chapter 4

Considering the possible structural representations of the intercalated species within each dimethyltin (IV) clay system, in conjunction with basal spacings of their respective air-dried X-ray diffraction spectra, the Me_2Sn^{2+} monomeric cation is confirmed to be the major species in the clay prepared at pH 2 6 and the $(Me_2Sn)_2(OH)_2^{2+}$ dimer, the major species in the clay prepared at pH 4 0 This is evidenced by the difference in the thermogravimetric plots by virtue of the peak near 170°C Furthermore this peak is a little more intense in the twice exchanged clay prepared at pH 4 0 Furthermore, from the water vapour sorption-desorption isotherms, the mass of water sorbed was greater for the

clay prepared at pH 2 6 This indicates that the major species intercalated in this system is neither as large nor as hydrophobic as the major species intercalated in the clay prepared at pH 4 0, allowing a larger volume of water to be adsorbed and as such more difficult to desorb

REFERENCES

CHAPTER 1 REFERENCES

1. Hadding, A , (1923), Z. Krist., 58, 108.
2. Pauling, L., (1930), Proc. Matl Acad Sci U S., 16, 578.
3 Damour, A.A., and Saluctat, D., (1847), Ann. Chim Phys., 21, 376.
4. Le Chatelier, H , (1887), Bull. Soc. Franc. Mineral , 10, 204
5 Hofmann, U , Endell, K , and Wilm, D , (1933), Z. Krist., 86, 340.
6 Marshall, D E , (1935), Z Krist., 91, 433.
7. Maegdefrau, E , and Hofmann, U , (1937), Z. Krist , 98, 299.
8. Hendricks, S B., (1942), J. Geol., 50, 276.
9. Grim, R.E , (1953), "Clay Mineralogy", McGraw-Hill, New York, N.Y.
10. Norish, K., (1954), Disc. Faraday Soc., 18, 120
11. Edelman, C.H., and Favejee, J.C.L., (1940), Z. Krist., 102, 417.
12. Brown, G., (1950), Clay Minerals Bull., 4, 109.
13. McConnell, D., (1950), Am. Mineralogist, 35, 166.
14. Franzer, G., Muller-Hesse, H., and Schwiete, H.E., (1955), Naturewiessenshaften, 42, 176.
15. Kelly, W.P., (1948), "Cation Exchange in Solids", Reinhold, New York.
16. Forschamer, G., (1946), Ann. Royal Agr. Coll. Sweden, 14, 1.

17. Pezeret, H., and Mering, J., (1958), Bull Groupe Franc. Argiles, 10, 26.

18. Mering, J , and Glaesser, R., (1954), Bull. Soc Franc. Mineral, 77, 519.

19. Walker, G.F., (1963), Proc. Intern. Clay Conf , Stockholm, 1, 177.

20. Walker, G.F., (1959), Nature, 184, 1392.

21. Wiegner, G., and Jenny, H., (1927), Kolloid-Z., 43, 268

22 Schachtschabel, P., (1940), Kolloid-Beihefte, 51, 199

23. Gedroiz, K., (1922), On The Absorptive Power of Soils, U.S. Dept. of Agriculture

24. Wiklander, L., (1946), Ann. Royal Agr. Coll Sweden, 14, 244

25 Hofmann, U., and Endell, J., (1939), Ver. Deut. Chemiker Beihefte, 35, 10

26. Theng, B K.G., (1974), "The Chemistry of Clay Organic Reactions", Adam Hilger, London.

27. Walker, G.F., (1961), "The X-Ray Identification and Crystal Structure of Clay Minerals", Mineral Soc. London.

28. Mooney, R.W., Keenan, A.G., and Wood, L.A., (1952), J. Am. Chem. Soc., 74, 1367.

29. El-Akkad, T.M., Flex, M.S., and Grundy, H.M., (1982), Thermochim Acta, 59, 9.

30. Grim, R.E., and Bradley, W.E., (1948), Am. Mineralogist, 33, 50.

31. Hofmann, U., Endell, K., and Wilm, D , (1934), Angew. Chem., 47, 539.

32. Hoffmann, R.W , and Brindley, G W., (1961), Am. Mineralogist, 46, 450.

33. Hendricks, S.B., (1941), J. Phys Chem., 45, 65

34. Brindley, G.W., and Hoffmann, R W , (1962), Clays Clay Minerals, 9, 546.

35. Serratosa, J.M., (1968), Am. Mineralogist, 53, 1244.

36 Barrer, R.M , (1984), in "Zeolites Science and Technology", Martinus Nijhoff Publishers, Netherlands, 4, 266.

37 Atkinson, D., and Curtbous, G., (1980), J. Chem Soc., Faraday Trans , 77, 897.

38 Sherry, H.S., (1969), "Ion Exchange", Marinskey, New York, Mariel Dekker, 2, 89.

39. Boari, G., Liberti, L., Passino, R., and Petruzelli, D., (1981), Water Res., 15, 337.

40. Breck, D.W., Eversole, W.G., and Milton, R.M., (1956), J. Am. Chem Soc , 78, 2338

41 Barrer, R.M., and Denny, P.J., (1961), J. Am. Chem. Soc., 971

42. Barrer, R.M., Denny, P.J., and Flanigen, E.M., (1962), U.S. Patent 3,306,922.

CHAPTER 2 REFERENCES

1. Fripiat, J.J., Cruz-Cumplido, M.I., (1974), Ann. Rev. Earth Planet. Sci. 2, 239.
2. Shimoyama, A, Johns, W.D., (1971), Nature (London) Phys Sci. 232, 140.
3. Johns, W.D., Shimoyama, A, (1972), Am. Assoc. Pet. Geol.Bull. 56, 2160.
4. Schnitzer, M., Kodama, H., (1977), "Minerals in Soil Environments", ed J.B Dixon and S B. Weed, Soil Science Society of America, Madison, Wis., Chap. 2
5. White, D.H., Erickson, J.C., (1980), J. Mol Evol. 16, 279.
6. Ballantine J A., Davies, M., Purnell, J.H., Rayanakorn, M., Thomas, J.M. and Williams, K.J., (1981), (a) J C.S. Chem. Comm. 8, (b) J.C S. Chem. Comm. 427.
7. Adams, J.M., Clement, D.E., and Graham, S.H., (1981), (b) J.Chem. Res. 254.
8. Elantawy, I.M., Baverex, M., (1978), Clays and Clay Minerals, 26, 285
9. Adams, J.M., Clapp, T V., Clement, D.E., (1983), Clay Minerals, 18, 411.
10. Adams, J.M., Bylina A., Graham, S.H., (1981 (a)). Clay Minerals, 16, 325.
11. Csicsery, S.M., (1976), in "Zeolite Chemistry and Catalysis", ed: J.A. Rabo, ACS monograph 171, Washington, U.S.A.

12. Vaughan, D.E.W., Lussier, R.J., and Magee, J.S., (1979), U.S. Patent, 4,176,090.

13 Adams, J.M., Martin, K., and McCabe, R.W., (1987), J. Inclusion Phenom, 5, 663.

14. Breen, C., Deane, A.T., Flynn, J.J. (1987), Clay Minerals, 22, 169.

15. Deane, A.T., (1987), Ph.D. Thesis, N.I.H.E., Dublin.

16. Mortland, M.M , Fripiat, J.J., Chaussidan, J., Utterhoevan, J., (1963), J Phys Chem , 67, 248.

17. Russell, J.D., (1965), J.C S. Trans. Faraday Soc., 61, 2284.

18 Thomas, J.M., (1982), "Intercalation Chemistry", ed Whittingham and Jacobson, Academic Press, New York. 56.

19. Dandy, A.J., (1971 (a)), J. Chem. Soc. 14, 2383.

20. Ward, J.W., (1968), J. Catal. 11, 251.

21. Weisz, P.B., Frilette, V.J., (1960), J. Phys. Chem. 64, 382.

22. Chen, N.Y., Maziuk, J., Schwartz, A.B., Weisz, P.B., (1968), 66, 154.

23. Theng, B.K.G., (1974), "The Chemistry of Clay-Organic Reactions" (Published. John Wiley & Sons, New York).

24. Adams, J.M., Clement, D E., and Graham, S.H., (1983), Clays and Clay Minerals, 31, 129.

25. Adams, J.M., Clement, D.E., and Graham, S.H , (1982 (b)), Clays and Clay Minerals, 30, 129

26. Bylina, A., Adams, J.M., Graham, S.H., Thomas, J.M , (1980), J.C.S Chem. Comm. 1003

27. Adams, J.M., Bylina, A., Graham, S.H., Thomas, J.M., (1979), J Catal. 58, 238.

28. Poutsma, M.L , (1976), in "Zeolite Chemistry and Catalysis", ed. A. Rabo, A C.S. Monograph, 171, 437.

29. Rabo, J.A , (1981), Catal. Rev. Sci. Eng., 23, 293.

30. Smith, J.V., (1971), Adv. Chem. Sci , 10, 171.

31. Rabo, J.A , Bezman, R.D., Poutsma, M.L., (1978), Acta. Phys Chem., 24, 39.

32. Coughlan, B., Carroll, W.M., and Kelly, T C., (1978), in. Chemistry and Industry, 4, 167.

33. Nevitt, B.A., and Tobias, R S., (1963), Chemistry and Industry, 40, 136.

34. Pinnavaia, T.J , (1983), Science, 220, 365.

35. Brindley, G.W., Sempels, R.E., (1977), Clay Minerals, 12, 229.

36. Barrer, R.M., and MacLeod, D.M., (1955), J.C.S. Trans. Faraday Soc., 51, 1290.

37. Leoppert, R.H., Mortland, M.M., and Pinnavaia, T.J., (1979), Clays and Clay Minerals, 27, 201.

38. Barrer, R.M., (1978), "Zeolites and Clay Minerals as Sorbents and Molecular Sieves", Academic Press, New York, 407.

39. Breck, D.W., (1980), "The Properties and Applications of Zeolites", ed R P. Townsend, The Chemical Society, London, 391.

40. Fripiat, J J., (1986), Clays and Clay Minerals, 34, 501.

41. Pinnavaia, T.J., Tzou, M , Landau, S.D., and Raythatha, H., (1984), J.Mol.Catal., 27, 195

42. Vaughan, D.E.W., and Lussier, R.J , (1980), Proc 5th Internat Conf. Zeolites, Naples, ed L.V.C. Rees - Heyden, London, 94.

43. Occelli, M.L., and Tindwa, R.M , (1983), Clays and Clay Minerals, 31, 22

44. Endo, T., Mortland, M M., and Pinnavaia, T.J., (1980), Clays and Clay Minerals, 28, 105.

45. Endo, T , Mortland, M.M , and Pinnavaia, T.J., (1981), Clays and Clay Minerals, 29, 153.

46. Van Damme, Crespin, H., Obrecht, F , Cruz, M.I., and Fripiat, J.J , (1978), J. Colloid Interface Sci., 66, 43.

47. Abdo, S., Cruz, M.I , and Fripiat, J.J., (1980), Clays and Clay Minerals, 28, 125.

48. Molloy, K.C., Breen, C., and Quill, K., (1987), Applied Organometallic Chemistry, 1, 21.

49. Glaeser, R., (1948), Clay Minerals Bull., 1, 88.

50. Parfitt, R.L , and Mortland, M.M., (1968), Soil Sci. Soc. Am. Proc. 32, 355.

51. Barrer, R.M., and MacLeod, D.M., (1954), J.C.S. Trans. Faraday Soc., 50, 980.

52. Dyal, R.S., and Hendricks, S.B., (1950), Soil Science, 69, 421

53. Van Assche, J.B., Van Cauwelaert, F.H., and Uytterhoeven, J B., (1973), Proc. Int. Clay Conf., 605.

54. Annabi-Bergaya, F., Cruz, M.I., Gatineau, L., and Fripiat, J.J (1979), Clay Minerals, 14, 249.

55. Annabi-Bergaya, F , Cruz, M I., Gatineau, L and Fripiat, J.J., (1980), Clay Minerals, 15, 219.

56. Annabi-Bergaya, F., Cruz, M.I., Gatineau, L., and Fripiat, J.J., (1980), Clay Minerals, 15, 225

57. Mortland, M M., (1970), Advan. Agron , 22, 75.

58. Farmer, V C., (1971), Soil Science, 112, 62.

59. German, W.L., and Harding, D.A., (1971), Clay Minerals, 9, 167.

60. Dekany, I., Szanto, F., Nagy, L.G., (1978), Progr. Colloid and Polymer Science. 256, 150.

61. "Zeolites Science and Technology" (1984), ed F. Ramoa Ribeiro, Martinus Nijhoff Publishers, Netherlands, 320

62. Breck, D.W., (1974), "Zeolite Molecular Sieves", Wiley, New York.

63. Brunauer, S., (1944), "The Adsorption of Gases and Vapours", Oxford University Press, 150.

64. Mac Ewan, D.M.C., (1961), "The X-Ray Identification and Crystal Structures of Clay Minerals", Mineralogical Soc., London, 143.

65. Weaver, C E., Wampler, J M., Pecuil, T E., (1967), Science 156, 204

66. Little, L H , (1966), "Infra Red Spectra of Adsorbed Species", Academic Press, London

67 Bancroft, G.M., Maddock, A.G., Burns, R.G , (1967), Geochim. Cosmochim Acta, 31, 2219.

68. Bancroft, G.M., Burns, R.G., Stone, A.J., (1968), Geochim. Cosmochim. Acta, 32, 547.

69. Malathi, N., Puri, S.P., Saraswat, J.P., (1969), J Phys. Soc. Japan, 26, 680.

70. Greenwood, N.N , Gibb, T.C , (1971), In "Mössbauer Spectroscopy", Chapman and Hall, London.

71. Ruiying, C., (1983), Kexue Tongbao, (Eng), 25, 416

72. Simopoulos, A., Petridis, D., Kostikas, A., and Gangas, N.H., (1988), Hyperfine Interactions, 41, 843.

73. Petridis, D., Bakas, T., Simopoulos, A., and Gangas, N.H., (1989), Inorg. Chem., 28, 2439.

74. Greene-Kelly, R., (1956), Clay Min. Bull., 2, 226.

75. Endo, T., Mortland, M.M., Pinnavaia, T.J. (1980), Clays and Clay Minerals, 28, 105.

76. Adams, J.M., Breen, C. (1981), J. Coll. Int. Sc., 89, 1.

77. Dunn, J.G., (1983), "Stanton Redcroft Technical Information Sheet No. 130".

78. Mackenzie, R.C., et. al., (1957), "The Differential Thermal Investigation of Clays", ed Mackenzie, Mineralogical Society, London, 45

79. Schultz, L.G. (1969), Clays and Clay Minerals, 17, 115.

80. Laura, R.D., and Cloos, P. (1970), Reunion Hispano-Belga de Minerals de la Arcilla, Madrid, 76.

81. Mackenzie, R.C (1964), Ber dt. Keram. Geo., 12, 696.

82. Johansen, R.T., and Dunning, H.M., (1959), Proc 6th Nat. Clay Conf , (Pub Pergammon Press, New York), 249.

83. Senich, D., Turgut, D., and Handy, R.L., (1967), Highw. Res Rec., 209, 23.

84. Keren, R., and Shainberg, I., (1975), Clays and Clay Minerals, 23, 193.

85. Yamanaka, S., Malla, P.B., and Komarneni, S., (1990), Journal of Colloid and Interface Science, 134, 51.

86. Malla, P.B., and Komarneni, S., (1990), Clays and Clay Minerals, 4, 363.

CHAPTER 3 REFERENCES

1. Bennet, H , and Reed, R A , (1971), "Chemical Methods of Silicate Analysis", Academic Press, London, 71.

2 Keren, R., and Shainberg, I , (1975), Clay Minerals, 23, 193

3 I.L. 357 Spectrophotometor Manual, (1980), Instrumentation Laboratory, U K.

4 Quill, K., (1987), Ph D Thesis, N I.H.E , Dublin

5 Cryostats for Mössbauer Spectrometer Set-up and Running Procedures, (1978), Cryophysics Ltd , Crowley Road, Oxford, U K.

6. Cryostats for Mössbauer Spectroscopy - Product and Application Note, (1978), Cryophysics Ltd., Crowley Road, Oxford, U.K.

7. O'Gorman, J.V , and Walker, P.L , (1973), Fuel, 52, 71.

8. Branson, K., and Newman, A C D., (1983), Clay Minerals 18, 277

9. Greenspan, L., (1977), J National Bureau of Standards, 81A, 89

10. Robinson, R.A., and Stokes, R H , (1965), "Electrolyte Solutions", Butterworths, London.

CHAPTER 4 REFERENCES

1. Cranshaw, T.W., Dale, B.W., Longworth, D.O., Johnson, C.E., (1985), "Mössbauer Spectroscopy and its Applications". (Pub. Cambridge University Press, U.K.).
2. Malathai, H., Puri, S.P., Saraswat, I.P., (1969), J.Phys.Soc. (Japan), 26, 680.
3. Bowen, H.L., Weed, S.P., Stevens, J.G., (1969), J. Amer. Min. 54, 72.
4. Ruiying, Cai. (1983). Kexue Tongbao, 28 (3), 416.
5. Blunden, S.J., Chapman, A.H., (1982), Environmental Technology Letters, 3, 267.
6. Mössbauer, R.L., (1958), Z. Physik, 151, 124.
7. Kuhn, W.,(1929), Phil. Mag., 8, 625.
8. Greenwood, N.N., Gibb, T.C., (1971), "Mössbauer Spectroscopy", pub. Chapman and Hall Ltd., London.
9. Berry, J., (1983), Phys. Bull, 34, 517.
10. Fitzsimmons, B.W., Teelry, N.J., Smith, A.W., (1969), J. Chem. Soc. (14), 143.
11. Gibb, T.G., (1976), "Principles of Mössbauer Spectroscopy", (Ed. A.D. Buckingham), pub. Chapmann and Hall Ltd., London.
12. Tobias, R.S., (1978), Am. Chem. Soc. Sym. Ser., 82, 130.
13. Tobias, R.S., Farrer, H.N., Hughes, M.B., and Nevett, B.A., (1966), Inorg. Chem., 5, 2052.

14. Tobias, R.S., and Yasuda, M., (1964), J. Phys. Chem., 68, 1820.

15. Tobias, R.S., Ogrins, I., and Nevett, B.A., (1962), Inorg. Chem., 1, 638.

16. Tobias, R.S., (1966), Organometal. Chem. Rev., 1, 93.

17. Brooks, J.J., Clarkson, R.W., and Allen, D.W., (1983), J. Organometallic Chemistry, 243, 411.

18. Parish, R.V. and Johnson, C.E. (1971). J.Chem. Soc. (A), 1906.

19. Davis, C.G. and Donaldson, J.D. (1968) J.Chem. Soc. (A), 946.

20. Petridis, D., Bakas, T., Simopoulos, A., and Gangas, N.H.J., (1989), Inorg. Chem., 28, 2439.

21. Stöckler, H.A. and Sano. H., (1968). Trans Faraday Soc., 64, 577.

22. Hill, J.C., Drago, R.S. and Herber, R.H., (1969), J. A,. Chem. Soc., 91, 1644.

23. Herber, R.H., Stockler, H.A., and Reichle, W.T., (1965), J. Chem. Phys., 42, 2447.

24. Cotton, F.A. and Wilkinson, G., (1980), "Advanced Inorganic Chemistry". (4th ed. published John Wiley & Sons, New York), 375.

25. Weast, R.C., (1985-1986), in "The Handbook of Chemistry and Physics", C.R.C. Press, U.K. 65 ed.

26. Cordey-Hayes, M., Peacock, R.D., and Vucelic, M., (1967), J. Inorg. Nuclear Chem., 29, 1177.

27. Poller, R.C., and Ruddick, J.H.R., (1969), J. Chem. Soc. (A)., 2273.

CHAPTER 5 REFERENCES

1 Farzanah, F and Pinnavaia, T J., (1983), Inorg Chem , 22, 2216

2 Pinnavaia, T J , (1983), Science, 220, 365

3 Adams, J M , Clapp, I V., and Clement, D.E., (1983), Clay Minerals, 18, 411.

4 Cullity B D , (1978), "Elements of X-ray Diffraction", 2nd ed , Addison-Wesley, London.

5. Theng, B K.G., (1974), "The Chemistry of Clay-Organic Reactions", Adam Hilger, London.

6 Bennet, H., and Reed, R.A., (1971), "Chemical Methods of Silicate Analysis", Academic Press, London, 71.

7. Grim, R.E , (1968), "Clay Mineralogy", McGraw-Hill, New York, 126.

8 Adams, J M., and Breen, C., (1982), J. Coll. Inter. Sc , 89, 272.

9 Deane, A.T., (1987), Ph.D. Thesis, National Institute for Higher Education, Dublin.

10. El-Akkad, T.M., Flex, N.S., Gruindy, H.M., El-Massry, S.R., and Hashed, S., (1982), Thermochim Alta, 59, 9.

11. Johansen, R.T., and Dunning, H.N., (1959), Proc. 6th Nat. Clay Conf., Pergammon Press, New York.

12. Barrer, R M., and McLeod, D.M., (1954), Trans Faraday Soc., 50, 980.

13. Keren, R., and Shainberg, I., (1975), Clays and Clay Minerals, 23, 193.

14. Branson, K., and Newman, A.C D., (1983), Clay Minerals, 18, 277.

15 Wendlandt, W.W., (1974), "Thermal Methods of Analysis", 2nd ed., Wiley-Interscience, New York

16. MacEwan, D M.C and Wilson, M.J., (1980), "Crystal Structures of Clay Minerals and their X-ray Identification", (G.W. Brindley and G. Brown, editors), Mineralogical Society London

17 Glasstone, S., and Lewis, D., (1965), "Elements of Physical Chemistry", 2nd ed, Macmillan & Co., London

18. Braunner, S., (1943), "The adsorption of Gases and Vapours, Physical Adsorption", Princeton University Press.

19. Martin, T.R., (1960), "Adsorbed Water on Clay· A Review". Nat. Conf. on Clays and Clay Minerals Proc., 9, 28.

20. Braunuer, S., Emmet, P.H , and Teller, E., (1938), J.Am.Chem Soc , 60, 309.

21. Barrer, R.M., (1984), "Zeolites· Science and Technology", ed F. Ramoa Ribeiro, NATO ASI Series E, No. 80, 227.

22. Lange, D., (1973), "Handbook of Chemistry", 11th ed., McGraw-Hill, Section 3, 118.

23. Porterfield, W., (1982), "Inorganic Chemistry", 1st ed., published by Addison Wiley.

24. Mortland, M.M., and Raman, K.V., (1968), Clays Clay Minerals, 16, 393.

25 Tillak, D., Tennakoon, B , Jones, W., and Thomas, J M , (1985), J Am Chem.Soc., 107, 2362.

26. Christiano, S.P , Wang, J , and Pinnavaia,T.J., (1985), J Inorg.Chem , 24, 1222.

27 Petridis, D , Bakas, T., Simopoulos, A , and Gangas, N.H J , (1989), Inorg. Chem., 28, 2439.

28. Tobias, R.S , and Yasuda, M., (1964), J. Phys. Chem , 68, 1820

29 Yamanaka, S , Malla, P B., and Komarneni, S., (1990), J Col Inter Sci , 134, 51.